

GUIDELINES FOR THE DESIGN OF PLAIN JOINTED RIGID PAVEMENTS FOR HIGHWAYS

(Fourth Revision)

Published by:

INDIAN ROADS CONGRESS

Kama Koti Marg,
Sector-6, R.K. Puram,
New Delhi-110 022

June, 2015

Price : ₹ ???/-
(Plus Packing & Postage)

IRC:58-2015

First Published : July, 1974
First Revision : June, 1988
Second Revision : Dec, 2002
Third Revision : Nov, 2011
Fourth Revision : June, 2015

(All Rights Reserved. No part of this publication shall be reproduced, translated or transmitted in any form or by any means without the permission of the Secretary General, Indian Roads Congress)

Printed by India Offset Press, Delhi-110 064

1000 Copies

CONTENTS

S. No.	Description	Page No.
	Personnel of the General Specifications and Standards Committee	i-ii
	Definition	1
	Introduction	6
1.	Overview of Landslided Hazards In India	8
2.	Landslide Features and Geometry	11
3.	Classification	16
4.	Landslide Hazard Mapping, Vulnerability and Risk Assessment	23
5.	Methods of Scientific Investigation of Slopes and Landslides	37
6.	Instrumentation, Monitoring, Forecasting and Early Warning of Landslides	43
7	Landslide Risk Reduction through Improved Planning, Design and Construction Practices	58
8.	Technology for Landslide Prevention and Remediation	72
9.	References	87
	Annexure 1	100

PERSONNEL OF THE HIGHWAYS SPECIFICATIONS AND STANDARDS COMMITTEE

(As on 12th January, 2015)

- | | | |
|----|--|--|
| 1. | Das, S.N.
(Convenor) | Director General (Road Development) & Special Secretary to Govt. of India, Ministry of Road Transport & Highways, New Delhi. |
| 2. | (Co-Convenor) | Addl. Director General, Ministry of Road Transport & Highways, New Delhi |
| 3. | Prasad, Vishnu Shankar
(Member-Secretary) | Chief Engineer (R) S, R&T, Ministry of Road Transport & Highways, New Delhi |

Members

- | | | |
|-----|----------------------|---|
| 4. | Basu, S.B. | Chief Engineer (Retd.), MORTH, New Delhi |
| 5. | Bongirwar, P.L. | Advisor, L & T, Mumbai |
| 6. | Bose, Dr. Sunil | Head, FPC Divn. CRRI (Retd.), Faridabad |
| 7. | Duhsaka, Vanlal | Chief Engineer, PWD (Highways), Aizwal (Mizoram) |
| 8. | Gangopadhyay, Dr. S. | Director, Central Road Research Institute, New Delhi |
| 9. | Gupta, D.P. | DG (RD) & AS (Retd.), MORTH, New Delhi |
| 10. | Jain, R.K. | Chief Engineer (Retd.), Haryana PWD, Sonipat |
| 11. | Jain, N.S. | Chief Engineer (Retd.), MORTH, New Delhi |
| 12. | Jain, Dr. S.S. | Professor & Coordinator, Centre of Transportation Engg., Dept. of Civil Engg., IIT Roorkee, Roorkee |
| 13. | Kadiyali, Dr. L.R. | Chief Executive, L.R. Kadiyali & Associates, New Delhi |
| 14. | Kumar, Ashok | Chief Engineer (Retd.), MORTH, New Delhi |
| 15. | Kurian, Jose | Chief Engineer, DTTDC Ltd., New Delhi |
| 16. | Kumar, Mahesh | Engineer-in-Chief, Haryana PWD, Chandigarh |
| 17. | Kumar, Satander | Ex-Scientist, CRRI, New Delhi |
| 18. | Lal, Chaman | Director (Project-III), NRRDA (Ministry of Rural Development), New Delhi |
| 19. | Manchanda, R.K. | Consultant, Intercontinental Consultants and Technocrats Pvt. Ltd., New Delhi |
| 20. | Marwah, S.K. | Addl. Director General, (Retd.), MORTH, New Delhi |
| 21. | Pandey, R.K. | Chief Engineer (Planning), MORTH, New Delhi |

22. Pateriya, Dr. I.K. Director (Tech.), NRRDA, (Ministry of Rural Development), New Delhi
23. Pradhan, B.C. Chief Engineer (NH), PWD, Bhubaneswar
24. Prasad, D.N. Chief Engineer (NH), RCD, Patna
25. Rao, P.J. Consulting Engineer, Faridabad
26. Raju, Dr. G.V.S. Engineer-in-Chief (R&B), Rural Roads, Director Research and Consultancy, Hyderabad
27. Representative of BRO (Shri B.B. Lal), ADGBR, HQ DGBR, New Delhi
28. Sarkar, Dr. P.K. Professor, Deptt. of Transport Planning, School of Planning & Architecture, New Delhi
29. Sharma, Arun Kumar CEO (Highways), GMR Highways Limited, Bangalore
30. Sharma, M.P. Member (Technical), NHAI, New Delhi
31. Sharma, S.C. DG (RD) & AS (Retd.), MORTH, New Delhi
32. Sinha, A.V. DG (RD) & SS (Retd.), MORTH, New Delhi
33. Singh, B.N. Member (Projects), NHAI, New Delhi
34. Singh, Nirmal Jit DG (RD) & SS (Retd.), MORTH, New Delhi
35. Vasava, S.B. Chief Engineer & Addl. Secretary (Panchayat) Roads & Building Dept., Gandhinagar
36. Yadav, Dr. V.K. Addl. Director General (Retd.), DGBR, New Delhi
37. The Chief Engineer (Mech.) (Shri Kaushik Basu), MORTH, New Delhi

Corresponding Members

1. Bhattacharya, C.C. DG (RD) & AS (Retd.), MORTH, New Delhi
2. Das, Dr. Animesh Professor, IIT, Kanpur
3. Justo, Dr. C.E.G. Emeritus Fellow, Bangalore
4. Momin, S.S. Former Secretary, PWD Maharashtra, Mumbai
5. Pandey, Dr. B.B. Advisor, IIT Kharagpur, Kharagpur

Ex-Officio Members

1. President, Indian Roads Congress (Bhowmik, Sunil), Engineer-in-Chief, PWD (R&B), Govt. of Tripura
2. Honorary Treasurer, Indian Roads Congress (Das, S.N.), Director General (Road Development), & Special Secretary to Govt. of India, Ministry of Road Transport & Highways
3. Secretary General, Indian Roads Congress (Nahar, Sajjan Singh)

SYMBOLS AND ABBREVIATIONS

Symbols and abbreviations are defined where they occur first. Some of them are local in nature and omitted from the following since they have no bearing in other sections.

A	=	Initial number of commercial vehicles per day in the year when road is opened to traffic
A_{cs}	=	Cross-sectional area of one tie bar, mm ²
A_s	=	Area of steel, mm ²
B	=	Lane width, m
b_d	=	Dowel diameter, mm
B^*	=	Permissible bond stress of concrete, MPa
B	=	Factor for transverse joint efficiency in top-down cracking
BUC	=	Bottom-up cracking
C	=	Cumulative number of commercial vehicles during the design period
C_s	=	Spacing of transverse joints, m
CBR	=	California Bearing Ratio, %
CFD	=	Cumulative Fatigue Damage
CVPD	=	Commercial vehicles per day
D_{60}	=	Particle size corresponding to 60% passing
D_{10}	=	Particle size corresponding to 10% passing
d	=	Depth of neutral axis from top surface
d_t	=	Diameter of tie bar, mm
DLC	=	Dry Lean Concrete
E	=	Modulus of elasticity of concrete, MPa
F_b	=	Allowable bearing stress in MPa
f	=	Coefficient of friction
F_{bmax}	=	Maximum bearing stress in MPa
f_{ck}	=	Characteristic compressive cube strength of concrete, MPa
f_{cr}	=	Characteristic flexural strength at 28 days, MPa
f'_{cr}	=	Target average flexural strength at 28 days, MPa
FEM	=	Finite Element Method
GSB	=	Granular sub-base
h	=	Thickness of slab, m
I	=	Moment of inertia, mm ⁴

I_c	=	Crack infiltration rate $m^3/day/m$
j	=	Total number of load groups
k	=	Modulus of subgrade reaction, $MP_{a/m} = k_{750}$
k_{mds}	=	Modulus of dowel support, MPa/m
K_p	=	Rate of infiltration through un-cracked pavement surface, $m^3/day/m$
k_ϕ	=	Modulus of subgrade reaction (MPa/m) with plate diameter Φ
k_{750}	=	Modulus of subgrade reaction (MPa/m) with plate diameter 750 mm
L	=	Length of tie bar, mm
L_d	=	Distance between free transverse joints
l	=	Radius of relative stiffness, m
LTE	=	Load Transfer Efficiency, %
MEPDG	=	Mechanistic Empirical Pavement Design Guide
N	=	Fatigue life
n	=	Design period, years
N_c	=	number of longitudinal joints/cracks
NCHRP	=	National Cooperative Highway Research Program
n_i	=	Number of expected repetitions for the i^{th} load group
N_i	=	Number of allowable repetitions (fatigue life) for the i^{th} load group
N_r	=	Fatigue life at load level 'r'
OMC	=	Optimum Moisture Content
P	=	Single/tandem axle load
P_{ci}	=	Pound per cubic inch
P_{ptb}	=	Perimeter of tie bar, mm
PQC	=	Pavement Quality Concrete
P_t	=	Load transferred by dowel bar, kN
q_i	=	infiltration rate per unit area, $m^3/day/m^2$
R	=	Flexural stiffness, MNm
r	=	Annual rate of growth of commercial traffic volume (expressed as decimal)
S_{st}	=	Allowable working stress of steel, MPa
S	=	Flexural stress in slab, MPa
SR	=	Stress Ratio
SR_r	=	Stress Ratio at load level 'r'

TCS	=	Tied Concrete Shoulder
TD	=	Temperature Differential
TDC	=	Top-down Cracking
U_c	=	Uniformity coefficient
W	=	Weight of slab, kN/m ²
W_c	=	Length of the transverse cracks or joints, m
W_p	=	Width of pavement subjected to infiltration, m
Z	=	Joint width, mm
Z_a	=	A factor corresponding to desired confidence level, which is 1.96 for 5% confidence level
α	=	Coefficient of thermal expansion, /°C
β	=	Relative stiffness of dowel bar embedded in concrete, MPa/m
γ	=	Unit weight of concrete, kN/cum
ϕ	=	Plate diameter, m
μ	=	Poisson's ratio of concrete
σ	=	Standard deviation of field test samples, MPa
Δ_T	=	Temperature differential in °C (also designated as T_D)

GUIDELINES FOR THE DESIGN OF PLAIN JOINTED RIGID PAVEMENTS FOR HIGHWAYS

1 INTRODUCTION

Guidelines for the Design of the Rigid Pavements for Highways were first published in 1974. The first revision of the guidelines was made in 1988 after the upward revision of the legal limit on the maximum laden axle loads of commercial vehicles from 8160 kg to 10200 kg. The second revision was brought out in 2002 to include fatigue damage concept in design. The third revision of the document was published in 2011.

Taking into account the further developments in the area of rigid pavements during the past years a revised draft of the guidelines was prepared by Dr. B.B. Pandey with the support of the Transportation Engineering Section of Civil Engineering Department of Indian Institute of Technology, Kharagpur. The Rigid Pavement Committee (H-3) deliberated on the document in a series of meetings and finalised it in its meeting held on 19th December, 2014 for placing before the Highways Specifications and Standards Committee (HSS). The HSS Committee approved the revised draft of IRC:58 “Guidelines for the Design of Plain Jointed Rigid Pavements for Highways” in its meeting held on 12th January, 2015. The Council of IRC in its 204th meeting held on 19th January, 2015 at Bhubaneswar (Odisha) approved the same after taking on board the comments offered by the members.

The Composition of H-3 Committee is as given below:

Jain, R.K.	-----	Convenor
Kumar, Satander	-----	Co-Convenor
Kumar, Raman	-----	Member-Secretary

Members

Bongirwar, P.L.	Prasad, Bageshwar
Ganju, Col. V.K.	Sachdeva, Dr. S.N.
Gautam, Ashutosh	Seehra, Dr. S.S.
Gupta, K.K.	Sengupta, J.B.
Jain, L.K.	Sharma, Late R.N.
Joseph, Isaac V.	Singla, B.S.
Kadiyali, Dr. L.R.	Sitaramanjaneyulu, K.
Krishna, Prabhat	Tipnis, Col. Manoj
Kumar, Ashok	Venkatesha, M.C.
Kurian, Jose	Rep. of CMA (Avtar, Ram)
Maiti, Dr. S.C.	Rep. of E-in-C Branch
Pandey, Dr. B.B.	

Corresponding Members

De, D.C.	Nakra, Brig. Vinod
Justo, Dr. C.E.G.	Reddi, S.A.
Madan, Rajesh	Thombare, Vishal

Ex-Officio Members

President, Indian Roads Congress	(Bhowmik, Sunil), Engineer-in-Chief, PWD (R&B), Govt. of Tripura
Honorary Treasurer, Indian Roads Congress	(Das, S.N.), Director General, (Road Development) & Special Secretary to Govt. of India, Ministry of Road Transport & Highways
Secretary General, Indian Roads Congress	Nahar, Sajjan Singh

2 SCOPE

3.1 The guidelines cover the design of plain jointed cement concrete pavements with and without tied concrete shoulders. These are applicable to roads having an average daily commercial vehicles more than 450 with laden weight exceeding 3 tonnes. IRC:SP:62 may be referred for design of low-volume Rural Roads.

3 GENERAL

3.1 The current version of IRC:58 aims at rationalising the design procedure by bringing it at par with current trends in design considering cumulative fatigue damage due to the combined effect of load and pavement temperature. The guidelines also include procedure for design of pavements with widened outer lane, tied concrete shoulder, pavements bonded to stabilized subbase as well as design of longitudinal, expansion and contraction joints.

3.2 The Salient Features of the Current Guidelines are:-

- i) Design of pavements considering the flexural stress under the simultaneous action of load and temperature gradient for different categories of axles.
- ii) Design considering sum of cumulative fatigue damages caused by single, tandem and tridem axle load applications due to tensile flexural stresses at the top and the bottom of the pavement slab.
- iii) Consideration of in-built permanent curl in the analysis of flexural stresses.
- iv) Design guidelines for pavements without concrete shoulders and with tied concrete shoulders.
- v) Consideration of Concrete slabs with unbonded as well as bonded cement bound subbase.
- vi) Design of pavements with widened outer lanes.

There can be many different considerations other than what are given above and designers may use their knowledge and experience.

3.3 The guidelines may need revision from time to time in the light of field performance of rigid pavements, future research findings and development of better analytical tools. It is recommended that all the organizations that are concerned with design, construction and maintenance of rigid pavements should keep a detailed record of the year of construction, Traffic, Subgrade CBR, properties and gradation of granular subbase, strength of Dry Lean Concrete (DLC) and Pavement Quality Concrete (PQC), roughness, cracking, faulting at joints and cracks, falling weight deflection data etc. so that these can be used in future revision of the guidelines.

4 CONCRETE PAVEMENT TYPES

4.1 Several types of concrete pavements have been used in different countries depending upon the climate, availability of materials, soil types, experience and traffic. A designer may select the most appropriate composition of a concrete pavement depending upon his/her experience. Typical cross sections of two pavements are shown in **Fig. 1**. When PQC is laid over a bituminous surface during the sunshine it is important to whitewash the surface of BC (**Fig. 1 (b)**) because black body absorbs more heat which may be injurious to concrete.

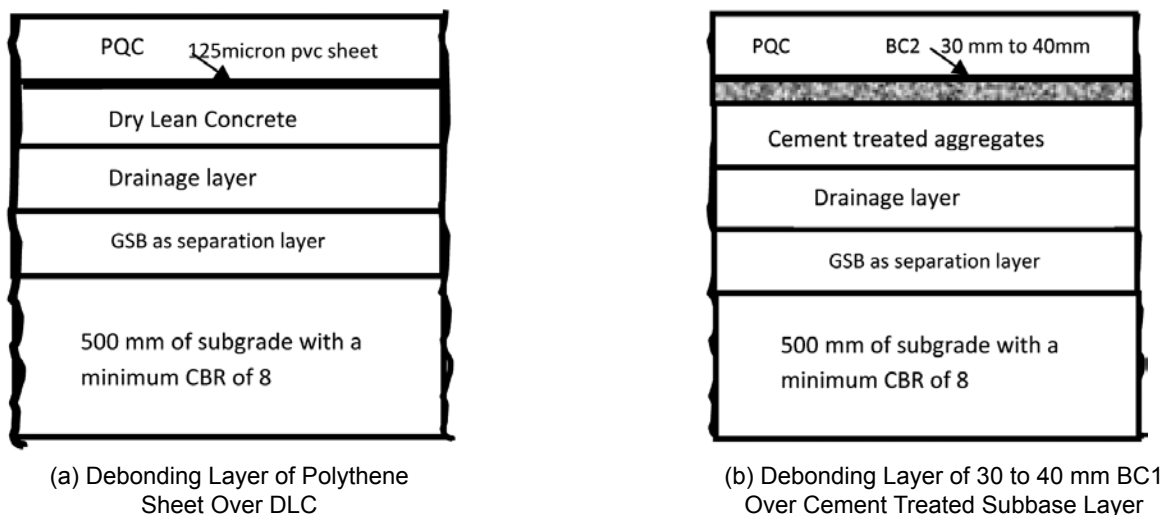


Fig. 1 Typical Cross Section of Concrete Pavements

Note : PQC: Pavement Quality Concrete, DLC: Dry Lean Concrete, BC: Bituminous Concrete, For Subgrade with $CBR \geq 8$, both the granular separation and drainage layers can be replaced with Synthetic geocomposite.

5 FACTORS GOVERNING DESIGN

5.1 The main factors governing design of concrete pavements are design period, design commercial traffic volume, composition of commercial traffic in terms of single, tandem, tridem and multi-axles, axle load spectrum, tyre pressure, lateral placement characteristics, directional distribution, strength of foundation and climatic considerations.

5.2 Axle Load Characteristics

Though the legal axle load limits in India are 10.2 tonnes (100 kN), 19.0 tonnes (186 kN) and 24.0 tonnes (235 kN) for single, tandem and tridem axles respectively, a large number of axles operating on National Highways carry much heavier loads than the legal limits. Data on axle load spectrum of the commercial vehicles is required to estimate the repetitions of single, tandem and tridem axles in each direction expected during the design period. Minimum percentages of commercial vehicles to be weighed should be 10% of the volume of Commercial Vehicles Per Day (CVPD) exceeding 6000, 15% of CVPD for 3000 to 6000 and 20% of CVPD if less than 3000. Axle load survey may be conducted for a continuous 48-hour period. The vehicles to be surveyed may be selected randomly to avoid bias. If the spacing of consecutive axles (wheel base) is more than 2.4 m, each axle shall be considered as a single axle. The intervals at which axle load groups should be classified for fatigue damage analysis are:-

Single axle	10 kN
Tandem axle	20 kN
Tridem axle	30 kN

For most of the commercial highway vehicles, the commonly used tyre inflation pressures range from about 0.7 MPa to 1.0 MPa. It is found that stresses in concrete pavements having thickness of 200 mm or higher are not affected significantly by the variation of tyre pressure. A tyre pressure of 0.8 MPa is adopted for design in these guidelines.

5.3 Wheel Base Characteristics

Information on typical spacing between successive axles of commercial vehicles is necessary to identify the proportion of axles that should be considered for estimating top-down fatigue cracking caused by axle loads during night period. The slab has the tendency of curling up due to negative temperature differential. Data on the spacing of axles may be collected during the traffic survey. As discussed in subsequent sections of these guidelines, if the spacing between any pair of consecutive axles is less than the spacing of transverse joints, such axles need to be considered in the design traffic for computing top-down fatigue cracking damage. Wheel bases of trucks of different models generally range from 3.6 m to more than 5.0 m whereas the commonly used spacing of transverse joints is 4.5 m. Thus, axles with spacing of more than 4.5 m will not contribute to top-down fatigue cracking. However, if the actual spacing of transverse joints is different from 4.5 m, design traffic for estimation of top-down cracking damage may be selected appropriately. The percentage of commercial vehicles with spacing between the front and the first rear axle less than the proposed spacing of the transverse joints in the concrete slab should be established from axle load survey.

5.4 Design Period

Cement concrete pavements may be designed to have a life span of 30 years or more. However, the design engineer should use his/her judgment about the design period taking into consideration factors such as traffic volume, uncertainty of traffic growth rate, the capacity of the road and the possibility of augmentation of capacity by widening.

5.5 Traffic Consideration

5.5.1 Design Lane

The lane carrying the maximum number of heavy commercial vehicles is termed as design lane. Each lane of a two-way two-lane highway and the outer lane of multi-lane highways can be considered as design lanes.

5.5.2 Design Traffic

5.5.2.1 Assessment of average daily traffic should normally be based on seven-day 24-hour count made in accordance with IRC:9 “Traffic Census on Non-Urban Roads”. The actual value of annual rate of growth ‘r’ of commercial vehicles should be determined using appropriate methods. As per IRC:SP:84, annual growth rate of commercial vehicles shall be taken to be a minimum of 5%. The traffic counts and the corresponding traffic estimates should indicate the day and night traffic trends as the traffic during the day hours is generally responsible for bottom-up cracking whereas the night time traffic may lead to top-down cracking.

5.5.2.2 The edge flexural stress caused by axle loads for bottom up cracking is maximum when the tyre imprint of the outer wheel touches the longitudinal edge. When the tyre position is away even by 150 mm from the longitudinal edge, stress in the edge region is reduced substantially. The edge flexural stress is small when the wheels are close to the transverse joints. Typical lateral distribution characteristics of wheel paths of commercial vehicles observed on Indian highways indicate that very few wheels of vehicles are tangential to the longitudinal edge or longitudinal joint on two-lane two-way roads and divided multi-lane highways. Some multi-lane divided highways have 8.5 m to 9.0 m wide carriageways with a single longitudinal joint in the Centre. The lane markings in these cases may not coincide with the longitudinal joint resulting in a larger proportion of wheel paths being positioned close to the longitudinal joint compared to the situation where the lane markings match the longitudinal joints.

5.5.2.3 Taking into consideration these issues, it is recommended that 25 percent of the total two-way commercial traffic may be considered as design traffic for two-lane two-way roads for the analysis of fatigue damage. In the case of four-lane and other multi-lane divided highways, 25 percent of the total traffic in the direction of predominant traffic may be considered for design of pavement.

5.5.2.4 The design traffic for top-down cracking analysis will usually be a fraction of the design traffic considered for bottom-up cracking analysis. Only those commercial vehicles with the spacing between the front axle and the first rear axle less than the spacing of transverse joints is considered for the analysis of top-down cracking. This percentage should be established from axle load / traffic survey. A default value of fifty percent of the design traffic for the bottom-up cracking analysis may be considered for the analysis of top down cracking.

5.5.2.5 In case of new highway links, where no traffic count data is available, data from roads of similar classification and importance may be used to predict the design traffic intensity.

5.5.2.6 Expected number of applications of different axle load groups during the design period can be estimated using the details of commercial traffic volume, expected rate of growth of commercial traffic, the information about axle load spectrum and the number of single, tandem and tridem axles obtained from axle load survey. Front axles (steering axle) with single wheels on either side cause only negligible bottom-up fatigue damage.

5.5.2.7 The cumulative number of commercial vehicles during the design period may be estimated from the following expression.

$$C = \frac{365 \times A \{ (1+r)^n - 1 \}}{r} \quad \dots (1)$$

Where,

- C = Cumulative number of commercial vehicles during the design period
- A = Initial number of commercial vehicles per day in the year when the road is opened to traffic
- r = Annual rate of growth of commercial traffic volume (expressed as decimal)
- n = Design period in years

5.5.2.8 The design cumulative number of axle load repetitions for fatigue damage can be obtained from the cumulative number of commercial vehicles as per Clauses 5.5.2.3 and 5.5.2.4.

5.6 Temperature Consideration

5.6.1 Temperature Differential

5.6.1.1 Temperature differential between the top and bottom fibres of concrete pavements causes the concrete slab to curl, giving rise to stresses. The temperature differential is a function of solar radiation received by the pavement surface, wind velocity, thermal diffusivity of concrete, latitude, longitude and elevation of the place and is thus affected by geographical features of the pavement location. As far as possible, temperature differential values estimated realistically for the given site using relevant geographical parameters and material characteristics should be used for analysis. In the absence of any local data, the maximum temperature differential values given in **Table 1** may be adopted for pavement design. The variation of temperature with depth is non-linear during the day time and nearly linear during night hours. The maximum temperature differential during the night is nearly half of the day time maximum temperature differential.

5.6.1.2 Temperature differentials are positive when the top surface of a pavement slab has the tendency to have a convex shape during the day hours and negative with a concave shape during the night. The axle load stresses should be computed for fatigue analysis when the slab is in a curled state due to the temperature differential during day as well as night hours.

Table 1 Recommended Maximum Temperature Differentials for Concrete Slabs

Zone	States/Regions	Max. Temperature Differential °C in Slab of Thickness			
		150 mm	200 mm	250 mm	300 mm to 400 mm
I	Hilly regions of Uttaranchal, West Bengal, Jammu & Kashmir, Himachal Pradesh and Arunachal Pradesh	12.5	13.1	14.3	15.8
II	Punjab, U.P., Uttaranchal, Gujarat, Rajasthan, Haryana and North M.P, excluding hilly regions	12.5	13.1	14.3	15.8
III	Bihar, Jharkhand, West Bengal, Assam and Eastern Orissa, excluding hilly regions and coastal areas	15.6	16.4	16.6	16.8
IV	Maharashtra, Karnataka, South M.P., Chattisgarh, Andhra Pradesh, Western Orissa and North Tamil Nadu, excluding hilly regions and coastal areas	17.3	19.0	20.3	21.0
V	Kerala and South Tamil Nadu, excluding hilly regions and coastal areas	15.0	16.4	17.6	18.1
VI	Coastal areas bounded by hills	14.6	15.8	16.2	17.0
VII	Coastal areas unbounded by hills	15.5	17.0	19.0	19.2

Note : The above temperature data was recommended by Central Road Research Institute, New Delhi in 1974. The data for colder hilly regions of Jammu & Kashmir, Himachal Pradesh, West Bengal, Uttaranchal and Arunachal Pradesh are suggested in Zone- I in the absence of available records.

5.6.2 Zero Stress Temperature Gradient

5.6.2.1 Cement concrete pavements are usually laid during the night hours in India due higher day temperatures. The pavement slabs laid during late night and early hours may have high positive temperature gradients due to intense solar radiation during the day hours and chemical reaction in the cemented mass before the setting of the concrete .Even when positive temperature differential occurs in concrete during the day time, the slab remains flat during the hardening process because of its plastic stage. The slab is stress free in this condition with higher temperature on the top surface and lower at the bottom fibre and the corresponding temperature gradient is known as ‘zero stress temperature gradient’. Research on in-service concrete pavements indicates that exposure of fresh concrete to sun and high air temperature during the hardening stage causes building of permanent curl in the concrete pavements which is nearly equivalent to the curl caused by a negative temperature differential of about 5°C. This equivalent negative temperature differential has to be added algebraically to the actual temperature differential prevailing at any time. Field investigations

on existing pavements located in different regions of the country will be necessary to establish the zero stress temperature gradient for different regions in India for future guidance.

5.6.2.2 If the maximum positive temperature differential during the day time is 20°C, the temperature differential for stress computation can be taken as 15°C. However, this 5°C reduction is generally not made so that the design for bottom-up cracking will be conservative.

5.6.2.3 During the night hours, if the temperature differential is 10°C, the total effective negative temperature differential can be taken as 15°C (10°C + 5°C). If mist spray of water can be applied over the curing compound during the period of intense solar radiation during day time, the built-in permanent curl will be less. It is safer to consider the effective negative temperature gradient for checking the slab for top-down cracking caused by the combined effect of traffic loads and night time negative temperature differential.

5.6.2.4 It is ideal to carry out hourly cumulative fatigue damage analysis but data for carrying out such an exercise is not available. It is suggested that the maximum positive and negative temperature differentials respectively may be assumed to be constant for the six hour period during the day between 10 AM and 4 PM and for the six hour period between 0 AM to 6 AM during night hours. The slab may be assumed to be free of curling stresses for the remaining 12 hours for the purpose of fatigue damage analysis as the fatigue damage caused by the combined action of load and temperature differential will be insignificant during this period. The timings refer to Indian Standard time and may be different for different geographical locations in India.

5.7 Embankment Soil and Characteristics of Subgrade and Subbase

5.7.1 CBR of embankment soil placed below the 500 mm select subgrade should be determined for estimating the effective CBR of subgrade and its 'k' value for design.

5.7.2 The nature of embankment foundation strata such as expansive clays, marine clays, soft clays, black cotton soil, etc. needs to be studied to take special measures like consolidation of the strata by accelerated pore pressure dissipation, removal of expansive black cotton soil strata and its replacement by non-expansive soil, use of geo synthetics to arrest tension cracks or soil stabilization etc. Soil swell can be controlled by surcharge loads or by placing the swelling soils in the lower part of an embankment. Selective grading and soil mixing is also helpful. In deep cut sections, removal of overburden soils causes soils to swell. It is, therefore, advisable to excavate deep cuts in advance of other grading work to allow expansion to occur and stabilize. Expansive soils should be compacted at 1-3 percent above Optimum Moisture Content (OMC) as determined by Modified Proctor compaction. The soil should not be allowed to dry out excessively before GSB and other layers are laid. If non-expansive soils are not available, it may be more economical to modify the existing soil with lime or cement or both. A thorough study needs to be undertaken on case specific basis and detailed treatment of foundation strata is beyond the scope of these guidelines.

5.7.3 Subgrade

5.7.3.1 The subgrade is usually considered as a Winkler foundation, also known as dense

liquid foundation. In Winkler model, it is assumed that the foundation is made up of springs supporting the concrete slab. The strength of subgrade is expressed in terms of modulus of subgrade reaction, k , which is defined as the pressure per unit deflection of the foundation as determined by plate load tests. The k -value is determined from the pressure sustained at a deflection of 1.25 mm. As k -value is influenced by test plate diameter, the standard test is to be carried out with a 750 mm diameter plate. IS:9214, "Method of Determination of Modulus of Subgrade Reaction of Soil in the Field" may be referred to for guidance in this regard. A frequency of one test per km per lane is recommended for assessment of k -value. If the foundation changes with respect to subgrade soil, type of subbase or the nature of formation (i.e. cut or fill) then additional tests may be conducted.

5.7.3.2 Though 750 mm is the standard plate diameter, smaller diameter plate can be used in case of homogeneous foundation from practical consideration and the test values obtained with plates of smaller diameter may be converted to the standard 750 mm plate value using equation 2.

$$k_{750} = k_{\phi} (1.21 \Phi + 0.078) \quad \dots (2)$$

where,

Φ = plate diameter, metre

k_{ϕ} = modulus of subgrade reaction (MPa/m) with plate diameter Φ metre

k_{750} = modulus of subgrade reaction (MPa/m) with plate diameter of 750 mm (k)

5.7.3.3 The estimate obtained from Equation 2 is regarded as approximate only. However, in case of layered construction, the tests conducted with smaller plates give greater weight age to the stronger top layer, and direct conversion to 750 mm plate values using Equation 2 results in somewhat over-estimation of the foundation strength.

5.7.3.4 The subgrade soil strength and consequently the strength of the foundation as a whole, is affected by its moisture content. Since it is not convenient to determine the k -value in the field at different moisture contents and densities, CBR tests may be carried out at field moisture content and field density both in soaked and un-soaked condition and the measured k -value from plate load test may be corrected in the ratio of CBR values under soaked and un-soaked conditions to obtain the k -value corresponding to the weakest condition of subgrade. The plate load test is time-consuming and expensive and, therefore, the design k -value is often estimated from soaked CBR value. The relationship between the CBR and k -value illustrated in **Table 2** can be used for this purpose.

Table 2 Relationship between K-Value and CBR Value for Homogeneous Soil Subgrade

Soaked CBR (%)	2	3	4	5	7	10	15	20	50	100
k -value (MPa/m)	21	28	35	42	48	55	62	69	140	220

Note: 100 pci = 2.77 kg/cm³ = 27.2 MPa/m

5.7.3.5 If the CBR of the 500 mm thick compacted subgrade is significantly larger than that of the embankment below it, the effective CBR of the subgrade can be estimated from **Fig. 2**.

5.7.3.6 A minimum CBR of 8% is recommended for the 500 mm of the select soil used as subgrade.

5.7.3.7 The in-situ CBR of the subgrade soil can also be determined quickly from the Dynamic Cone Penetrometer (60° cone) tests using the following relationship (ASTMD 6951).

$$\log_{10} \text{ CBR} = 2.465 - 1.12 \log_{10} N \quad \dots (3)$$

Where,

N = rate of cone penetration (mm/blow)

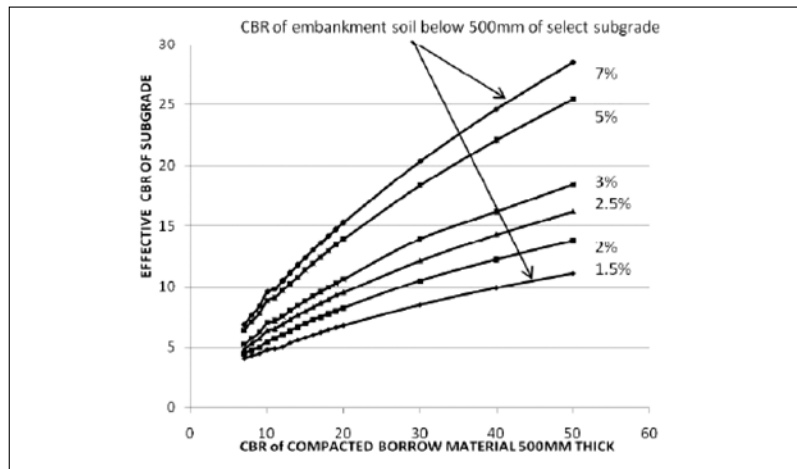


Fig. 2 Chart for Estimation of Effective CBR of Subgrade

5.7.3.8 The modulus of subgrade reaction of the subgrade of an in-service pavement or of a prepared foundation can also be determined by conducting Falling Weight Deflectometer (FWD) tests. The k-value of the subgrade back calculated from FWD test data is the dynamic k-value. The corresponding static k-value, which should be used for analysis, can be estimated as 50% of the dynamic k-value obtained from FWD test as recommended AASHTO 1993 Pavement Design Guide.

5.7.3.9 The subgrade needs to be protected by providing separation and drainage layers of Granular Subbase (GSB) above it to prevent (i) excessive softening of subgrade and GSB and (ii) erosion of the subgrade and subbase particularly under adverse moisture condition and heavy dynamic loads. GSB Gr I/II/V/VI (MORTH 5th rev) may be as used as separation layer to prevent fines from migrating to the drainage layer and coke it. IRC:15, IRC:SP:42 and IRC:SP:50 may be referred to for the design criteria of the separation layer also known as filter layer. International practice for drainage layer is discussed in **Appendix VI**. The gradations for the drainage layers may be adopted from several gradations given in the **Appendix VI** since GSB of MORTH have low permeability as discussed in **Appendix VI**. Open graded drainage layer is unstable under construction traffic and it may be stabilized with 1.5 to 2% bitumen or 3% bituminous emulsion or 2 to 2.5% cement to impart stability to it. Commercially available synthetic geo-composite layer can also be used at the interface of subgrade and granular subbase layer for separation and drainage in place

of granular layers. It will also not allow the migration of fine particles to the granular layer while maintaining a good horizontal permeability.

5.7.4 *Stabilised Subbase*

5.7.4.1 The main purpose of the subbase is to provide a uniform, stable and permanent support to the concrete slab laid over it. It must have sufficient strength so that it is not subjected to disintegration and erosion under heavy traffic and adverse environmental conditions such as excessive moisture, freezing and thawing. In the light of these requirements, a subbase of Dry Lean Concrete (DLC) having a 7-day average compressive strength of 7 MPa determined as per IRC:SP:49 over GSB is recommended for highways. Minimum recommended thickness of DLC for major highways is 150 mm. For PQC bonded to DLC the 7 day strength of DLC should not be less than 10 MPa. The surface of DLC is to be roughened with wire brush within 3-6 hours of laying.

5.7.4.2 Availability of good quality aggregates has become a big hurdle in the construction of pavements because of closures of old quarries, restriction on opening of new quarries from environmental considerations. Similar problems are being faced in other countries also. International practice on the use of cemented/stabilized subbases is discussed in **Appendix I**. In the light of international experience, a minimum characteristic 28-day compressive strength of 7 MPa is recommended for cement treated subbases with recycled or marginal aggregates while ensuring that the support is permanent, uniform and non-erodible. Use of BC2 as per MORTH (5th rev) as a debonding layer over cement treated GSB shown in **Fig. 1 (b)** is recommended to allow expansion and contraction of the pavement slabs. The dense graded BC is resistant against stripping and concrete pavements with a debonding layer of BC shown in **Fig. 1(b)** are known to give good performance. Loss of weight of cement treated subbases shall not exceed 14% after 12 cycles of “Wetting and Drying Test/freezing and thawing” tests as per BIS:4332 (Part IV) - 1968. Freezing and thawing test is relevant for snow bound regions of Kashmir, Ladakh, Himachal Pradesh, Arunachal Pradesh etc.

5.7.4.3 In the case of problematic subgrades such as clayey and expansive soils appropriate provisions shall be made for a blanket course in addition to the subbase as per the relevant stipulations of IRC:15.

5.7.4.4 Effective k-values of different combinations of subgrade and subbase (untreated granular and cement treated granular) can be estimated from **Table 3**. For concrete pavements laid over a bituminous subbase, the k-value can be adopted from IRC:SP:76. k-values for different combinations of DLC subbase (with DLC having minimum 7-day compressive strength of 7 MPa) thicknesses laid over granular subbase consisting of separation and drainage layers can be adopted from **Table 4**. The contribution of granular subbase placed below the DLC layer can be ignored for estimating the effective modulus of subgrade reaction of the foundation. The values given in **Table 4** are based on the analysis given in the Pavement Design Guide AASHTO:1993 and an upper limit of 300 MPa/m is recommended considering the loss of subgrade support caused by heavy traffic.

Table 3 k-Values for Granular and Cement Treated Subbases

k-Value of Subgrade (MPa/m)	Effective k (MPa/m) of Untreated Granular Subbase of Thickness (mm)			Effective k (MPa/m) of Cement Treated Subbase of Thickness (mm)*		
	150	225	300	100	150	200
28	39	44	53	76	108	141
56	63	75	88	127	173	225
84	92	102	119	-	-	-

Note: 100 pci = 2.77 kg/cm³ = 27.2 MPa/m.* adapted from Portland Cement association

Table 4 k-Values for Dry Lean Concrete Subbase

k-value of Subgrade (MPa/m)	21	28	42	48	55	62
Effective k for 100 mm DLC, (MPa/m)	56	97	166	208	278	300
Effective k for 150 mm DLC, (MPa/m)	97	138	208	277	300	300

* **Note:**The above k values are extrapolated from AASHTO-1993.The maximum recommended value is 300 MPa/m

Note: 100 pci = 2.77 kg/cm³ = 27.2 MPa/m

5.7.5 Separation Layer Between DLC and Concrete Slab

The interface layer between the concrete slab and the DLC layer can be made smooth to reduce the inter layer friction thereby allowing relative movement between the slab and DLC layer and prevent reflection cracking in the pavement slab. A de-bonding interlayer of polythene sheet white or transparent having a minimum thickness of 125 micron is recommended as per the current practice in India. Wax based compound in place of plastic sheet has popularly been used with success in most countries including India in one of the National Highway projects. Bituminous concrete 2 shown in **Fig. 1(b)** is another option. The international practice on bond breaking interlayer is described in **Appendix-II**.

5.8 Concrete Strength

5.8.1 Flexural strength of concrete is required for the purpose of design of concrete slab. Flexural strength can be obtained after testing the concrete beam as per procedures given in IS: 516. Alternatively, it can be derived from the characteristic compressive strength of concrete as per IS 456-2000 using the following relationship:

$$F_{cr} = 0.7 \times \sqrt{f_{ck}}$$

Where,

F_{cr} = flexural strength (modulus of rupture), MPa

f_{ck} = characteristic compressive cube strength of concrete, MPa

5.8.2 Concrete mix design is usually based on 28 days strength. In the case of concrete pavement, 90 days strength for thickness design can be permitted in view of the fact that

(i) the concrete pavement is opened to traffic long after the construction (ii) the number of repetitions of load is very small during initial period of 90 days even if the pavement is opened to traffic after 28 days (iii) cumulative fatigue damage of concrete is very low during the first 90 days and (iv) the stress analysis is done for a terminal condition of the pavement slab when load transfer efficiencies of transverse and tied concrete shoulder joints are low. Increasing the 28 days flexural strength by a factor of 1.10 may be used to get 90 days strength. In no case should 28 days flexural strength of pavement quality concrete be less than 4.5 MPa.

5.8.3 Target mean flexural strength to be achieved while designing the Mix should be such that there is 95 percent probability that the characteristic strength would be achieved when the Mix is produced in the field (confidence level = 5%).

The target mean flexural strength is given by the following equation

$$f'_{cr} = f_{cr} + Z_a \sigma \quad \dots (4)$$

where,

- f_{cr} = characteristic flexural strength at 28 days, MPa
- f'_{cr} = target mean flexural strength at 28 days, MPa
- Z_a = a factor corresponding to the desired confidence level, which is 1.96 for 5% confidence level
- σ = standard deviation of field test samples, MPa

Modulus of elasticity and Poisson's ratio of concrete

5.8.4.1 The modulus of elasticity (E) and Poisson's ratio (μ) of cement concrete vary with concrete materials and strength. The elastic modulus increases with increase in strength, and Poisson's ratio decreases with increase in the modulus of elasticity. While it is desirable that the values of these parameters are ascertained experimentally for the concrete mix and for the materials actually to be used in the construction, this information may not always be available at the design stage. A 25% variation in E and μ values will have only a marginal effect on the flexural stresses in the pavement concrete. Following values were adopted for stress analysis for the concrete with 28-day flexural strength of 4.5 MPa (4.95 MPa for 90-day strength).

Modulus of elasticity of concrete, E = 30,000 MPa

Poisson's ratio, μ = 0.15

5.8.5 *Coefficient of Thermal Expansion*

The coefficient of thermal expansion of concrete (α) is dependent to a great extent on the type of aggregates used in concrete. However, for design purpose, a value of $\alpha = 10 \times 10^{-6}/^{\circ}\text{C}$ is adopted.

5.8.6 *Fatigue Behaviour of Cement Concrete*

5.8.6.1 Due to repeated application of flexural stresses by the traffic loads, progressive fatigue damage takes place in the cement concrete slab in the form of gradual development of micro-cracks especially when ratio between the applied flexural stress and the flexural strength of concrete is high. This ratio is termed as Stress Ratio (SR). If the SR is less than

0.45, the concrete is expected to sustain infinite number of repetitions. As the stress ratio increases, the number of load repetitions required to cause cracking decreases. The relation between fatigue life (N) and stress ratio is given as:

$$N = \text{unlimited for } SR < 0.45$$

$$N = \left[\frac{4.2577}{SR - 0.4325} \right]^{3.268} \quad \text{When } 0.45 \leq SR \leq 0.55 \quad \dots (5)$$

$$\log_{10} N = \frac{0.9718 - SR}{0.0828} \quad \text{For } SR < 0.55 \quad \dots (6)$$

5.8.6.2 These fatigue criteria are used for checking the adequacy of the pavement slab on the basis of Miner’s hypothesis. It is assumed that the fatigue resistance not consumed by repetitions of one load is available for repetitions of other loads. The above fatigue criteria developed by Portland Cement Association (PCA, 1984) are conservative and these can be used for the analysis of bottom-up and top-down cracking. The validity of the PCA fatigue equations in the light of recent developments is discussed in **Appendix III**.

6 DESIGN OF SLAB THICKNESS

6.1 Critical Stress Condition

6.1.1 In-service cement concrete pavements are subjected to stresses due to a variety of factors acting simultaneously. The severest combination of different factors that induce the maximum stress in the pavement will give the critical stress condition. The flexural stress due to the simultaneous application of traffic loads and temperature differentials between the top and bottom fibres of a concrete slab is considered for design of pavement thickness. The effect of moisture change is opposite to that of temperature change and is not normally considered critical to thickness design. The flexural stress at the bottom layer of the concrete slab is the maximum during the day hours when the axle loads act midway on the pavement slab while there is a positive temperature gradient as illustrated in **Fig. 3 and 4**. This condition is likely to produce Bottom-Up Cracking (BUC).

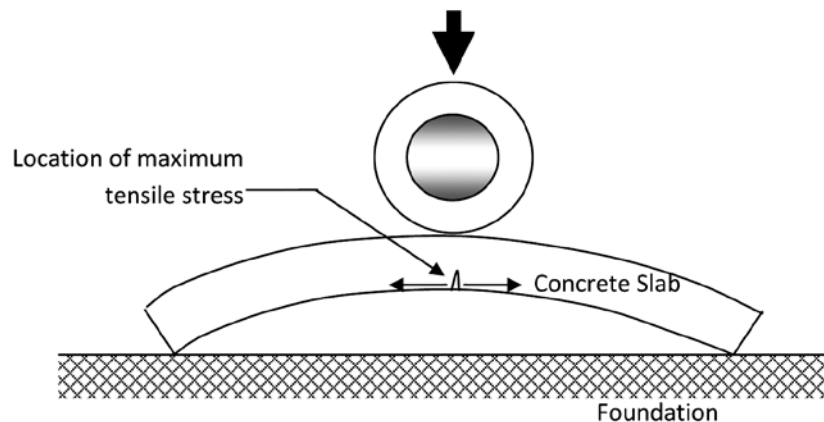


Fig. 3 Axle Load Placed in the Middle of the Slab during Mid-Day

6.1.2 Locations of points of maximum flexural stress at the bottom of the pavement slab without tied concrete shoulder for single, tandem and tridem axles are shown in **Fig. 4**. The

tyre imprints are tangential to the longitudinal edge. For tied concrete shoulders also, the maximum stress occurs at the same locations. Single axles cause highest stress followed by tandem and tridem axles respectively. Spacing between individual axles for tandem and tridem axles varies from 1.30 m to about 1.40 m. There is practically no difference in stresses for axle spacing between 1.30 m and 1.40 m. A spacing of 1.30 m has been used in these guidelines for stress computation.

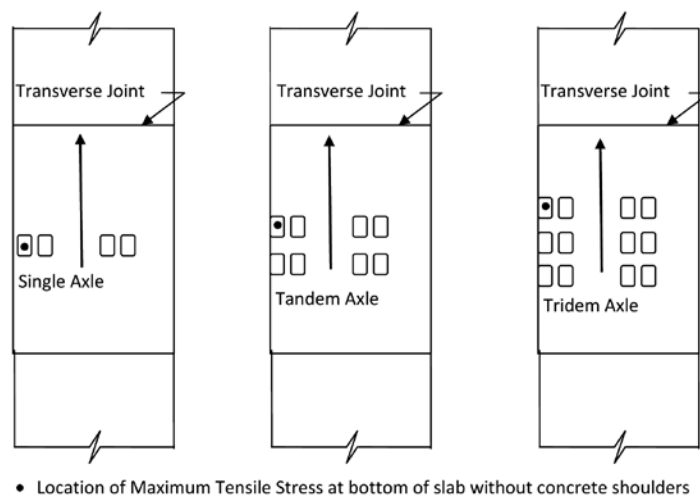


Fig. 4 Placement of Axles for Maximum Edge Flexural Stress at Bottom of the Slab without Concrete Shoulders

6.1.3 During the night hours, the top surface is cooler than the bottom surface and the ends of the slab curl up in a concave shape resulting in loss of support for the slab as shown in **Fig. 5**. Due to the restraint provided by the self-weight of concrete and by the dowel connections, temperature tensile stresses are caused at the top. **Fig. 5** shows the placement of axle loads close to transverse joints when there is negative temperature gradient during night period causing high flexural stresses in the top layer leading to top-down cracking. Positioning of axles of different configurations on the slab with successive axles placed close to the transverse joints is shown in **Fig. 6**. These axle positions can initiate Top-Down Cracking (TDC) during the night hours when the pavement has the tendency to curl up. Built-in permanent curl induced during the curing of the concrete slab further aggravates the problem.

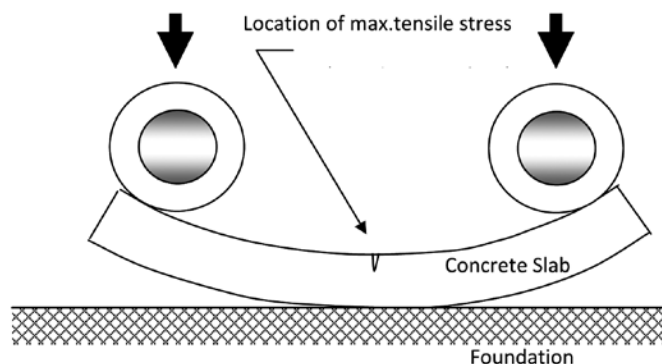


Fig. 5 Placement of Two Axles of a Commercial Vehicle on a Slab Curled During Night Hours

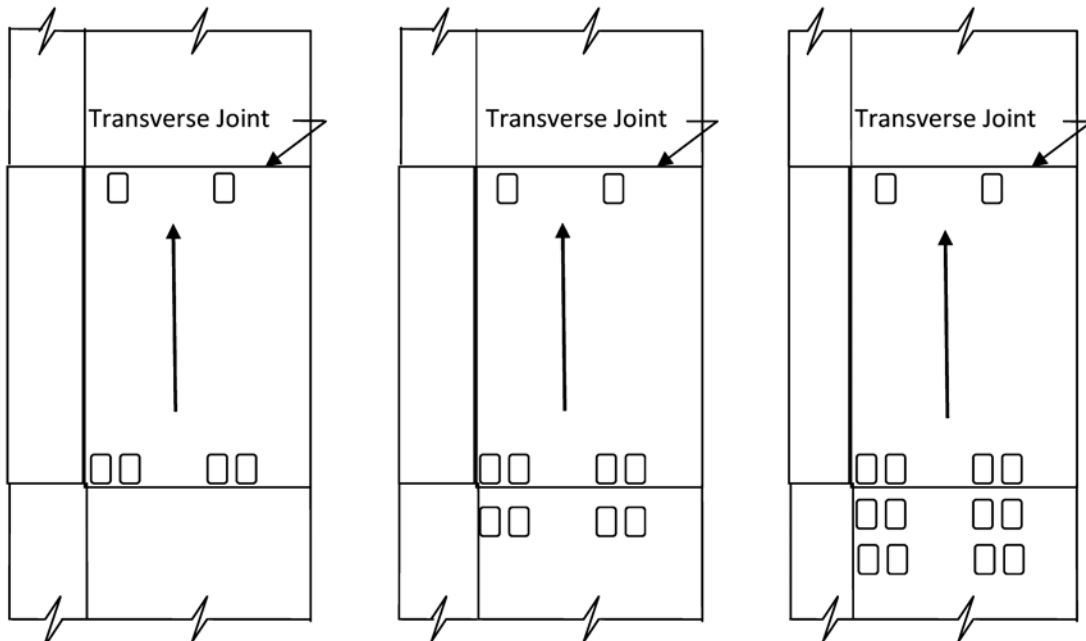


Fig. 6 Different Axle Load Positions Causing Tensile Stress at the Top Fibre of the Slab with Tied Concrete Shoulder

6.2 Calculation of Flexural Stress

6.2.1 Since the loads causing failure of pavements are mostly applied by single, tandem, tridem and other multiple axles, stresses should be determined for the conditions illustrated in **Figs. 3 to 6**. The IITRIGID software used in IRC:58-2002 for the computation of flexural stress in the edge region due to single and tandem axle loads was based on Picket and Ray (1951)'s work on computation of stresses in infinite slabs. The software is still valid for computation of load stress in the edge region of pavements without any concrete shoulder without any temperature gradient. Finite Element Method (FEM) is more appropriate for stress computation for a wide variety of load, temperature, geometry and boundary conditions. Finite element analysis has been carried out using IITSLAB-II, a software developed at IIT Kharagpur, to compute flexural stress due to the combined action of load (single, tandem and tridem axles) and different temperature differentials (positive and negative).

6.2.2 For a single axle load of 200 kN and zero temperature differential (**Fig. IV-30, Appendix IV**), it can be seen that flexural stresses decrease with increase in k-values for all thicknesses. If there is a positive temperature differential of 17°C, the same axle load causes higher flexural stresses in thicker slabs (**Fig. IV-45**) for higher k-values. For a thickness in the region of 270 mm, there is practically no effect of modulus of subgrade reaction on flexural stresses. Increasing the subgrade modulus to high values does not help in thickness design due to high curling stresses caused by a stiff support.

6.2.3 The following combinations of pavements and loading were considered for the analysis of bottom-up and top-down cracking. For bottom-up cracking case, the combination of load and positive non-linear temperature differential (**Fig. 3**) has been considered whereas for top-down cracking analysis, the combination of load and negative linear temperature

differential (**Fig. 5**) has been taken. For bottom-up cracking analysis, single/tandem axles have been placed on the slab in the positions indicated in **Fig. 4**. In bottom-up cracking case, single axle load causes the largest edge stress followed by tandem and tridem axles. Since the stresses due to tridem axles are small, they were not considered for stress analysis for bottom-up cracking case. For top-down cracking analysis, the load position considered for analysis is as shown in **Fig. 6**. As indicated in the figure, only one axle of single/tandem/tridem axle units has been considered for analysis in combination with front axle. Front axle weight has been assumed to be 50% of the weight of one axle of the rear axle unit (single/tandem/tridem) for analysis.

6.2.4 *Analysis has been done for the Following Cases.*

Bottom-up Cracking

- Pavement with tied concrete shoulders for single rear axle
- Pavement without concrete shoulders for single rear axle
- Pavement with tied concrete shoulders for tandem rear axle
- Pavement without concrete shoulders for tandem rear axle

Top-down Cracking

- Pavements with and without dowel bars having front steering axle with single tyres and the first axle of the rear axle unit (single/tandem/tridem) placed on the same panel as depicted in **Fig. 6**.

6.2.5 For heavy traffic conditions, dowel bars are usually provided across transverse joints for load transfer. Tied concrete shoulders are also necessary for high volume roads. However, for smaller traffic volumes smaller than 450 commercial vehicles/day, tied concrete shoulders and dowel bars are not generally warranted. The results of the Finite Stress Analysis has been used for the computation of flexural stresses for pavements with and without (a) dowelled transverse joints and (b) tied concrete shoulders. Terminal Load Transfer Efficiencies (LTE) for dowelled transverse joints and tied joints between the slab and concrete shoulder have been taken as 50% and 40% respectively for stress computation though MEPDG guide (NCHRP, 2004) recommends LTE values of 60% and 50% respectively for dowelled and tied joints. This has been done to make design more conservative considering the overloading in India.

6.2.6 The results of Finite Element Analysis of a large number of concrete pavements with different pavement configurations subjected to various combinations of axle loads and temperature differentials have been presented in the form of charts in **Appendix IV**. The slab size is taken as 3.5 m x 4.5 m. The charts can be used to obtain the edge flexural stress caused by a specified magnitude of single/tandem axle (positioned as indicated in **Fig. 4**) in combination with a specified positive temperature differential for a given pavement structure. Linear interpolation can be done for obtaining stresses for intermediate loads and temperatures from the charts given in **Appendix IV**.

6.2.7 The finite element analysis results have been used to develop regression equations for estimation of the flexural tensile stress for bottom-up as well as top-down cracking cases. While a single regression equation was found to be adequate for estimation of flexural tensile stress in the slab for top-down cracking case, separate equations were developed for the bottom-up cases for different pavement types and foundation strengths. The regression equations are presented in **Appendix V**.

6.2.8 Designers can develop their own excel sheets for analysis and design using the regression equations given in **Appendix V**. A programmed excel file is available with the guidelines in a compact disc which can be used for thickness design for different trials.

6.3 Cumulative Fatigue Damage Analysis

6.3.1 For a given slab thickness and other design parameters, the pavement shall be checked for cumulative bottom-up and top-down fatigue damages. For bottom-up cracking, the flexural stress at the edge due to the combined action of single or tandem rear axle load and positive temperature differential is considered. This stress can either be selected from the stress charts given in **Appendix IV** or by using the regression equations given in Appendix V. Charts explain clearly the interplay of thickness, modulus of subgrade reactions, axle loads and temperature differentials. Similarly, for assessing the top-down fatigue damage caused by repeated cycles of axle loads and negative temperature differential, flexural stress can be estimated using the equation given in **Appendix V**.

6.3.2 The flexural stress is divided by the design flexural strength (modulus of rupture) of the cement concrete to obtain Stress Ratio (SR). If the Stress Ratio (SR) is less than 0.45, the allowable number of cycles of axle load is infinity. For stress ratio values greater than 0.45, allowable repetitions of different axle load groups can be estimated using equations 5 and 6. The concrete slab undergoes fatigue damage through crack growth induced by repeated cycles of loading. Total cumulative fatigue damage caused to the slab during its service life should be equal to or less than one.

6.3.3 Analysis indicates that contribution to CFD for bottom-up cracking is significant only during 10 AM to 4 PM because of higher stresses due to simultaneous action of wheel load and positive temperature gradient. Thus, the day hour traffic during the six hour period is to be considered for bottom-up cracking analysis. For the top-down cracking analysis, only the CFD caused during the period between 0 AM and 6 AM is significant. Hence, the six hourly night time traffic may be considered for computing CFD for top-down cracking analysis. If the exact proportions of traffic expected during the specified six-hour periods are not available, it may be assumed that the total night time traffic is equally distributed among the twelve night hours. Similarly, the total day time traffic may be assumed to be distributed uniformly during the twelve day hours. The Cumulative Fatigue Damage (CFD) expressions for bottom-up and top-down cracking cases are given by Equations 7 and 8 respectively. The time indicated in the equations will vary depending on the geographical location of the project site but the duration of each period may practically remain the same.

$$CFD(BUC) = \sum_i^j \frac{n_i}{N_i} (10AM \text{ to } 4PM) \quad \dots (7)$$

$$CFD(TDC) = \sum_i^j \frac{n_i}{N_i} (0AM \text{ to } 6AM) \quad \dots (8)$$

Where,

N_i = allowable number of load repetitions for the i^{th} load group during the specified six-hour period

n_i = predicted number of load repetitions for the i^{th} load group during the specified six-hour period

j = total number of load group

6.3.4 Design Criterion of Rigid Pavements

6.3.4.1 If the sum of cumulative fatigue damages (i) due to wheel load and curling stresses at the bottom and (ii) wheel load and curling stresses at the top is less than 1, the pavement is safe. In other words, a pavement is deemed to have failed if sum of cumulative damages is greater than one.

Thus if $CFD(BUC) + CFD(TDC) \leq 1$, the pavement is safe from large scale cracking.

The design thickness may be increased by 10 mm to (i) to permit two retexturing and (ii) grinding to rectify faulting during the service life.

6.3.4.2 India is a large country with varied climate in different regions. The recommendations for six hourly traffic for fatigue analysis for day and night hours may not be valid for all regions. Designers are recommended to carry out hourly or two hourly fatigue damage analysis for all the twenty four hours to examine the safety of the pavement for which hourly temperature data for pavement is necessary for analysis.

6.3.4.3 Many well designed concrete pavement display cracks within a short period of five years due to loss of support caused by permanent deformation and erosion of GSB and subgrade in the presence of water and heavy loads, locked dowel bars, shrinkage cracks etc. rather than fatigue cracks caused by structural deficiency. These factors deserve careful consideration for a satisfactory performance of pavements.

6.4 Erosion Consideration

6.4.1 AASHO Road Test indicated that erosion of the foundation is an important mode of failure in concrete pavements in addition to fatigue cracking and must be considered in the design and maintenance. Analysis of the AASHO road test data by Portland Cement Association (PCA, 1980) suggests that the erosion of the foundation was caused largely by tandem and multi-axle vehicles in the presence of moisture and that single axles were mostly responsible for fatigue cracking of slabs. Since tandem, tridem and multi-axle vehicles form a large percentage of the total commercial vehicles on highways in India, erosion data along with the condition of GSB and the subgrade need to be collected for revision of the future guidelines whenever there is a major rehabilitation such as panel replacement. The DLC

subbase recommended in the guidelines is non-erodible but very heavy commercial vehicles may cause erosion of granular materials and subgrade soils in the presence of water that might enter from median, cracks and joints. This is one of the reasons for longitudinal cracking along the wheel path on many highways. Record of pavement performance data including loss of erodible material from untreated subgrade and subbase of the concrete pavements will be necessary for modification of the guidelines since erosion is dependent on the quality of subbase and subgrade, climatic conditions as well as the gross weight of the vehicles. Ground Penetrating Radar or Falling Weight Deflectometer can indicate the extent the voids formed below a DLC layer.

6.5 Drainage Layer

6.5.1 New pavements are practically impermeable but with the passage of time, the joints, median and cracks allow the water to infiltrate into the pavement. Entrapped water in the subgrade and granular subbase causes erosion of the foundation material under dynamic loading due to pulsating pore water pressure generated by moving heavy tandem and tridem axle loads. It may be mentioned that pavement deflection due to heavy tandem and tridem axles can be as high as 1.0 mm which may result in the formation of voids below the pavement due to the permanent deformation of the foundation material. Presence of excess moisture accumulated in the unbound foundation layers due to infiltration or due to thawing in snow-bound regions is conducive for development of permanent deformation in these layers being rendered soft due to excess moisture.

6.5.2 To facilitate quick disposal of water that may enter into the subgrade, a drainage layer together with a separation layer may be provided beneath the DLC subbase throughout the road width. The separation layer prevents fines from pumping up from the subgrade to the drainage layer. It also provides a platform for the construction of the drainage layer. The amount of water infiltrating into the pavement should be assessed and a drainage layer having the required permeability needs to be designed. The minimum permeability of 300 m/day or greater is recommended. It is essential to design the drainage layer appropriately for major highways in areas having annual rainfall in excess of 1000 mm. Local experience is the best guide. The drainage layer can be treated with 2 to 2.5% bitumen/cement or 2.5 to 3% bitumen emulsion to obtain a stable platform to permit the movement of construction traffic without any sideways displacement and/or shoving of the open graded aggregates. If granular layers are not needed because of high strength subgrade, synthetic geo-composite can be used for separation and drainage with a reduced thickness of levelling course of granular layer over the subgrade.

6.5.3 On an examination of use of different Granular Sub Bases (GSB) given in CI 401.2.2 of MORTH Specifications 5th Revision as a drainage layer, laboratory tests indicate that the GSB have permeability values less than 12 metre per day which is indicative of their poor drainage capability and hence they are not suitable for drainage layers. Permeability of a number of gradations of drainage layers as per the international practice are shown in **Appendix VI**. The gradings of granular subbase of MORTH Specifications may be modified to correspond to one of the gradings given in **Appendix VI** so that a permeability of more

than 300 m/day is obtained for high volume highways. Thickness of the drainage layer will depend upon the permeability as well as the quantity of infiltration of water into the pavement. Stabilisation with cement or bitumen emulsion to provide the necessary stability may be necessary for open graded drainage layer. Engineers may use their judgement about stabilizing the drainage layer. Laboratory tests should be done to verify that the drainage layer has the required permeability. A discussion on gradations parameters such as Uniformity coefficient, D_{60} and D_{10} parameters which control permeability of aggregates to a great extent is given in **Appendix VI** where D_{60} and D_{10} are particle sizes corresponding to 60% and 10% passing and UC is the ratio of D_{60} and D_{10} . Los Angeles abrasion value of the aggregates used for drainage layer should be less than 40% to limit degradation during compaction. Field tests conducted by Ridgeway (1976) in USA indicated that it is the duration of the rainfall rather than its intensity that is critical for infiltration of water into the pavement. It was found that the infiltration rate (I_c) through the joints/cracks was 0.223 m³/day/m and this value can be used for design of drainage layer. The infiltration rate per unit area, q_i ((m³/day/m²), can be expressed as

$$q_i = I_c \left(\frac{N_c}{W_p} + \frac{W_c}{C_s W_p} \right) + K_p \quad \dots (9)$$

where,

- I_c = crack infiltration rate, m³/day/m
- N_c = number of longitudinal joints/cracks
- W_p = width of pavement subjected to infiltration, m
- W_c = length of the transverse cracks or joints, m
- C_s = spacing of transverse joints, m
- K_p = rate of infiltration through un-cracked pavement surface (m³/day/m²), which is almost negligible for cement concrete.

Details of gradations of the drainage layers as per international practice and an example of design of drainage layer are given in **Appendix VI**.

6.6 Tied Concrete Shoulder and Widened Outer Lane

6.6.1 Tied cement concrete shoulders are recommended to protect the edge of high volume highway pavements. These guidelines provide for design of concrete pavements with tied concrete shoulders for high volume roads. Widening of outer lanes of concrete pavement by 0.5 m to 0.6 m can be adopted for two-lane two-way roads to reduce the flexural stresses in the wheel path region. Analysis of typical concrete pavements shows that provision of a widened outer lane functioning as a monolithic concrete shoulder reduces the edge flexural stress by 20 to 30%. This will result in reduction of pavement thickness. The total quantity of concrete may remain the same as that without shoulder. Rough texture, if provided to the widened part, will bring in additional safety to vehicles particularly during night hours. Thicknesses of pavements with widened outer lane as well as tied concrete shoulder are almost the same. An example of designing concrete pavements with widened outer lanes has been included in **Appendix VII**.

6.7 Bonded Rigid Pavement

6.7.1 A concrete pavement laid over a sustained slope on ghat sections may slip if a debonding layer of polythene membrane is provided between the concrete slab and Dry Lean Concrete (DLC). PQC may be laid directly over DLC and the monolithic action of the two layers can be exploited to reduce the pavement thickness. The DLC surface may be made rough with wire brush within 3 to 6 hours of placement and a bonding agent of water and cement slurry may be applied over the surface before laying of PQC. For monolithic pavements, transverse joints may be formed in the DLC layer also by cutting grooves to 1/3rd of its depth exactly at the same locations where transverse joints are to be provided in the upper PQC layer in order to prevent random reflection cracking of upper layer due to cracks in the un-jointed DLC layer. This is recommended by Portland Cement association. An example of design of bonded rigid pavement is given in **appendix VII**. There is no limit on the strength of DLC in such cases and 7-day compressive strength of the DLC layer in bonded rigid pavement should not be less than 10 MPa.

6.7.2 Finite Element can be used for design of bonded pavement. The method of equivalent flexural stiffness is used in the guidelines. A granular subbase of 200 mm to 250 mm thickness may be provided below the DLC layer for bonded concrete pavement for separation and drainage. The effective modulus of subgrade reaction of the subgrade-granular subbase combination can be estimated from **Table 3**. Total slab thickness (h) over the granular layer is worked out for the given traffic and other design parameters. A part of the PQC of thickness 'h' is replaced with 150 mm of DLC so that the combined flexural stiffness of the pavement slab layer (thickness of h₁) and DLC layer (thickness of h₂) is equal to or greater than the flexural stiffness of the slab of thickness 'h' over the granular layer. Flexural stiffness of a slab of thickness, h, is given as

$$\frac{EI}{1-\mu^2} = \frac{Eh^3}{12(1-\mu^2)} \quad \dots (10)$$

Where,

E, μ, I, h are the modulus of elasticity, Poisson’s ratio, moment of inertia and thickness of the slab respectively. If the design thickness of the slab considering slab over a granular layer and subgrade is “h”, and if it is proposed to provide a DLC layer of thickness “h₂” bonded to the concrete slab of thickness “h₁”, the thickness of the concrete slab (h₁) can be obtained by equating the flexural stiffness of the design slab to the combined flexural stiffness of the DLC layer and concrete slab.

Fig. 7 shows the bonded section with neutral axis in the pavement slab.

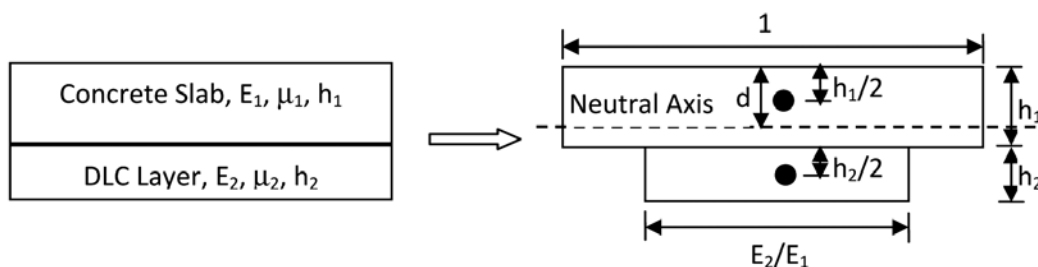


Fig. 7 Concept used for Obtaining Combined Flexural Stiffness

The neutral axis depth 'd', shown in **Fig. 7**, can be computed using Equation 11.

$$d = \frac{0.5(h_1^2) + \left(\frac{E_2}{E_1}\right)h_2(h_1 + 0.5h_2)}{h_1 + \left(\frac{E_2}{E_1}\right)h_2} \quad \dots 11$$

The flexural stiffnesses of the two layers can be determined using Equations 12 and 13 respectively.

$$\text{Flexural stiffness (1, PQC)} = \frac{E_1 \left(\frac{h_1^3}{12} + h_1(d - 0.5h_1)^2 \right)}{1 - \mu_1^2} \quad \dots 12$$

$$\text{Flexural Modulus (2, DLC)} = \frac{E_2 \left[\frac{\left(\frac{E_2}{E_1}\right)h_2^3}{12} + \left(\frac{E_2}{E_1}\right)h_2 \left(h_1 + \frac{h_2}{2} - d \right)^2 \right]}{(1 - \mu_2^2)} \quad \dots (13)$$

6.7.3 The combined flexural stiffness of the two layers should be equal to or more than the requirement of design flexural stiffness given by equation 10. 28-day strength of DLC having a 7-day compressive strength of 10 MPa may be close to 13.6 MPa. The 'E' of DLC as per IS:456 (2000) will be about 18439 MPa ($5000 (F_{ck})^{0.5}$). However, as thin DLC layer is expected to crack due to shrinkage, contraction and the construction traffic because of its lower tensile strength, the effective modulus of the DLC layer may be taken as $E = 1000 \times f_{ck} = 13600$ MPa (AUSTROADS, 2004). Poisson's ratio of DLC may be taken as 0.2.

6.8 Anchor Beam and Terminal Slab

6.8.1 During the hot season, the concrete slabs expand and this will result in the build-up of horizontal thrust on dirt-wall/abutment of structures. To contain this thrust, RCC anchor beams are generally provided in the terminal slab. One or more expansion joints may also be provided to accommodate the expansion. The terminal slab, therefore, will have to be reinforced to strengthen it. The details of the anchor beam and terminal slab are discussed in IRC:15.

6.9 Recommended Procedure for Slab Design

6.9.1 The following steps may be followed for design. Examples of design of different categories of concrete pavements using the current guidelines are given in **Appendix VII**.

Step 1 : Stipulate design values for the various parameters

Step 2 : Select a trial design thickness of pavement slab

Step 3 : Compute the repetitions of axle loads of different magnitudes and different categories during the design life

- Step 4 : Find the proportions of axle load repetitions operating during the day and night periods
- Step 5 : Estimate the axle load repetitions in the six-hour-period during the day time. The maximum temperature differential is assumed to remain constant during the 6 hours for analysis of bottom-up cracking
- Step 6 : Estimate the axle load repetitions in the six-hour period during the night time. The maximum negative temperature differential during night is taken as half of day-time maximum temperature differential. Built in negative temperature differential of 5°C developed during the setting of the concrete is to be added to the temperature differential for the analysis of top-down cracking. Only those vehicles with spacing between the front (steering) axle and the first rear axle less than the transverse joint spacing need to be considered for top-down cracking analysis.
- Step 7 : Compute the flexural stresses at the edge due to the single and tandem axle loads for the combined effect of axle loads and positive temperature differential during the day time. Determine the stress ratio (Flexural stress/Modulus of Rupture) and evaluate the Cumulative Fatigue Damage (CFD) for single and tandem axle loads.
- Step 8 : Compute the maximum flexural stress in the top surface of the pavement slab with the front axle near the approaching transverse joint and the rear axle close to the following joint in the same panel under negative temperature differential. Determine the stress ratio and evaluate the CFD for different axle loads for the analysis of top-down cracking.
- Step 9 : Sum of CFD for the BUC and TDC. If the sum is less than 1.0, the pavement slab is safe against fatigue cracking.

6.9.2 The entire design process is programmed on an excel sheet and it is included in a CD enclosed with these guidelines. This will enable the designer to make several trials conveniently. The designer has to provide modulus of the subgrade reaction of the foundation supporting the pavement slab, 28 day strength of concrete, temperature differential; traffic data such as rate of traffic growth, axle load spectrum, proportion of single, tandem and tridem axles, proportion of trucks with wheel base less than transverse joint spacing (say 4.5 m). All relevant traffic and material data are inputs to the excel sheet.

6.9.3 It is worth noting that concrete strength increases with age. The excel sheets provide designs by considering 90-day strength of paving concrete (The minimum 28 day flexural strength is taken as 4.5 MPa). Any other strength including that of high performance concrete can be the input. 90 day strength can safely be used because of the following considerations.

- i) Design traffic for edge stress calculation is taken as 25% against only 2 to 3% axles that actually move near the edge.

- ii) Assumption of low terminal load transfer efficiency at transverse and longitudinal joints for stress calculation. Load induced flexural stress in the early years of pavements will only be a fraction of computed stress.
- iii) The conservative assumption of highest temperature differential being constant for 6 hours both during the day and night hours throughout the design period leads to high computed CFD.
- iv) Conservative recommendation of dowel bar design. There is hardly any gap between the concrete slabs at transverse joints due to the absence of expansion joints but a gap of 5 mm is assumed in the design of dowel bar.
- v) The warping due moisture gradient across the depth of the concrete is opposite to that of the curling due to the temperature gradient and hence the curling caused by temperature gradient is nullified to some extent by the warping caused by the moisture gradient.

7 DESIGN OF JOINTS

7.1 Spacing and Layout

7.1.1 Great care is needed in the design and construction of joints in cement concrete pavements, as these are critical locations having significant effect on the pavement performance. The joints also need to be effectively sealed, and maintained well.

7.1.2 Cement Concrete Pavements have different types of transverse joints given as:

- i) Contraction joints
- ii) Construction joints
- iii) Expansion joint
- iv) Longitudinal joint

7.1.3 Contraction joints are transverse joints which relieve the tensile stresses in concrete pavements. The joint spacing of a concrete pavement depends upon the type of coarse aggregates and the average temperature fluctuation in different seasons. The spacing of contraction joints should be limited to 4.5 m to prevent top-down cracking during the night hours.

7.1.4 Expansion joints are transverse joints to allow expansion of concrete slab due to rise in average temperature in summer months. These joints are difficult to maintain and they get filled up with dirt and other incompressible materials causing locking of the joints and preventing expansion of concrete slabs. They are, therefore, no longer in use except near permanent structure like bridges and culverts which may be damaged by the thrust of the expanding concrete slab due to rise in temperatures.

7.1.5 Construction joints should, as far as possible, be placed at the location of contraction joints except in case of emergency when a key joint may be used.

7.1.6 Longitudinal joints are required in pavements of width greater than 4.5 m to allow for transverse contraction and warping.

7.2 Load Transfer at Transverse Joints

7.2.1 Load transfer to relieve part of the load stresses in edge and corner regions of pavement slab at transverse joints is provided by means of mild steel round dowel bars. In coastal and high rainfall areas, coated/corrosion resistant dowel bars are often used to provide long term load transfer. The coating may be zinc or lead based paint or epoxy coating. Dowel bars enable good riding quality to be maintained by preventing faulting at the joints. For general provisions in respect of dowel bars, stipulations laid down in IRC:15, may be followed. More dowel bars may be provided under the wheel path of heavy commercial vehicles in the light of past experience. Designer may use his/her discretion after a study of the traffic pattern.

7.2.2 From the experience gained all over the world, it is found that it is only the bearing stress in the concrete that is responsible for the performance of dowel bars at the joints. High concrete bearing stress can fracture the concrete surrounding the dowel bars, leading to the looseness of the dowel bar and the deterioration of the load transfer system with eventual faulting of the slab. Larger diameter dowel bars are found to provide better performance. Maximum bearing stress (F_{bmax}) between the concrete and dowel bar is obtained from equation 14.

$$F_{bmax} = \frac{k_{mds} P_t (2 + \beta Z)}{4\beta^3 EI} \quad \dots (14)$$

Where,

- β = relative stiffness of the bar embedded in concrete, $\text{mm}^{-1} = \sqrt[4]{\frac{k_{mds} b_d}{4EI}}$
- k_{mds} = modulus of dowel support, MPa/m
- b_d = diameter of the dowel, m
- z = joint width (5 mm for contraction joint and 20 mm for expansion joint), in mm
- E = modulus of the elasticity of the dowel bar, MPa
- I = moment of inertia of the dowel, mm^4
- P_t = load transferred by design dowel bar, kN

7.2.3 The modulus of dowel support ranges from 80,000 to 4,15,000 MPa/m. A typical value of 415,000 MPa/m may be adopted for design since only the fourth root of the k-value affects the computation of β .

7.2.4 Each dowel bar should be designed for the maximum load being transferred by it for the allowable bearing pressure. Equation 15, based on the expression given by the American Concrete Institute (ACI) Committee-225 may be used for calculation of the allowable bearing stress on concrete.

8 TIE BARS FOR LONGITUDINAL JOINTS

8.1 The longitudinal joint is expected to open up during the service period (in case of heavy traffic, expansive subgrades, etc.) and tie bars may be provided in accordance with the recommendation of IRC:15., For the sake of convenience of the designers the design procedure recommended in IRC:15 is given here.

8.2 Design of Tie Bars

8.2.1 The area of steel required per metre length of joint may be computed using equation 16.

$$A_s = \frac{bfw}{S_{st}} \quad \dots (16)$$

In which,

- A_s = area of steel in mm², required per m length of joint
- b = lane width in metres
- f = coefficient of friction between pavement and the subbase/base (usually taken as 1.5)
- W = weight of slab in kN/m² and
- S_{st} = allowable working stress of steel in MPa

8.2.2 The length of any tie bar should be at least twice that required to develop a bond strength equal to the working stress of the steel. The formula for estimating the length of tie bar is given as equation 17.

$$L = \frac{2 S_{st} A_{cs}}{B^* P_{ptb}} \quad \dots (17)$$

In which:

- L = length of tie bar (mm)
- S_{st} = allowable working stress in steel (MPa)
- A_{cs} = cross-sectional area of one tie bar (mm²)
- P_{ptb} = perimeter of tie bar (mm), and
- B^* = permissible bond stress of concrete (i) for deformed tie bars = 2.46 MPa, (ii) for plain tie bars – 1.75 MPa.

8.2.3 Reinforced Cement Concrete needs to be provided in pavement panels in curved portions of radius less than 45 m and at underpasses on steep gradients, and for slabs having man-hole cover slab having L/B (length to breadth) ratio more than 1.5 and in other similar situations.

8.2.4 To permit warping at the joint, the maximum diameter of tie bars may be limited to 16 mm, and to avoid concentration of tensile stress they should not be spaced more than 750 mm apart. The calculated length, L, may be increased by 50 to 80 mm to account for any

inaccuracy that may occur in the placement during construction. An example of design of tie bar is given in **appendix IX**.

8.2.5 Typical tie bar details for use at central longitudinal joint in double-lane rigid pavements with a lane width of 3.50 m are given in **Table 6**. The same specifications may be used for the tied concrete shoulder also.

Table 6 Details of Tie Bars for Longitudinal Joint of Rigid Pavements

Slab Thickness mm	Tie Bar Details				
	Diameter (d) mm	Max. Spacing, mm		Minimum Length, mm	
		Plain	Deformed	Plain	Deformed
150	8	330	530	440	480
	10	520	830	510	560
200	10	390	620	510	560
	12	560	900	580	640
250	12	450	720	580	640
300	12	370	600	580	640
	16	660	1060	720	800
350	12	320	510	580	640
	16	570	910	720	800

Note: The recommended details are based on the following values of different design parameters: $S_{st} = 125$ MPa for plain bars, 200 MPa for deformed bars; bond stress for plain bars = 1.75 MPa, for deformed bars = 2.46 MPa as per IRC:15. Tie bars deformed/plain shall conform to IS 1786 and IS 432 respectively.

9 REINFORCEMENT IN CONCRETE SLAB TO CONTROL CRACKING

9.1 Jointed reinforced concrete pavement is adopted for longer slabs with transverse joint spacing greater than 5.0. Reinforcement in concrete pavements, is intended to hold the cracked faces tightly together, so as to prevent opening of the cracks and to maintain aggregate interlock required for load transfer. It does not increase the flexural strength of unbroken slab when used in quantities which are considered economical.

9.2 Reinforcement in concrete slabs counteracts the tensile stresses caused by shrinkage and contraction due to temperature or moisture changes. The maximum tension in the steel across the crack equals the force required to overcome friction between the pavement and its foundation, from the crack to the nearest joint or free edge. This force is the greatest in the middle of the slab where the cracks occur first. Reinforcement is designed for this critical location. However, for practical reasons reinforcement is kept uniform throughout the length for short slabs.

9.3 The amount of longitudinal and transverse steel required per m width or length of slab is computed by the following formula:

$$A_s = \frac{L_d f W}{2 S_{st}} \quad \dots (18)$$

in which

A_s = area of steel in mm² required per m width or length of slab

- L_d = distance (m) between free transverse joints (for longitudinal steel) or free longitudinal joints (for transverse steel).
- f = coefficient of friction between pavement and subbase/base (usually taken as 1.5),
- W = weight of the slab in kN/m^2 and S_{st} = allowable working stress in steel in MPa (usually taken as 50 to 60 per cent of the minimum yield stress of steel)

9.4 Since reinforcement in the concrete slabs is not intended to contribute towards its flexural strength, its position within the slab is not important except that it should be adequately protected from corrosion. Since cracks starting from the top surface are more critical because of ingress of water when they open up, the general preference is for the placing of reinforcement about 50 to 60 mm below the surface. Reinforcement is often continued across longitudinal joints to serve the same purpose as tie bars, but it is kept at least 50 mm away from the face of the transverse joints and edge. In special cases, the steel reinforcement shall be provided in acute curve portions, under passes, steep gradients and slabs having man-hole covers and slabs having length to breadth ratio more than 1.5 and at acute angled corners.

10 WIDENING OF CONCRETE PAVEMENTS FROM 4 LANES TO 6 LANES

10.1 The rapid increase in traffic demands an up-gradation of existing concrete roads and additional lanes are to be added to accommodate the increasing traffic. In order to convert the existing 4-lane facility to 6-lane facility, one 3.5 m wide lane has to be added on each side of the pavement as illustrated in **Fig. 8**. The outer 1.5 m of the lane becomes part of the shoulder. The newly added lane should be tied to the shoulder of existing pavement. Tie bars can be placed by drilling holes along the longitudinal edge of shoulder of the existing pavement and epoxy grouting. The side faces may be chipped by mechanical equipment before concreting.

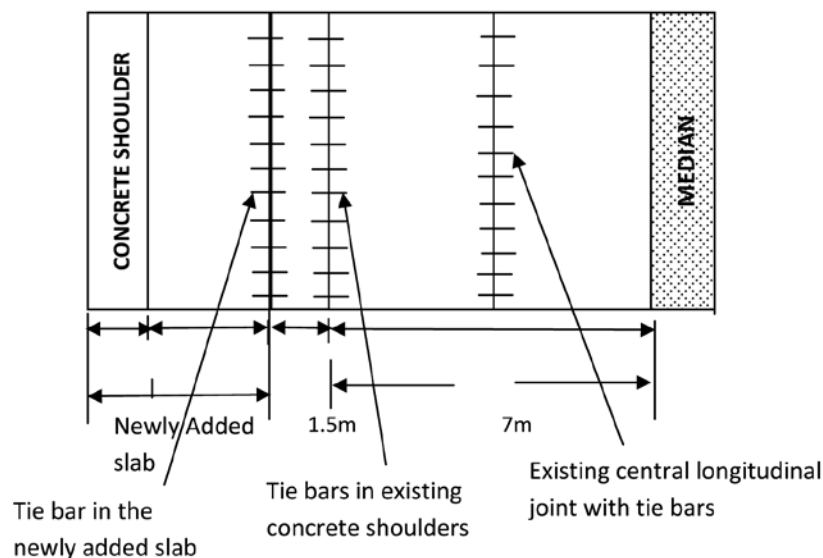


Fig. 8 Illustration of Addition of a Lane to an Existing Pavement

11 LIST OF REFERENCES

1. ASTM D4429-9, Standard test methods for CBR of soils in place.
2. http://www.pavementpreservation.org/concrete/Concrete_Pavement_Rehab.pdf
3. AASHTO (1993), 'AASHTO Guide for Design of Pavement Structures', American Association of State Highway and Transport Officials, Washington D.C.
4. AUSTROADS (2004), 'A Guide to the Structural design of Road Pavements' ARRB Transport Research Ltd, Australia.
5. PCA (1980) "Joint design for concrete highways and street pavements", Portland Cement Association USA.
6. NCHRP (2004), "2002 Design Guide of New and Rehabilitated Structures," Draft Final Report, NCHRP Study 1-37A, National Cooperative Highway Research Program, Washington, DC.
7. MORTH (2001) Specifications for Road and Bridge Works, Published by Indian Road Congress, New Delhi, 2001.
8. A.T. Papagiannakis, E.A. Masad (2008), 'Pavement design materials' John Wiley & Sons, Inc.
9. Ridgeway, H.H.(1976), 'Infiltration of water through pavement surface', Transportation Research Record, Transportation Research Board, 616, pp 98-100.
10. Cedergren H R (1974), 'Drainage of Highway and Airfield Pavements, John Wiley and Sons'.
11. IRC:SP:42-2014,'Guidelines of Road Drainage' Indian Roads Congress.
12. IRC:SP:50-2013,'Guidelines on Urban Drainage' Indian Roads Congress.
13. IS:4332 (Part IV) - 1968 Methods of test for stabilized soils part 4 wetting and drying, and freezing and thawing tests for compacted soil-cement mixtures.
14. Pickett, G, and G.K. Ray (1951). 'Influence Charts for Concrete Pavements', Transactions, ASCE, Vol. 116, pp. 49-73.
15. Croney, D. and Croney, P. (1992) 'The Design and Performance of road pavements' second edition, 1992, McGraw Hills International Series in Civil Engineering.
16. Patel Chintankumar K.(2010), 'Theoretical Investigation of Crack in Concrete Pavement with Tied Concrete Shoulder' M. Techthesis, Transportation Engineering section, Civil Engineering Department, IIT Kharagpur.
17. Jamshid Armaghani and Roger Schmitt (2006), 'Long-Life Concrete Pavements-The Florida Perspective' Int. Conf. on Long-Life Concrete Pavements Chicago, Illinois, USA.

18. V.V. Subramanian (1964), 'Investigation on Temperature and Friction Stresses in Bonded Cement Concrete Pavement' Ph. D thesis Transportation Engineering Section, Civil Engineering Department, IIT Kharagpur.
19. IRC:SP:76-2008, 'Tentative guide lines for Conventional, Thin and Ultra-Thin White Topping', Indian Roads Congress, New Delhi.
20. Kohn, S.D. and Tayabji,S.D.(2003), "Best Practice for Airport Portal and Cement Concrete Pavement Construction', IPRF-01-G-002-1, Washington, DC: Innovative Pavement Research Foundation. <http://www.iprf.org/products/main.htm>
21. Neville, A.M. and Brooks, J.J. (2010) "Concrete Technology", Prentice Hall.
22. IRC:SP:62-2014. Guidelines for the Design and Construction of Cement Concrete Pavement for Rural Roads.
23. IRC:15-2011, Standard Specifications and Code of Practice for Construction of Concrete Roads , Indian Roads Congress, New Delhi.
24. IRC:37-2012, Tentative Guidelines for Design of Flexible Pavements, Indian Roads Congress, New Delhi.
25. ASTM D559 - 03 Standard Test Methods for Wetting and Drying Compacted Soil-Cement Mixtures.
26. ASTM D560 - 03 Standard Test Methods for Freezing and Thawing Compacted Soil-Cement Mixtures.
27. Norbert Delatte, 'Concrete Pavement Design, Construction, and Performance' Taylor & Francis, 2008.
28. ASTM D6951-09, 'Standard Test Method for Use of the Dynamic Cone Penetrometer in Shallow Pavement Applications'.
29. American Concrete Pavement Association (1992), ' Design of Concrete Pavements for City Streets' Information Series Is184P, Skokie, USA.
30. Ghabchi, R., M. Zaman, Kamzee, H and Singh, Dharamveer (2014), 'Effect of shape Parameters and Gradation on Laboratory-Measured Permeability of Aggregate bases.' Int. J. of Geomechanics, ASCE, May 2014, ISSN 1532-3641/04014070-1 to 04014070-11.

APPENDIX - I

INTERNATIONAL PRACTICES ON THE USE OF CEMENTED SUBBASES FOR CEMENT CONCRETE PAVEMENTS

While a DLC subbase of 10 MPa, 7 day average compressive strength has been the common practice in India, non-availability of good quality aggregates is causing problems to road construction activity in India and other countries due to closure of quarries, restriction on new quarry sites from environmental considerations. It is worth-while to examine the international practice in the construction of cemented/stabilized subbases adopted in this regard. The subbases used for heavy-duty pavements have to be uniform and provide permanent support without erosion under adverse conditions of wetting and drying as well as freezing and thawing.

Standards and specifications adopted in different countries for subbase layer vary widely. A maximum of 28 day compressive strength of 8.5 MPa is recommended in US and Canada for heavy duty highway pavements to provide a non-erodible support. AUSTROADS (2004) recommends a characteristic 28 day compressive strength of 5 MPa with flyash and 7 MPa without flyash. Marginal as well as recycled concrete aggregates are being increasingly used as they are able to meet the afore-mentioned strength requirements. The cementitious subbases must satisfy the relevant durability criteria so that they do not erode. Loss of weight shall not exceed 14% after 12 cycles after wetting and drying / freezing and thawing tests conducted as per ASTM D559-03 (2010) and ASTM D560-03 (2010).

The revised IRC:58-2015 with reduced strength of DLC having a 7 day strength of 7MPa is conformity with the international practice. Marginal as well as recycled concrete aggregates can be used in cement treated subbase shown in **Fig. 1(b)** since the strength requirement is moderate now.

APPENDIX - II

INTERNATIONAL PRACTICE ON USE OF DEBONDING LAYER OVER STABILIZED/CEMENTED SUBBASE

Concrete slabs expand and contract with temperature and moisture changes. High strength stabilized subbase layers have a rough texture offering high frictional restraint to the concrete pavement movement causing cracking at early stages when the concrete is weak. The most common practice has been use of two layers of wax emulsion. Choke stone has been used in many projects in USA as a de-bonding layer .It is a small size uniformly graded stone layer usually 13-25 mm thick below the PQC slab .The bond prevention quality of choke stone is reported to be superior to that of a wax base liquid membrane forming curing compound or asphalt emulsion as per experience in USA . The nominal size of aggregates in choke stone material is 9.5 mm. Bituminous surface dressing has also been used as a debonding layer. A debonding layer of dense graded Bituminous Concrete is resistant to damage by moisture and pavements have given better performance than other debonding layers. Nonwovenneedle-punched geotextile fabric inter layer also is in use many countries.

APPENDIX - III

VALIDITY OF FATIGUE EQUATIONS ADOPTED IN THE GUIDELINES

A new fatigue model for concrete pavement given below was developed by American Concrete Pavement Association. The fatigue model is practically the same as the PCA model adopted in the guidelines for a reliability of 90.

... (III.1)

$$\log_{10} N_r = \left[\frac{-SR_r^{-10.24} \{\log_{10}(R)\}}{0.0112} \right]^{0.217}$$

where,

N_r = fatigue life at load level r

SR_r = stress ratio at load level r = $\frac{\text{stress caused at load level } r}{\text{modulus of rupture of concrete}}$

R = Reliability which is taken as 0.90 corresponding to 90% reliability = 10% of the concrete slab is expected to undergo fatigue cracking at the end of design period.

Suggested reliability values for different types of roads are :-

Village roads	60%
District roads	70%
State highways	80%
National highways and expressways	90%

Appendix- IV Stress Charts for Bottom-up Cracking Analysis

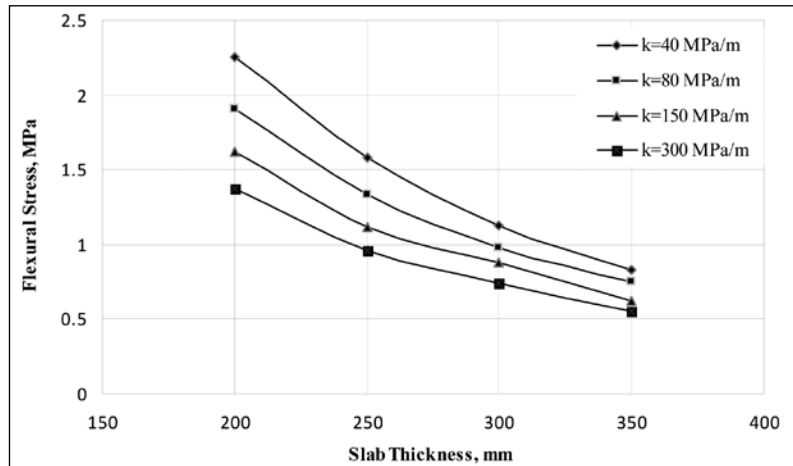


Fig. IV.1 Stress due to Single Axle Load of 80 kN, $\Delta T = 0^\circ\text{C}$, without Concrete Shoulder

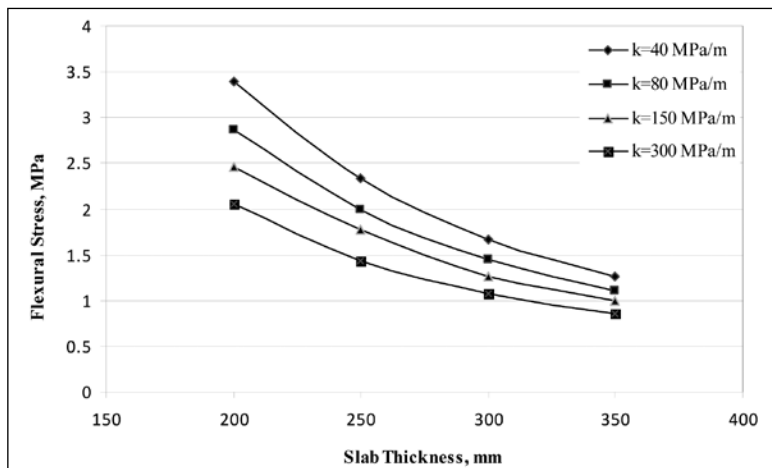


Fig. IV.2 Stress due to Single Axle Load of 120 kN, $\Delta T = 0^\circ\text{C}$, without Concrete Shoulder

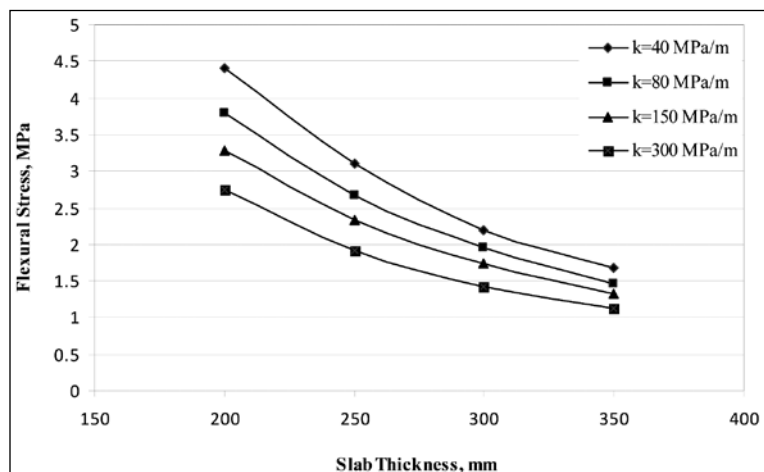


Fig. IV.3 Stress due to Single Axle Load of 160 kN, $\Delta T = 0^\circ\text{C}$, Without Concrete Shoulder

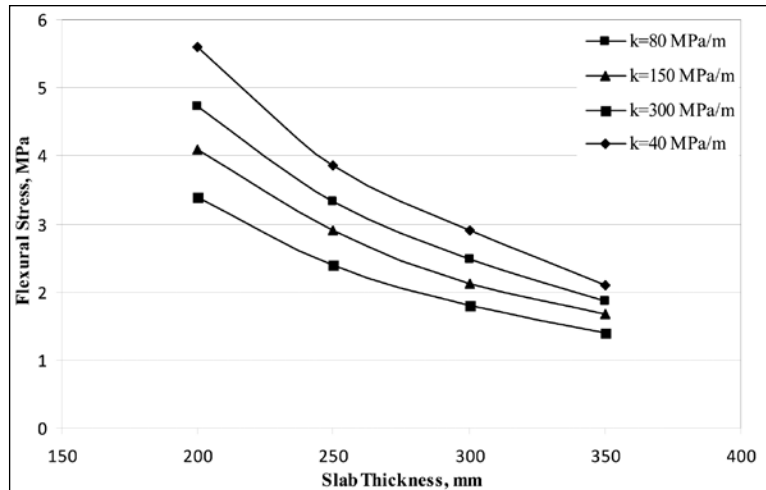


Fig. IV.4 Stress due to Single Axle Load of 200 kN, $\Delta T = 0^\circ\text{C}$, Without Concrete Shoulder

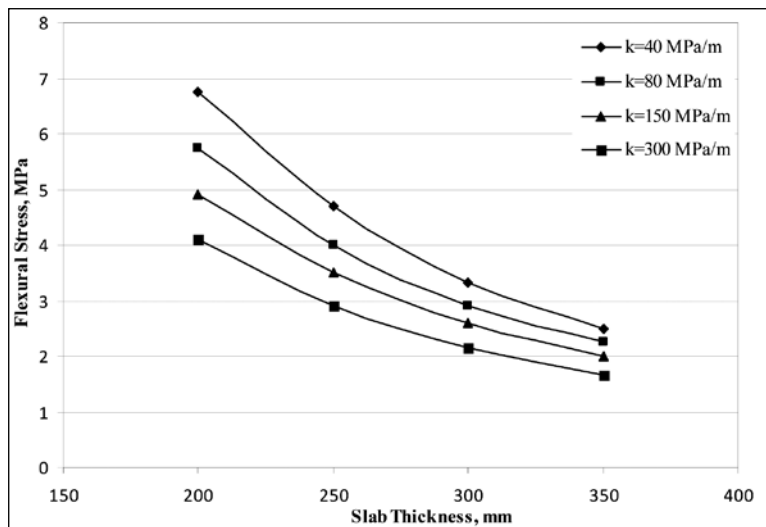


Fig. IV.5 Stress due to Single Axle Load of 240 kN, $\Delta T = 0^\circ\text{C}$, Without Concrete Shoulder

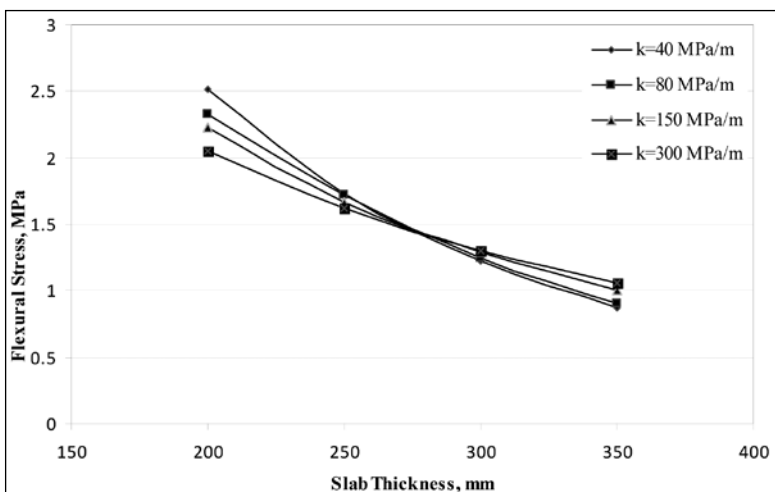


Fig. IV.6 Stress due to Single Axle Load of 80 kN, $\Delta T = 8^\circ\text{C}$, Without Concrete Shoulder

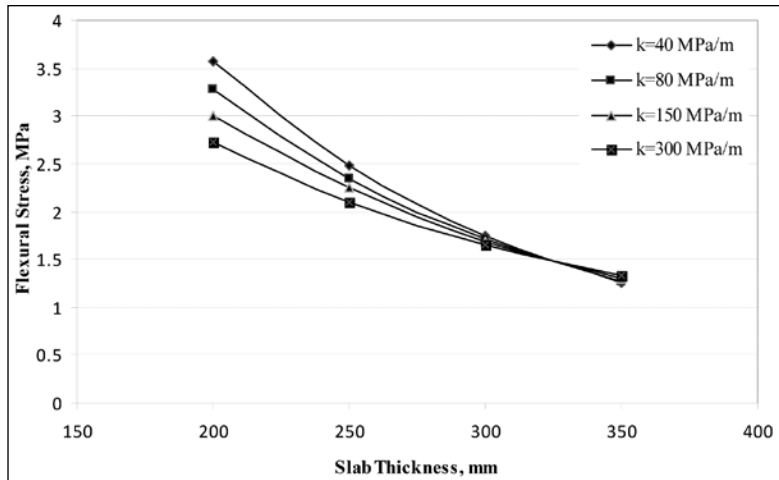


Fig. IV.7 Stress due to Single Axle Load of 120 kN, $\Delta T = 8^\circ\text{C}$, Without Concrete Shoulder

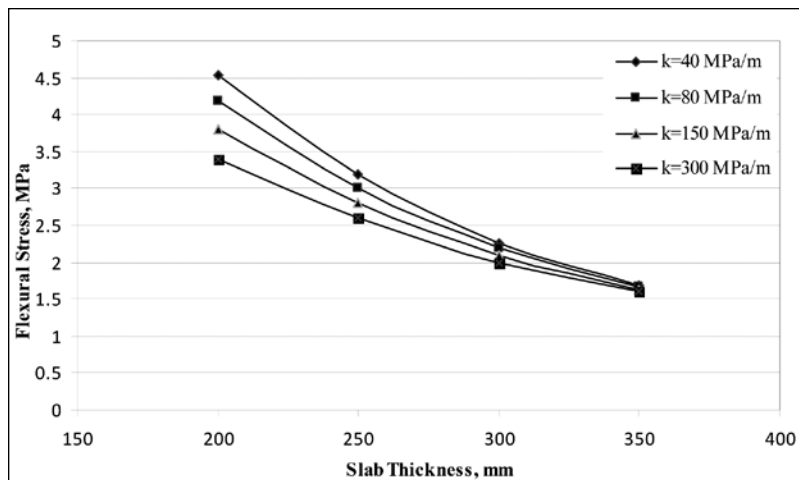


Fig. IV.8 Stress due to Single Axle Load of 160 kN, $\Delta T = 8^\circ\text{C}$, Without Concrete Shoulder

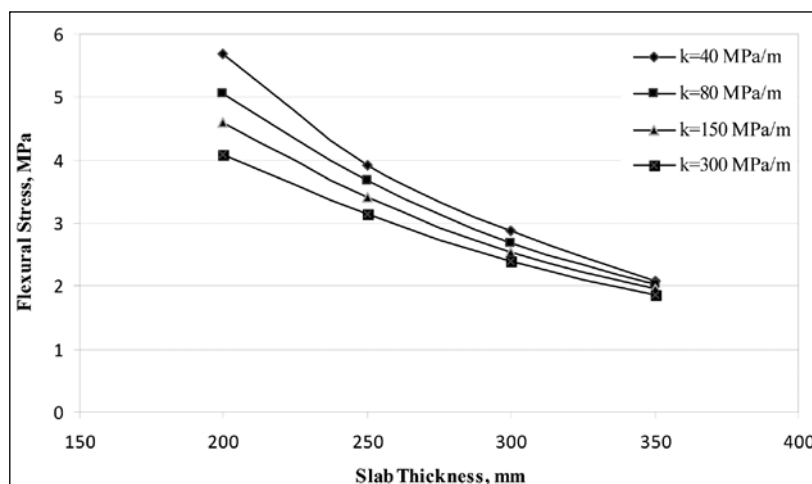


Fig. IV.9 Stress due to Single Axle Load of 200 kN, $\Delta T = 8^\circ\text{C}$, Without Concrete Shoulder

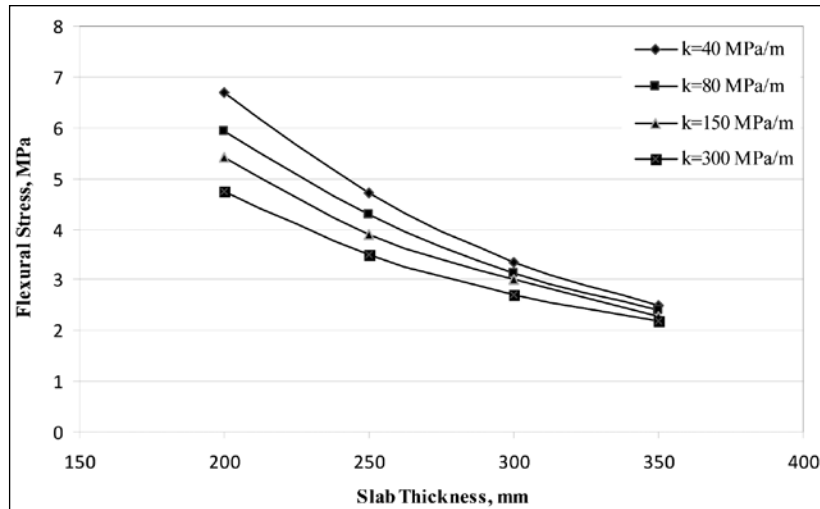


Fig. IV.10 Stress due to Single Axle Load of 240 kN, $\Delta T = 8^\circ\text{C}$, Without Concrete Shoulder

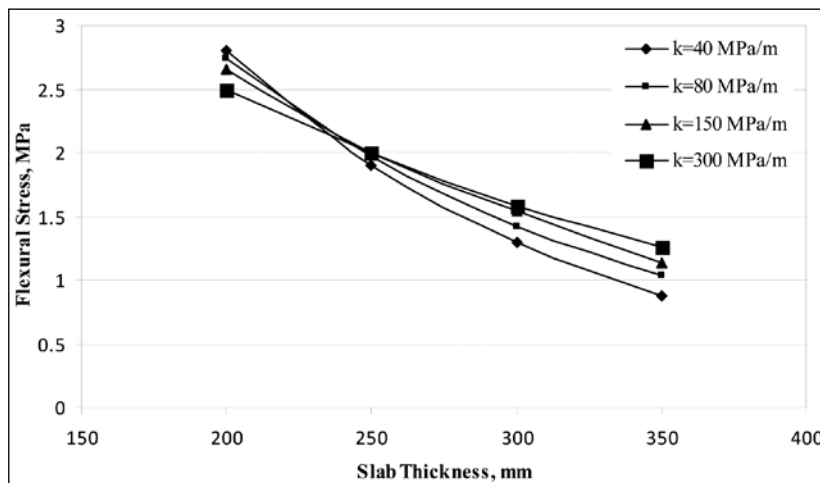


Fig. IV.11 Stress due to Single Axle Load of 80 kN, $\Delta T = 13^\circ\text{C}$, Without Concrete Shoulder

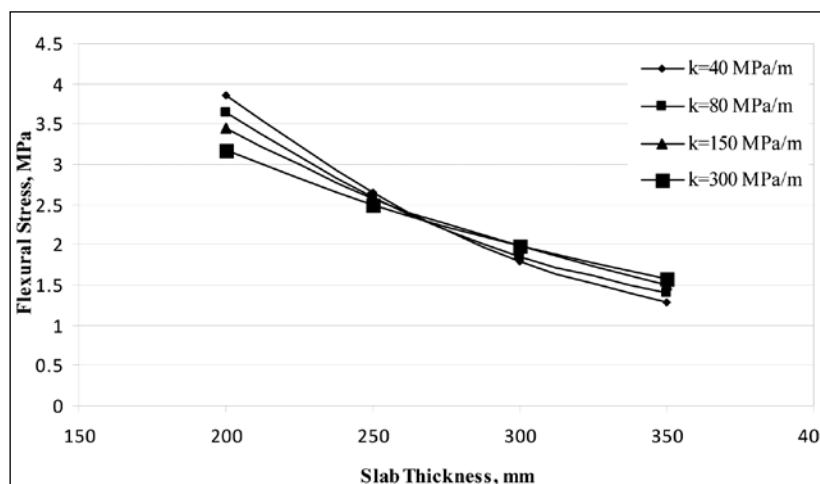


Fig. IV.12 Stress due to Single Axle Load of 120 kN, $\Delta T = 13^\circ\text{C}$, Without Concrete Shoulder

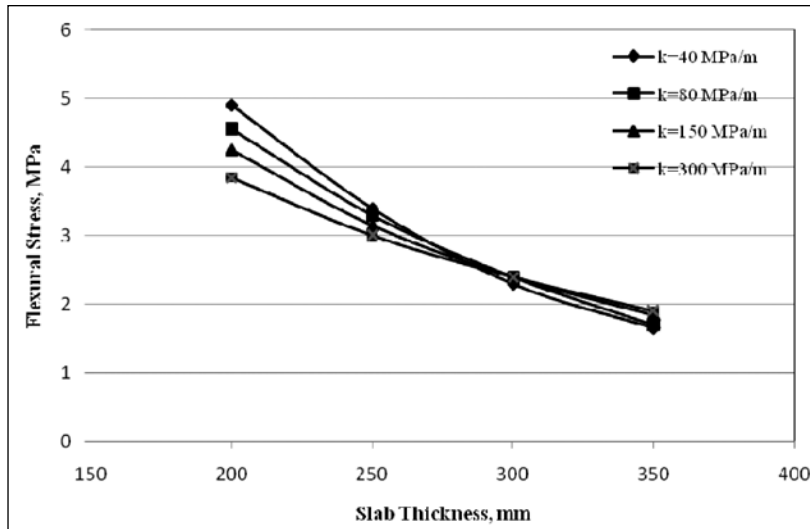


Fig. IV.13 Stress due to Single Axle Load of 140 kN, $\Delta T = 13^\circ\text{C}$, Without Concrete Shoulder

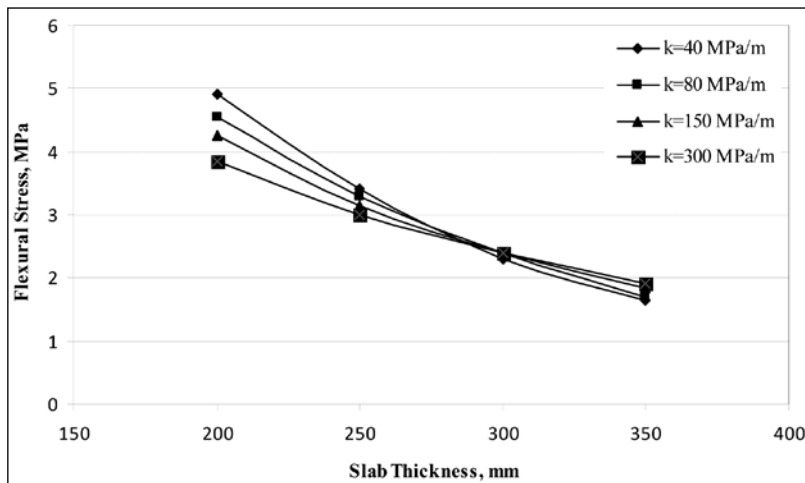


Fig. IV.14 Stress due to Single Axle Load of 160 kN, $\Delta T = 13^\circ\text{C}$, Without Concrete Shoulder

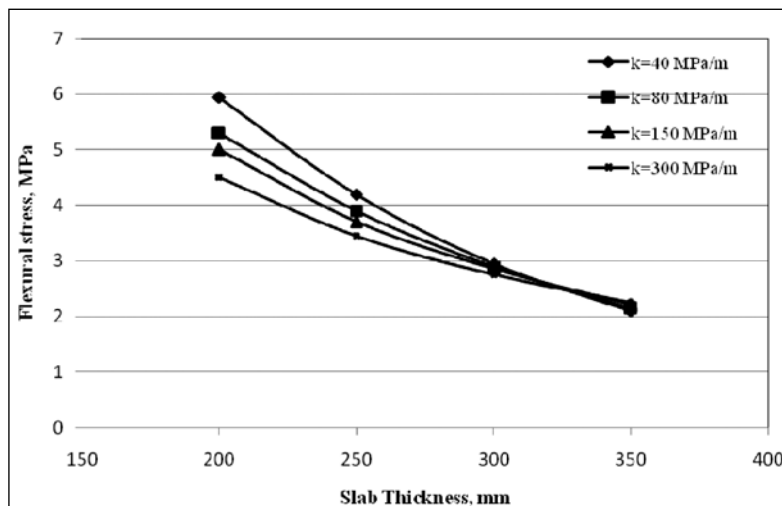


Fig. IV.15 Stress due to Single Axle Load of 200 kN, $\Delta T = 13^\circ\text{C}$, Without Concrete Shoulder

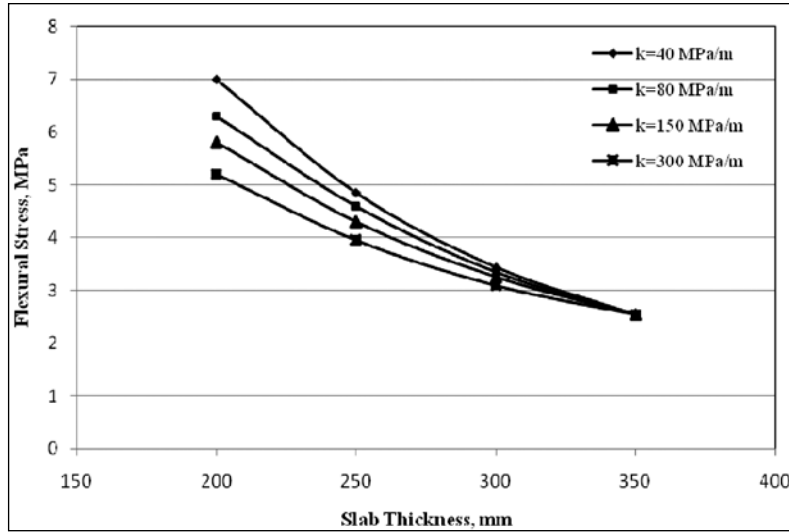


Fig. IV.16 Stress due to Single Axle Load of 240 kN, $\Delta T = 13^\circ\text{C}$, Without Concrete Shoulder

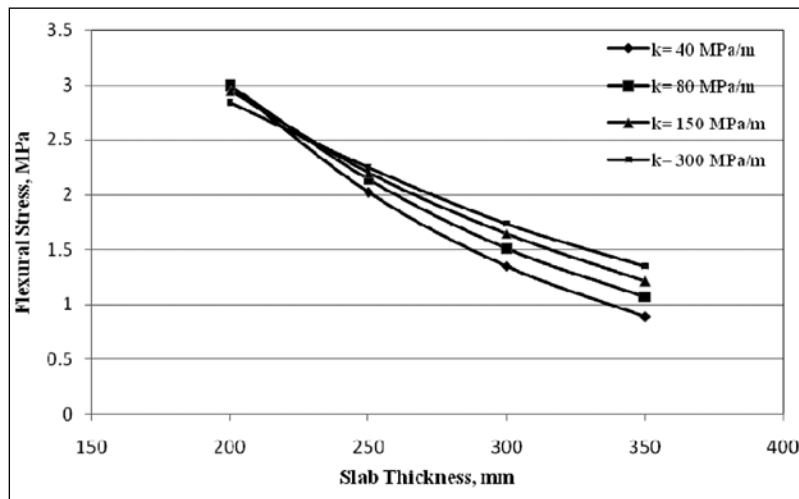


Fig. IV.17 Stress due to Single Axle Load of 80 kN, $\Delta T = 17^\circ\text{C}$, Without Concrete Shoulder

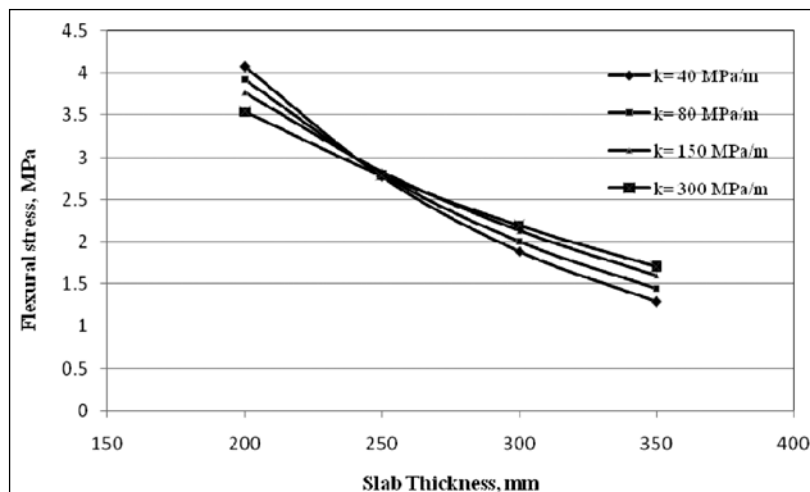


Fig. IV.18 Stress due to Single Axle Load of 120 kN, $\Delta T = 17^\circ\text{C}$, Without Concrete Shoulder

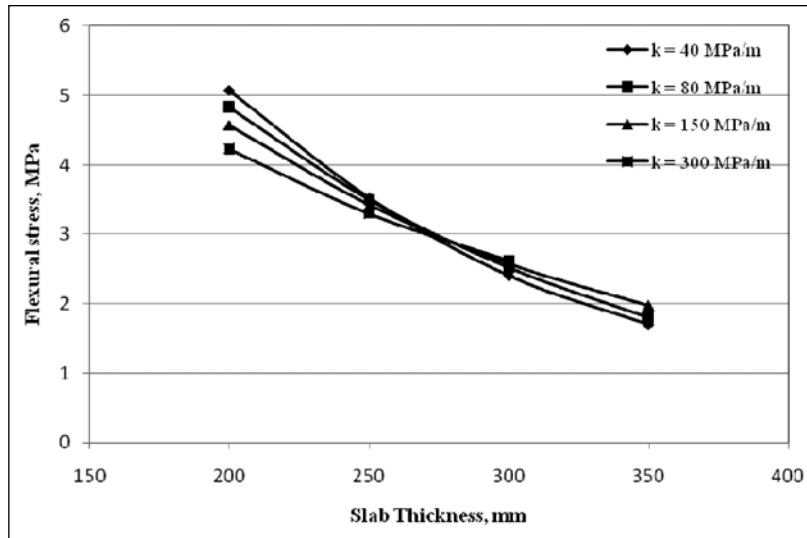


Fig. IV.19 Stress due to Single Axle Load of 160 kN, $\Delta T = 17^\circ\text{C}$, Without Concrete Shoulder

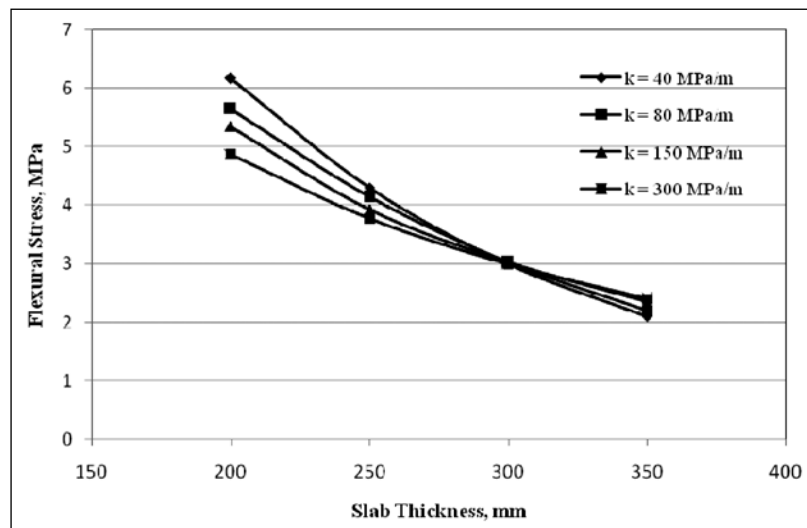


Fig. IV.20 Stress due to Single Axle Load of 200 kN, $\Delta T = 17^\circ\text{C}$, Without Concrete Shoulder

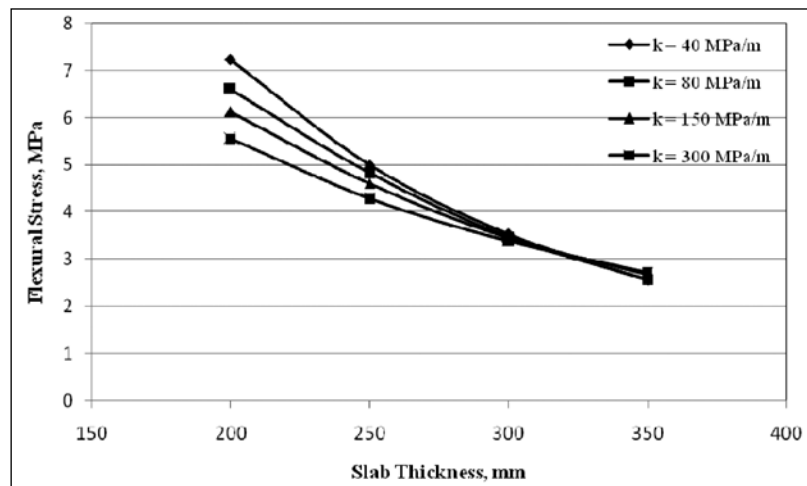


Fig. IV.21 Stress due to Single Axle Load of 240 kN, $\Delta T = 17^\circ\text{C}$, Without Concrete Shoulder

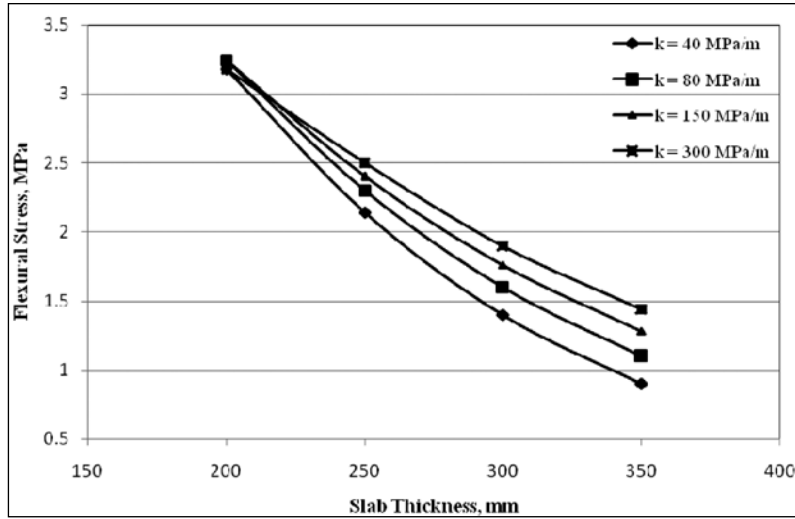


Fig. IV.22 Stress due to Single Axle Load of 80 kN, $\Delta T = 21^\circ\text{C}$, Without Concrete Shoulder

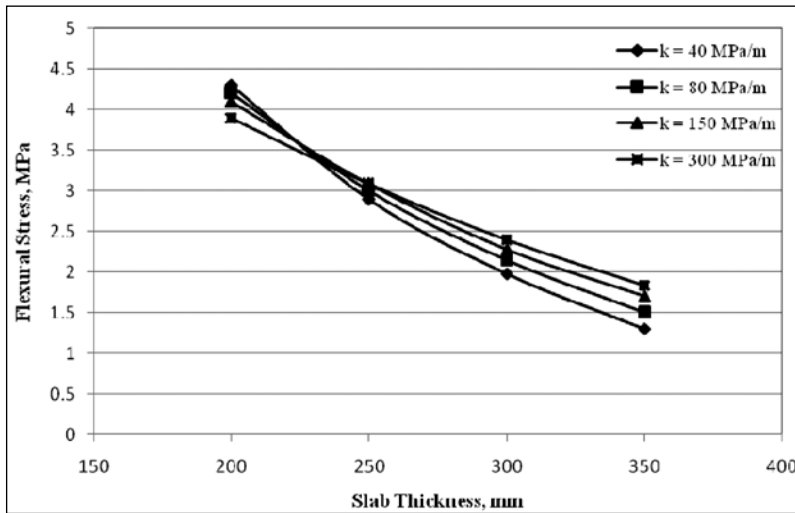


Fig. IV.23 Stress due to Single Axle Load of 120 kN, $\Delta T = 21^\circ\text{C}$, Without Concrete Shoulder

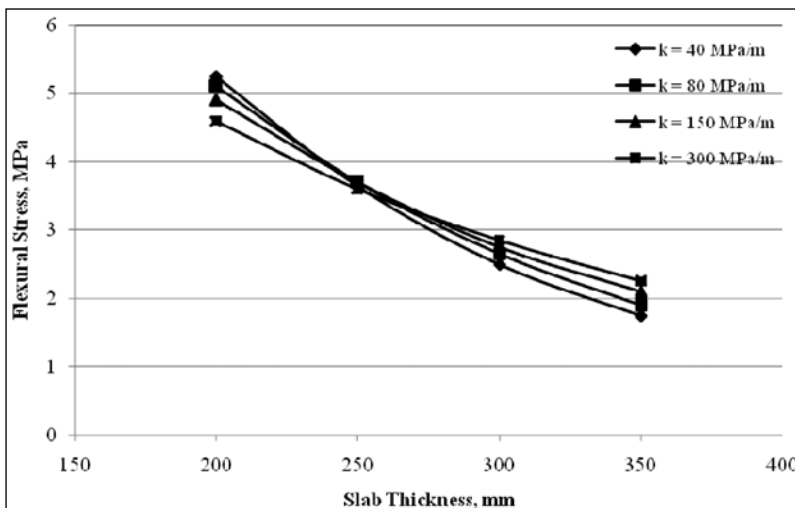


Fig. IV.24 Stress due to Single Axle Load of 160 kN, $\Delta T = 21^\circ\text{C}$, Without Concrete Shoulder

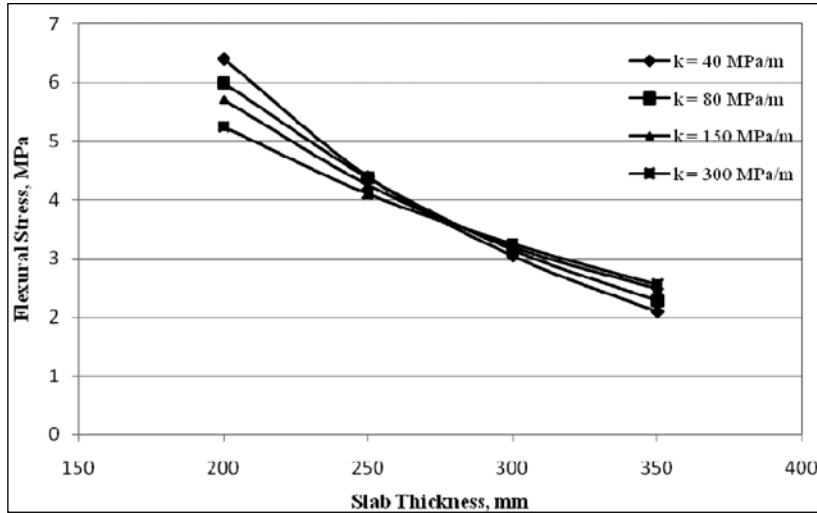


Fig. IV.25 Stress due to Single Axle Load of 200 kN, ΔT = 21°C, Without Concrete Shoulder

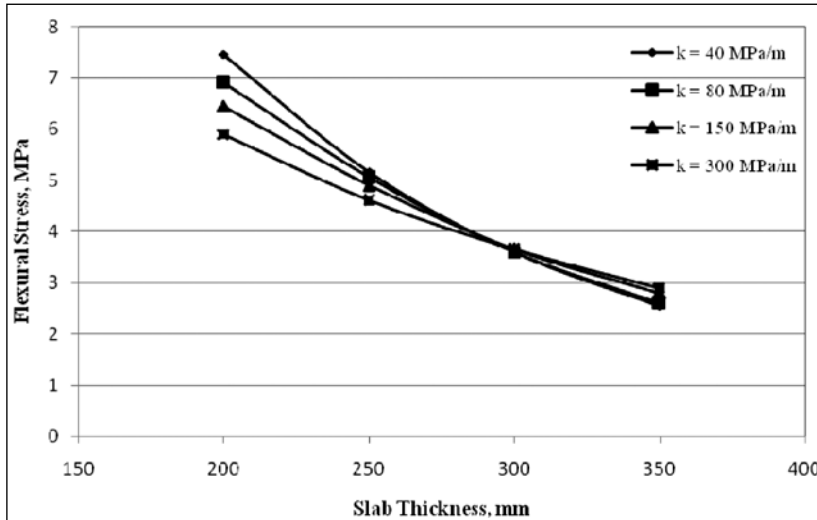


Fig. IV.26 Stress due to Single Axle Load of 240 kN, ΔT = 21°C, Without Concrete Shoulder

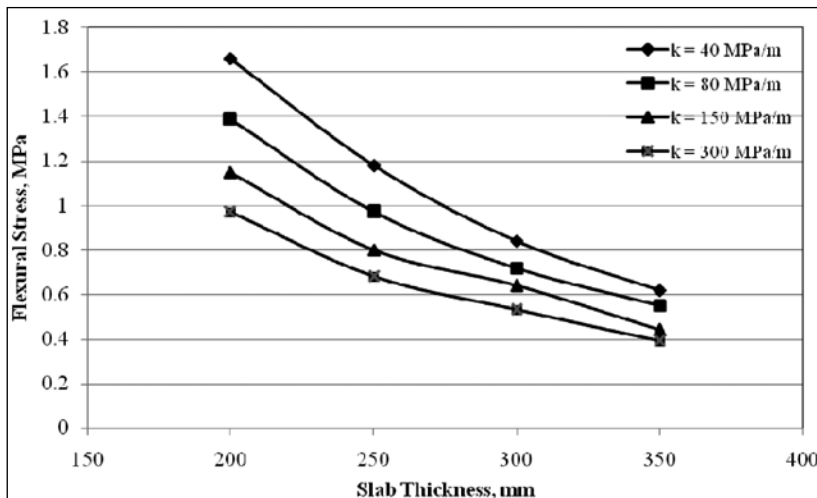


Fig. IV.27 Stress due to Single Axle Load of 80 kN, ΔT = 0°C, With Tied Concrete Shoulder

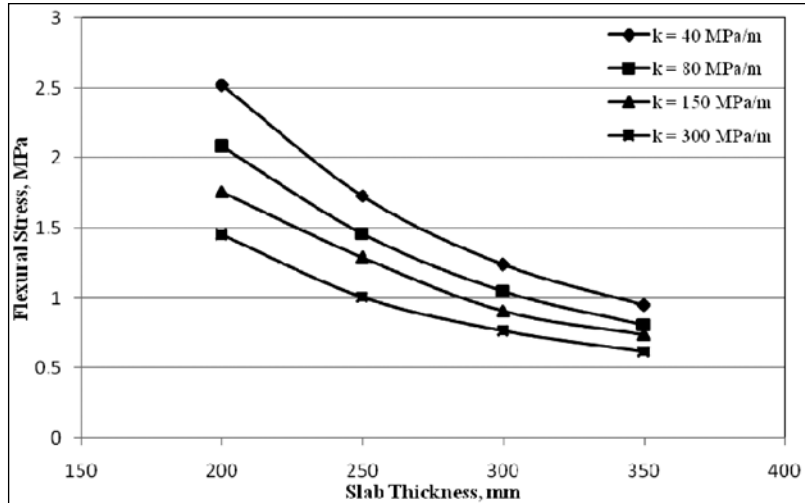


Fig. IV.28 Stress due to Single Axle Load of 120 kN, $\Delta T = 0^\circ\text{C}$, With tied Concrete Shoulder

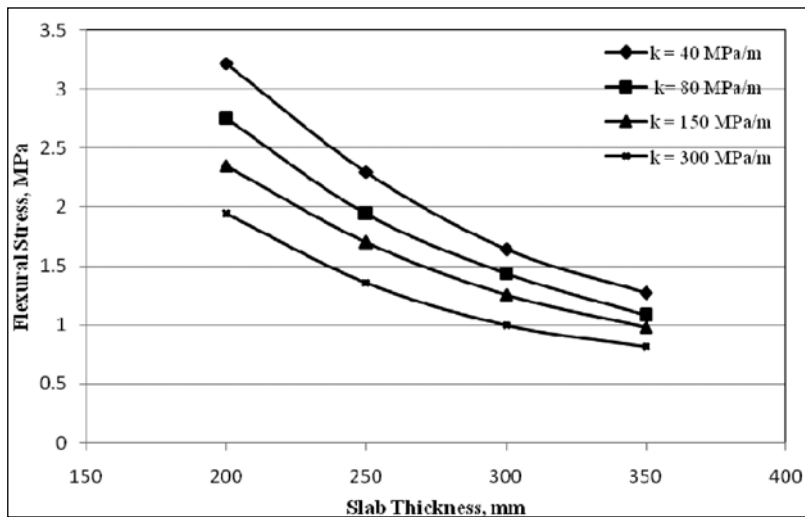


Fig. IV.29 Stress due to Single Axle Load of 160 kN, $\Delta T = 0^\circ\text{C}$, With Tied Concrete Shoulder

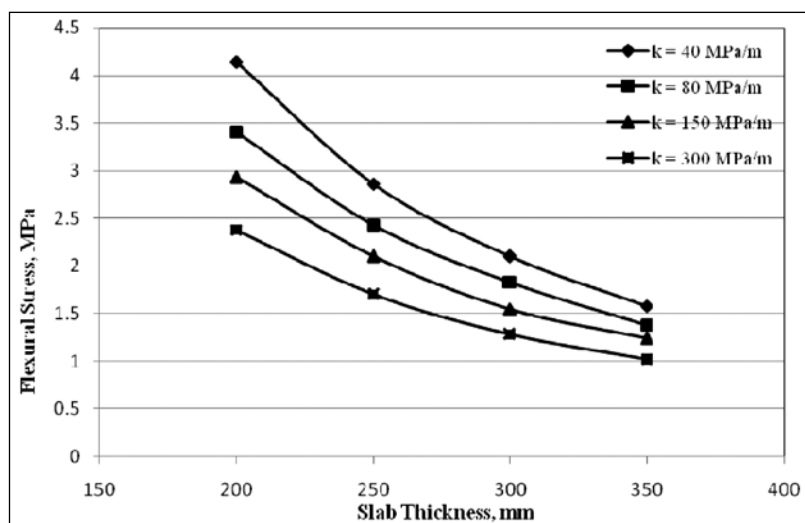


Fig. IV.30 Stress due to Single Axle Load of 200 kN, $\Delta T = 0^\circ\text{C}$, With Tied Concrete Shoulder

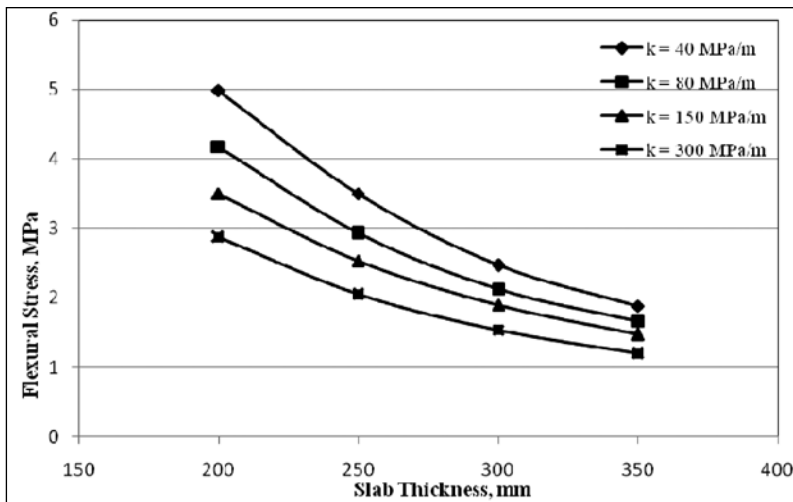


Fig. IV.31 Stress due to Single Axle Load of 240 kN, $\Delta T = 0^\circ\text{C}$, With Tied Concrete Shoulder

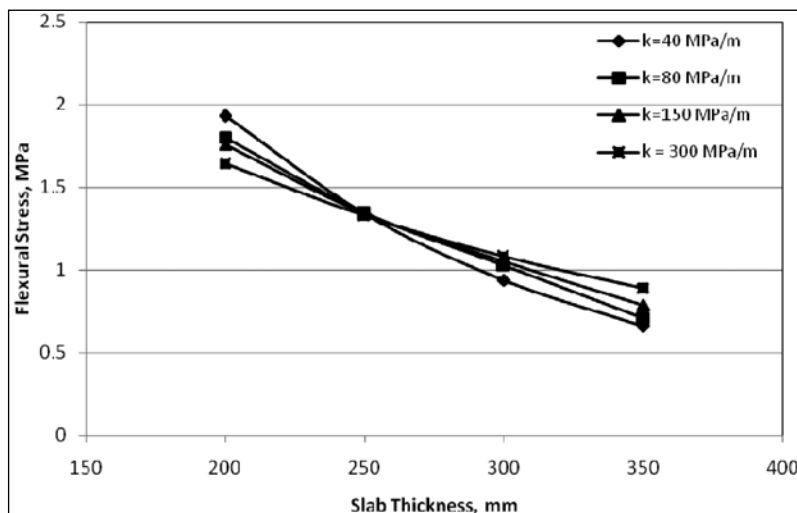


Fig. IV.32 Stress due to Single Axle Load of 80 kN, $\Delta T = 8^\circ\text{C}$, With Tied Concrete Shoulder

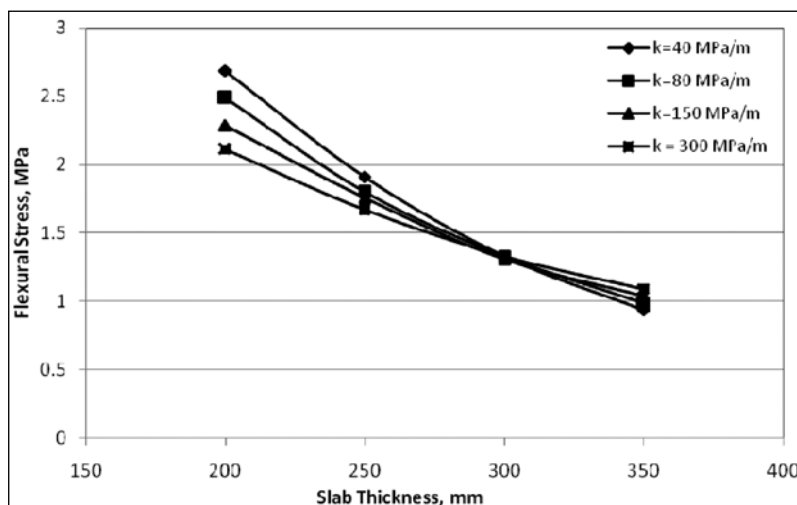


Fig. IV.33 Stress due to Single Axle Load of 120 kN, $\Delta T = 8^\circ\text{C}$, With Tied Concrete Shoulder

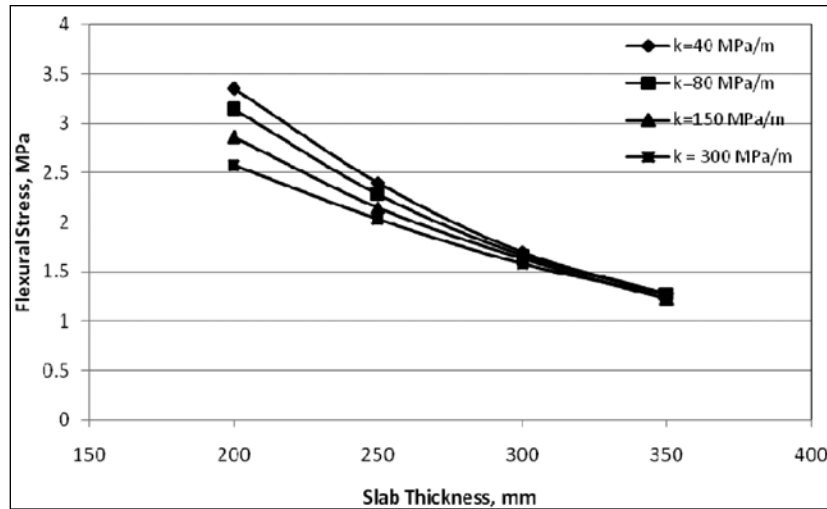


Fig. IV.34 Stress due to Single Axle Load of 160 kN, $\Delta T = 8^\circ\text{C}$, With Tied Concrete Shoulder

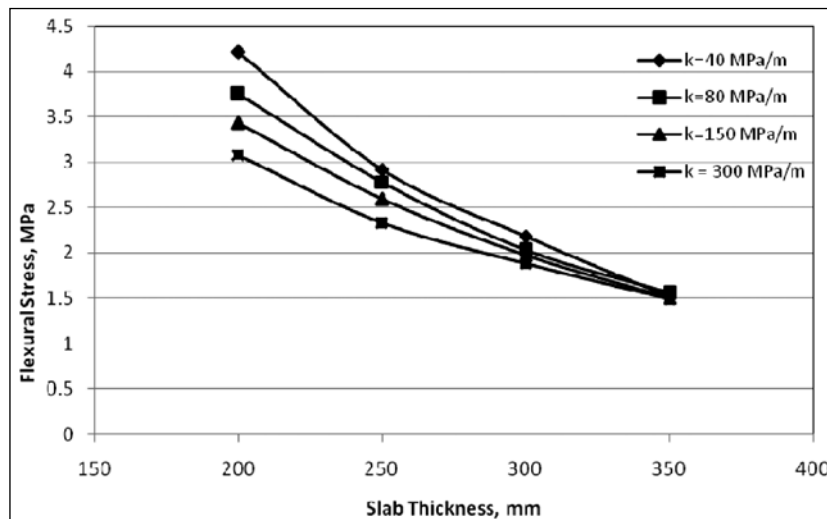


Fig. IV.35 Stress due to Single Axle Load of 200 kN, $\Delta T = 8^\circ\text{C}$, With Tied Concrete Shoulder

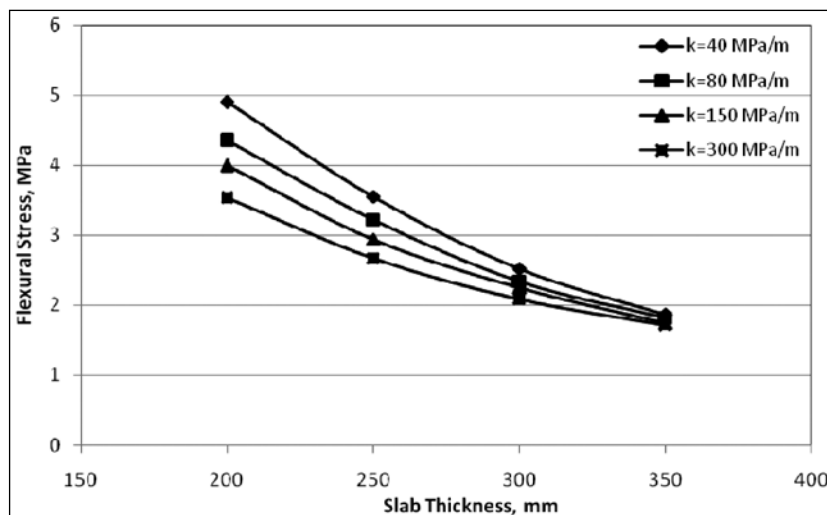


Fig. IV.36 Stress due to Single Axle Load of 240 kN, $\Delta T = 8^\circ\text{C}$, With Tied Concrete Shoulder

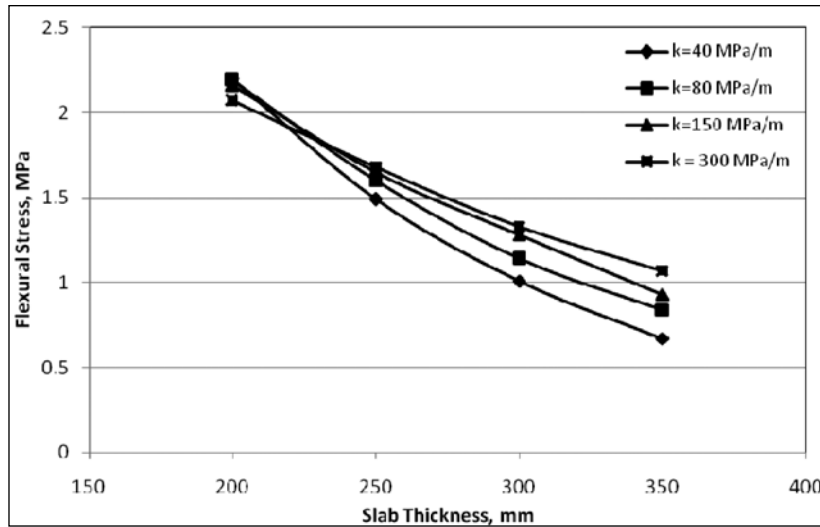


Fig. IV.37 Stress due to Single Axle Load of 80 kN, $\Delta T = 13^\circ\text{C}$, With Tied Concrete Shoulder

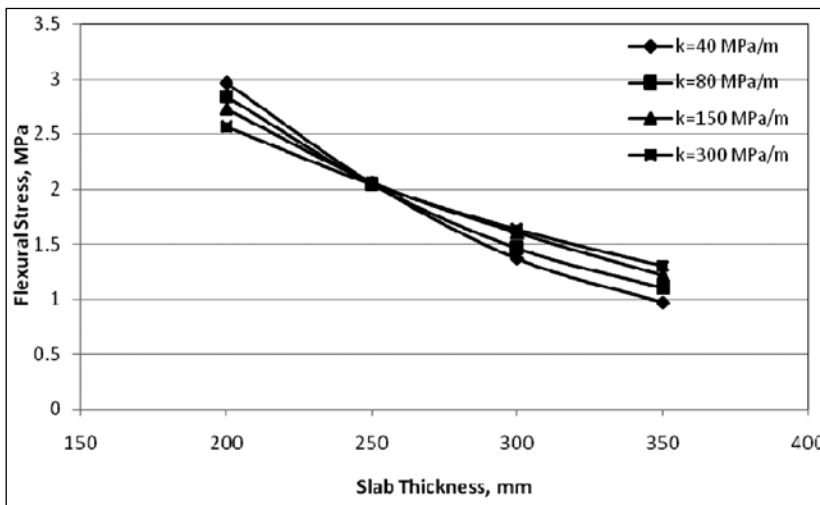


Fig. IV.38 Stress due to Single Axle Load of 120 kN, $\Delta T = 13^\circ\text{C}$, With Tied Concrete Shoulder

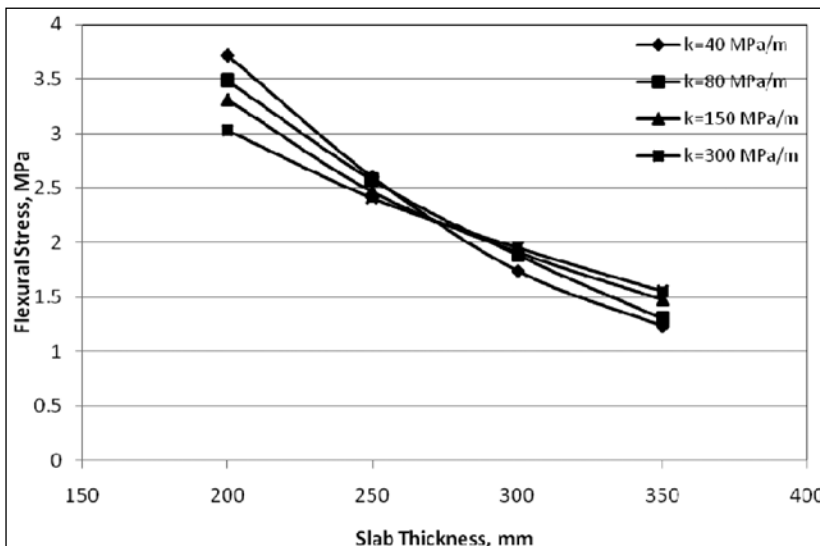


Fig. IV.39 Stress due to Single Axle Load of 160 kN, $\Delta T = 13^\circ\text{C}$, With Tied Concrete Shoulder

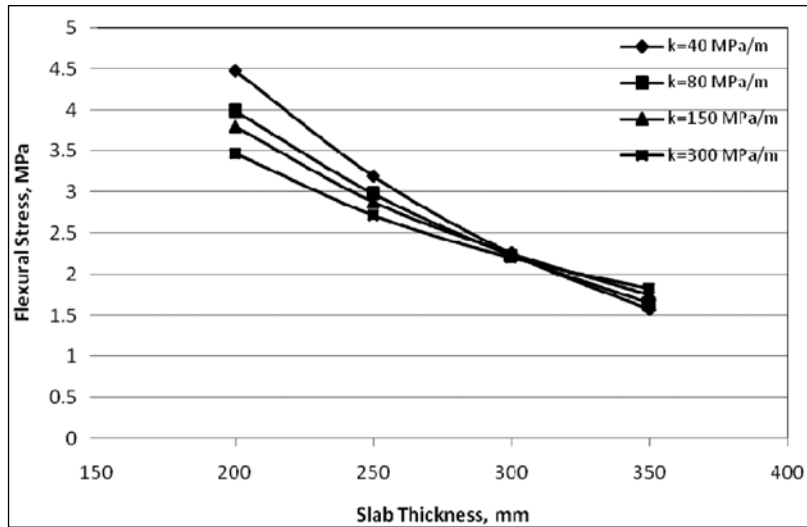


Fig. IV.40 Stress due to Single Axle Load of 200 kN, $\Delta T = 13^\circ\text{C}$, With Tied Concrete Shoulder

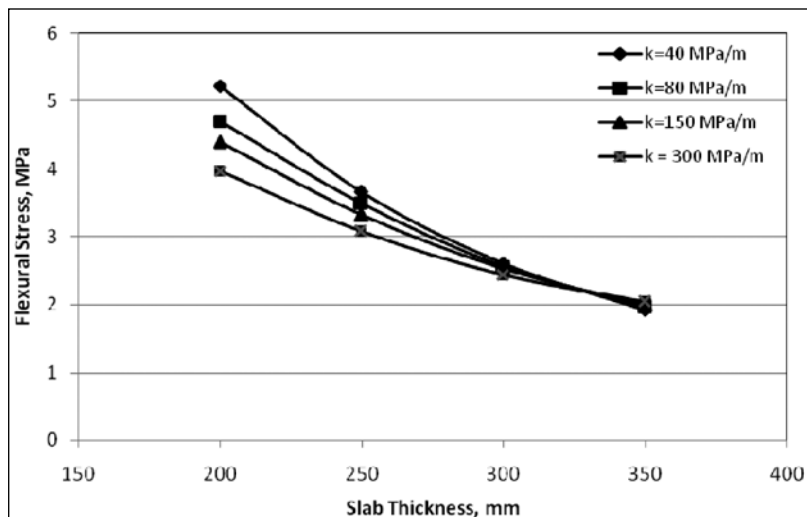


Fig. IV.41 Stress due to Single Axle Load of 240 kN, $\Delta T = 13^\circ\text{C}$, With Tied Concrete Shoulder

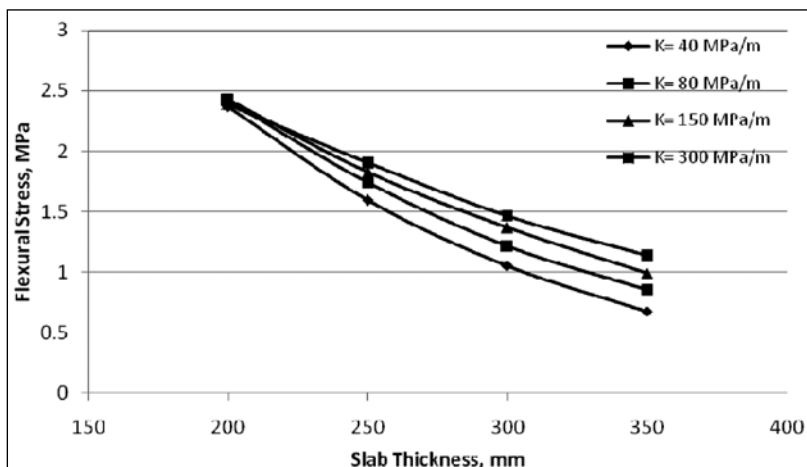


Fig. IV.42 Stress due to Single Axle Load of 80 kN, $\Delta T = 17^\circ\text{C}$, With Tied Concrete Shoulder

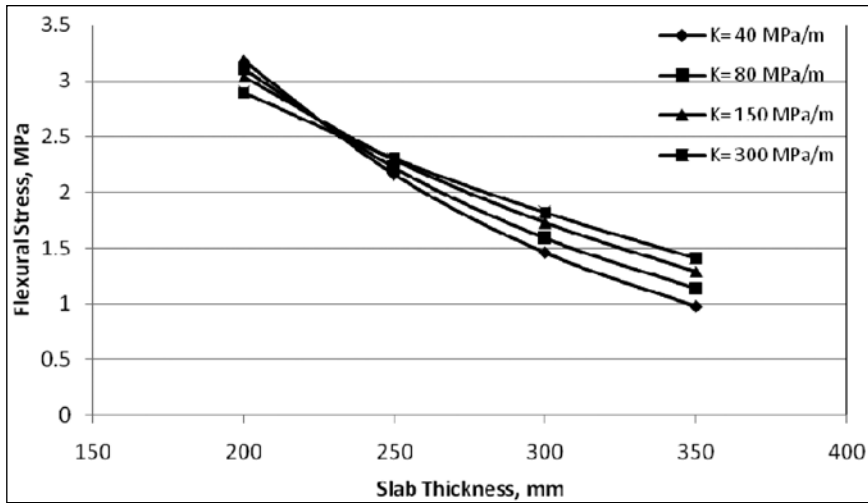


Fig. IV.43 Stress due to Single Axle Load of 120 kN, $\Delta T = 17^\circ\text{C}$, With Tied Concrete Shoulder

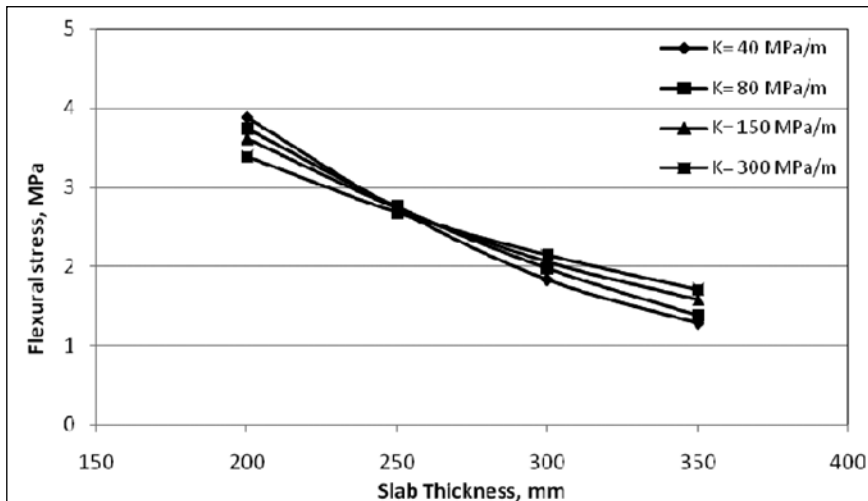


Fig. IV.44 Stress due to Single Axle Load of 160 kN, $\Delta T = 17^\circ\text{C}$, With Tied Concrete Shoulder

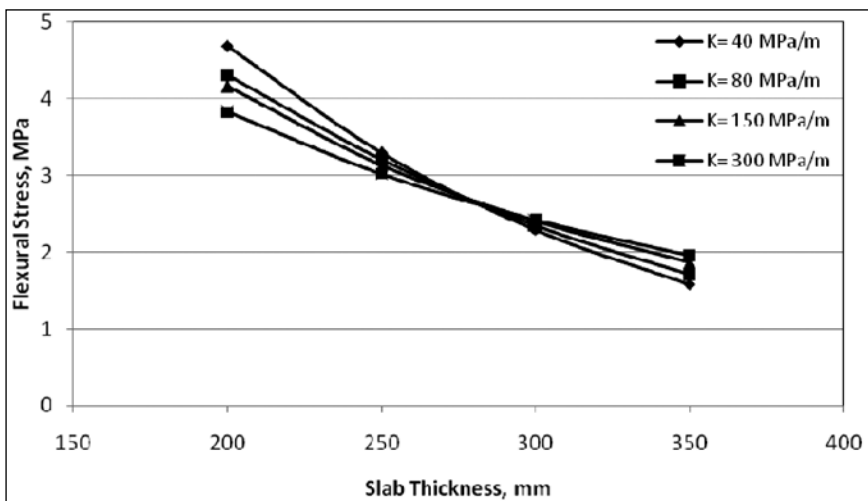


Fig. IV.45 Stress due to Single Axle Load of 200 kN, $\Delta T = 17^\circ\text{C}$, With Tied Concrete Shoulder

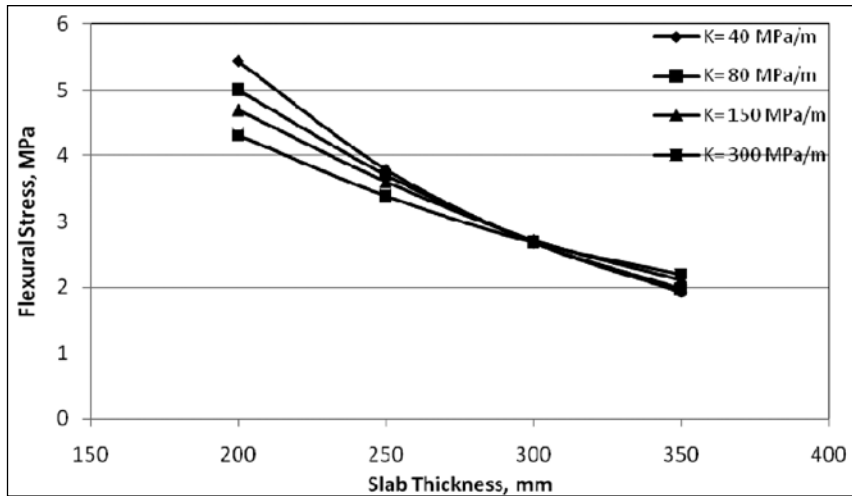


Fig. IV.46 Stress due to Single Axle Load of 240 kN, $\Delta T = 17^\circ\text{C}$, With Tied Concrete Shoulder

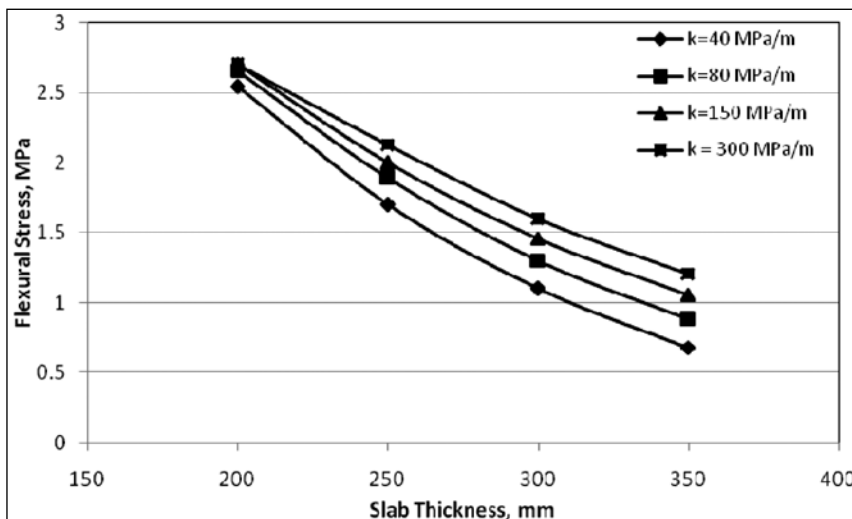


Fig. IV.47 Stress due to Single Axle Load of 80 kN, $\Delta T = 21^\circ\text{C}$, With Tied Concrete Shoulder

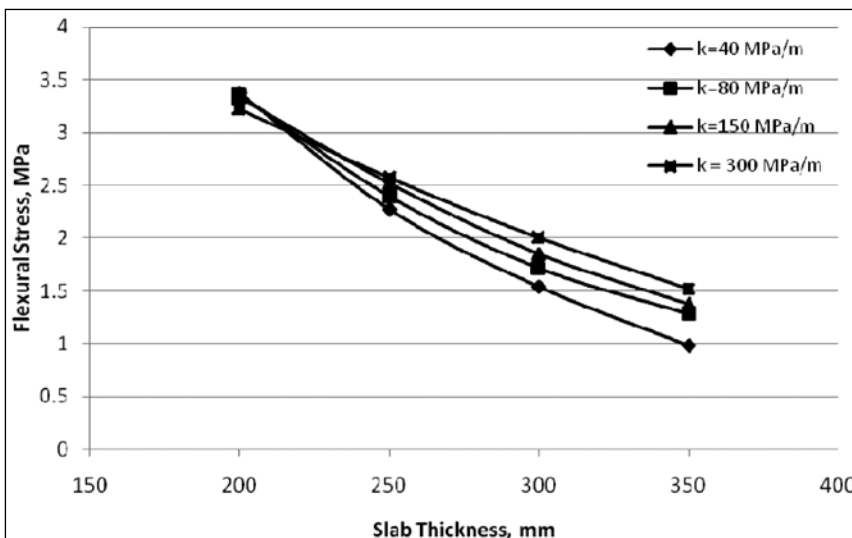


Fig. IV.48 Stress due to Single Axle Load of 120 kN, $\Delta T = 21^\circ\text{C}$, With Tied Concrete Shoulder

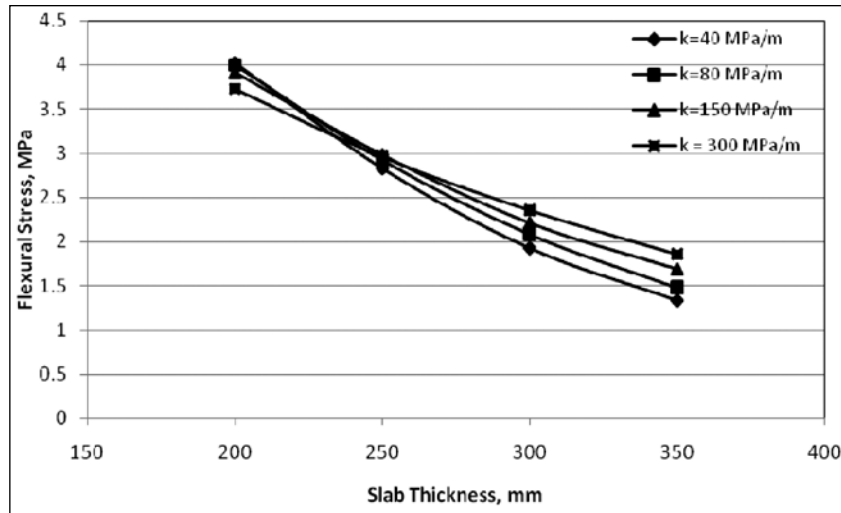


Fig. IV.49 Stress due to Single Axle Load of 160 kN, $\Delta T = 21^\circ\text{C}$, With Tied Concrete Shoulder

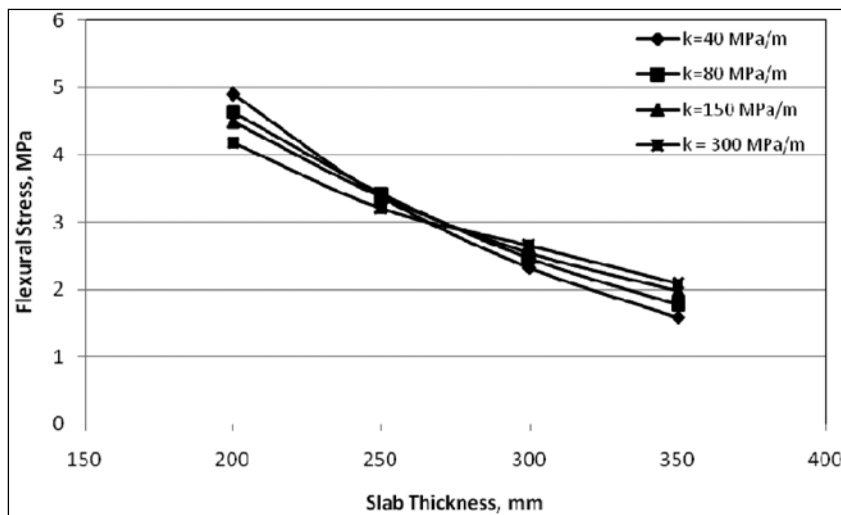


Fig. IV.50 Stress due to Single Axle Load of 200 kN, $\Delta T = 21^\circ\text{C}$, With Tied Concrete Shoulder

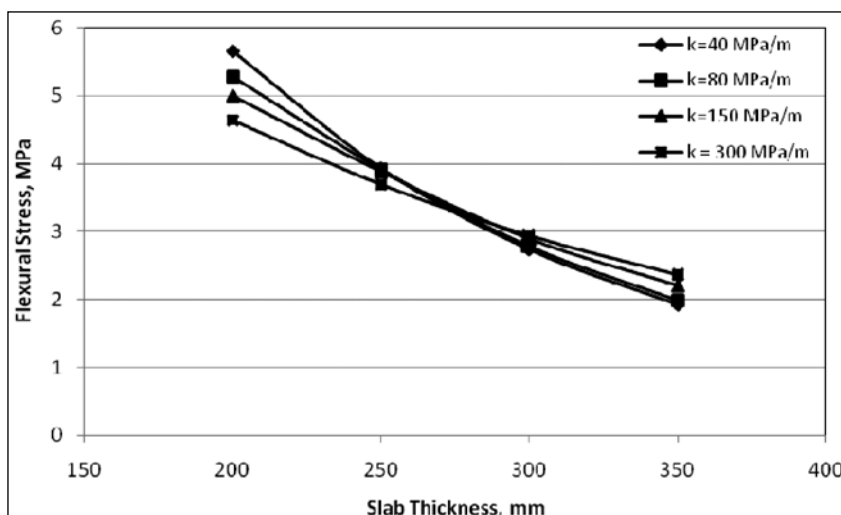


Fig. IV.51 Stress due to Single Axle Load of 240 kN, $\Delta T = 21^\circ\text{C}$, With Tied Concrete Shoulder

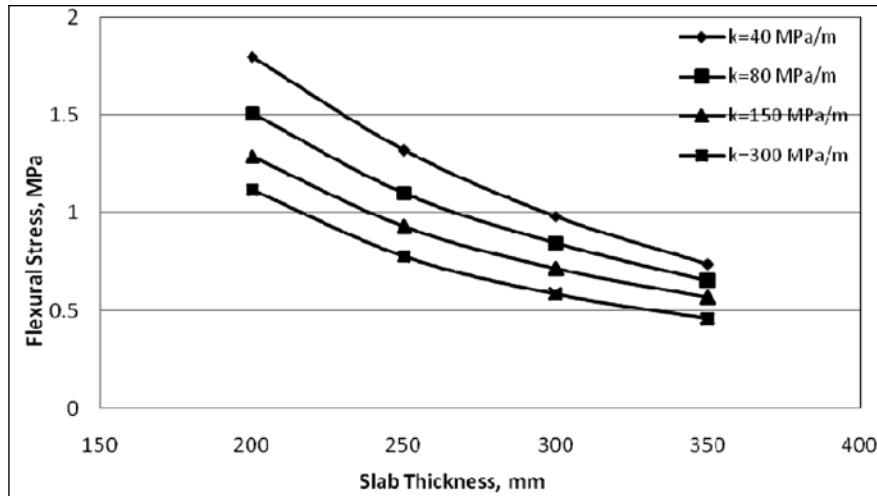


Fig. IV.52 Stress due to Tandem Axle Load of 160 kN, $\Delta T = 0^\circ\text{C}$, Without Concrete Shoulder

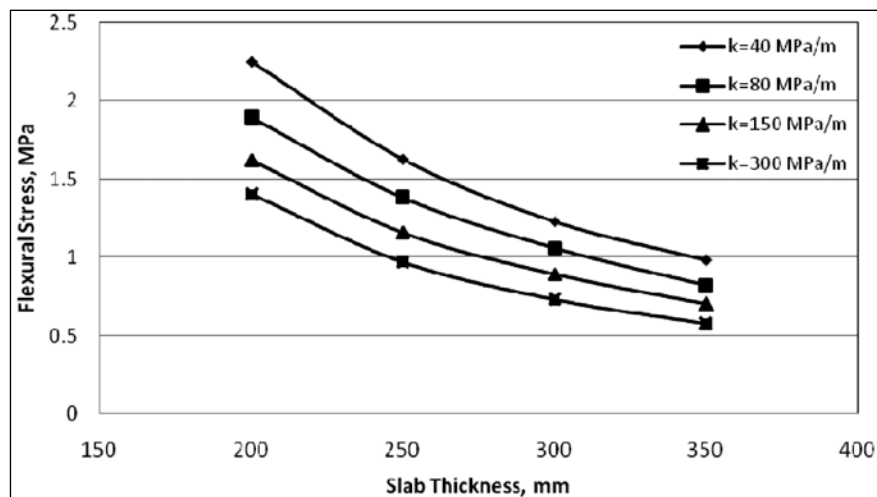


Fig. IV.53 Stress due to Tandem Axle Load of 200 kN, $\Delta T = 0^\circ\text{C}$, Without Concrete Shoulder

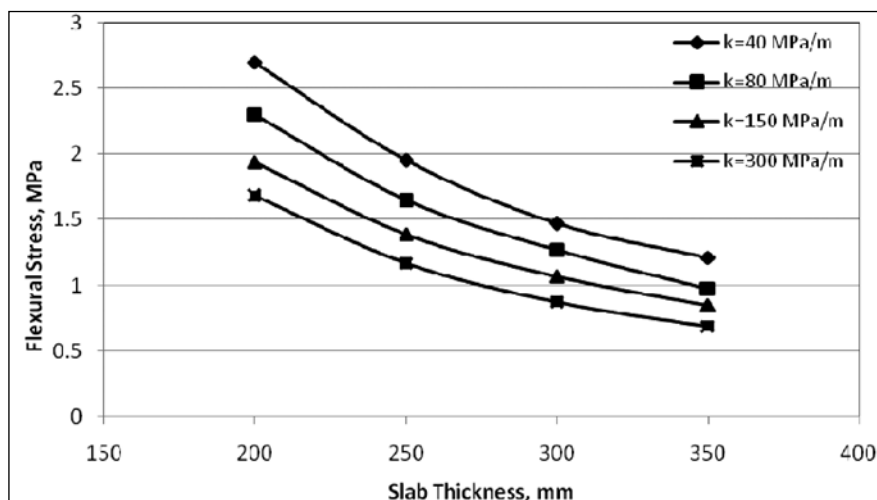


Fig. IV.54 Stress due to Tandem Axle Load of 240 kN, $\Delta T = 0^\circ\text{C}$, Without Concrete Shoulder

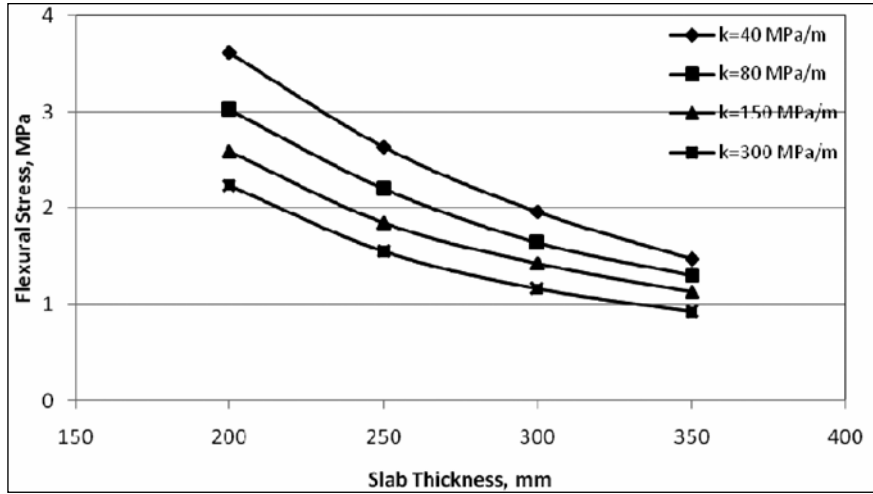


Fig. IV.55 Stress due to Tandem Axle Load of 320 kN, $\Delta T = 0^\circ\text{C}$, Without Concrete Shoulder

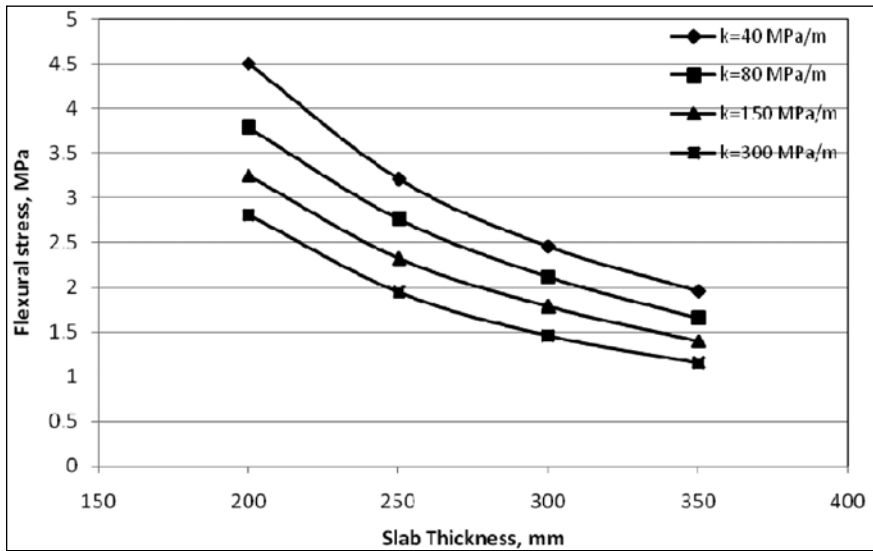


Fig. IV.56 Stress due to Tandem Axle Load of 400 kN, $\Delta T = 0^\circ\text{C}$, Without Concrete Shoulder

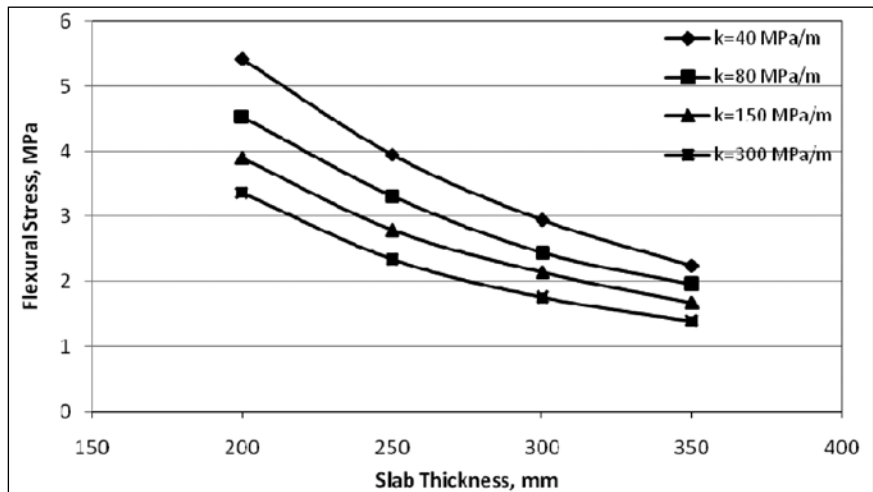


Fig. IV.57 Stress due to Tandem Axle Load of 480 kN, $\Delta T = 0^\circ\text{C}$, Without Concrete Shoulder

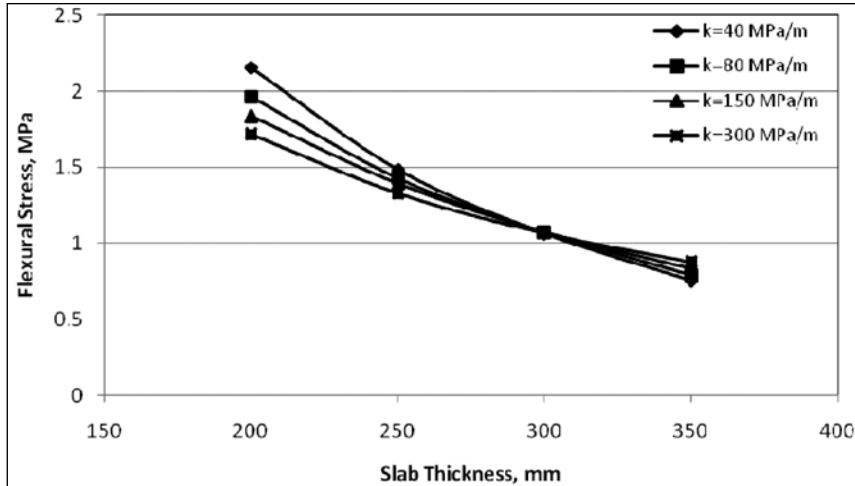


Fig. IV.58 Stress due to Tandem Axle Load of 160 kN, $\Delta T = 8^\circ\text{C}$, Without Concrete Shoulder

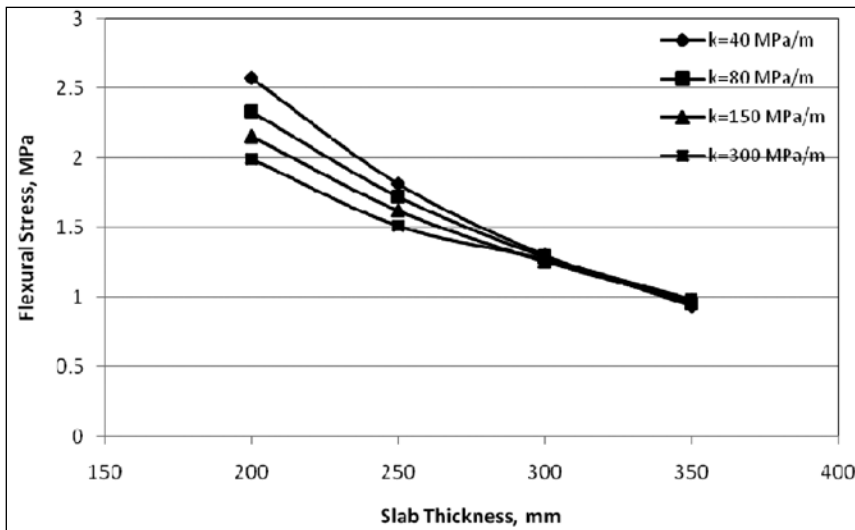


Fig. IV.59 Stress due to Tandem Axle Load of 200 kN, $\Delta T = 8^\circ\text{C}$, Without Concrete Shoulder

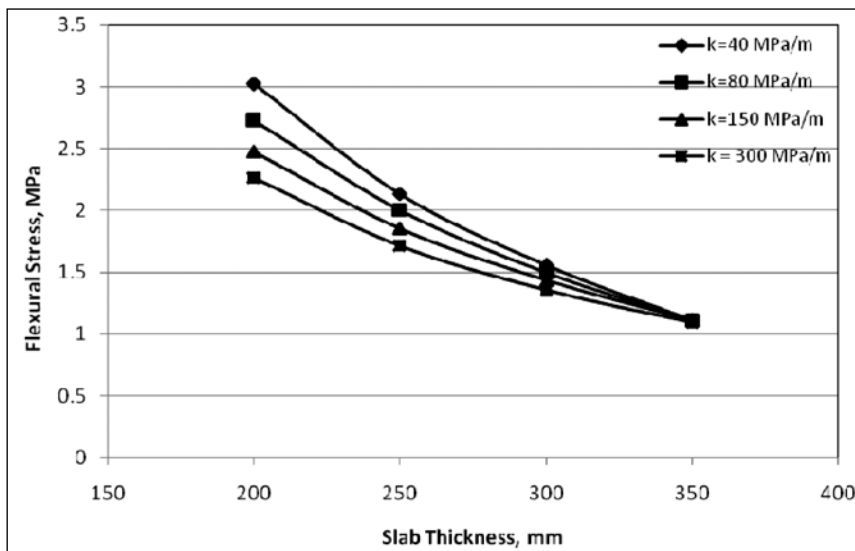


Fig. IV.60 Stress due to Tandem Axle Load of 240 kN, $\Delta T = 8^\circ\text{C}$, Without Concrete Shoulder

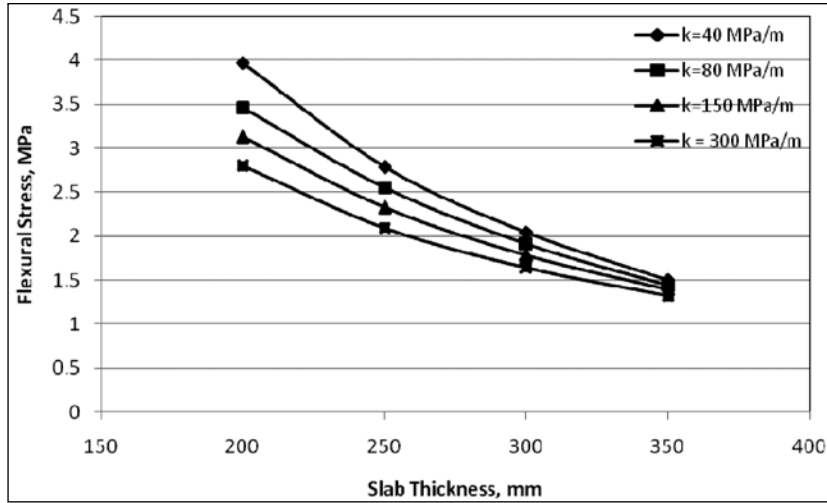


Fig. IV.61 Stress due to Tandem Axle Load of 320 kN, $\Delta T = 8^\circ\text{C}$, Without Concrete Shoulder

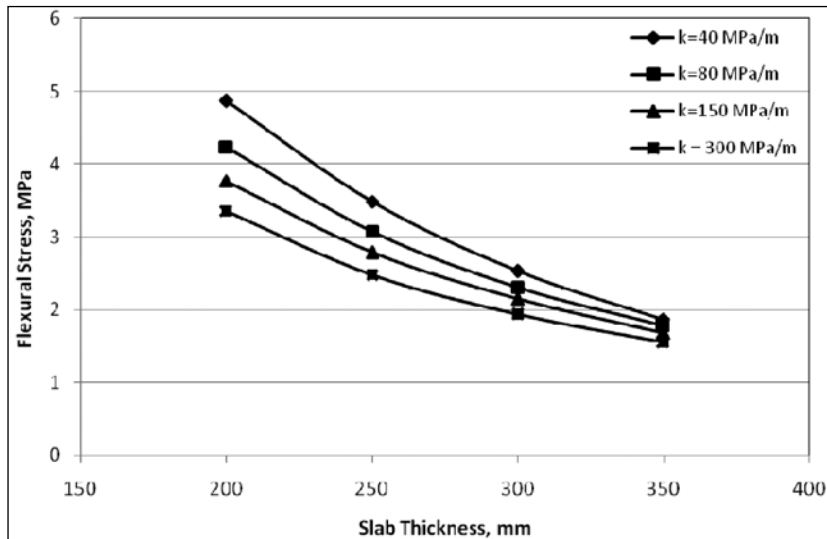


Fig. IV.62 Stress due to Tandem Axle Load of 400 kN, $\Delta T = 8^\circ\text{C}$, Without Concrete Shoulder

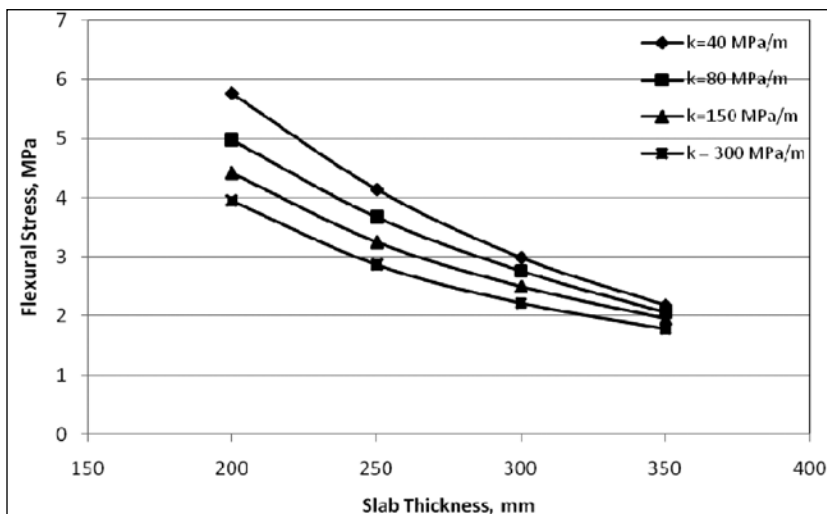


Fig. IV.63 Stress due to Tandem Axle Load of 480 kN, $\Delta T = 8^\circ\text{C}$, Without Concrete Shoulder

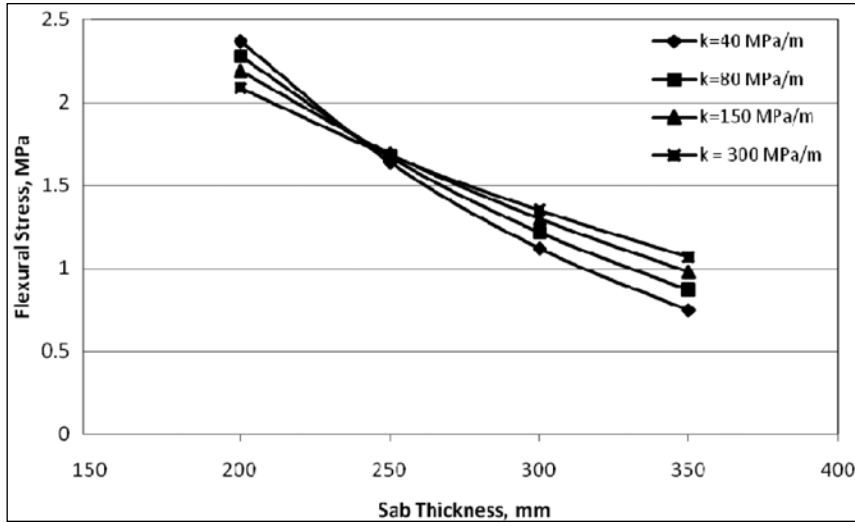


Fig. IV.64 Stress due to Tandem Axle Load of 160 kN, $\Delta T = 13^\circ\text{C}$, Without Concrete Shoulder

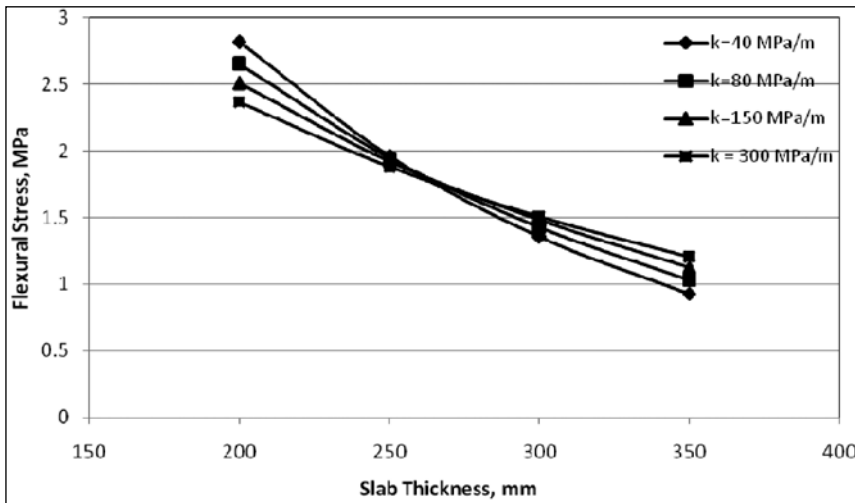


Fig. IV.65 Stress due to Tandem Axle Load of 200 kN, $\Delta T = 13^\circ\text{C}$, Without Concrete Shoulder

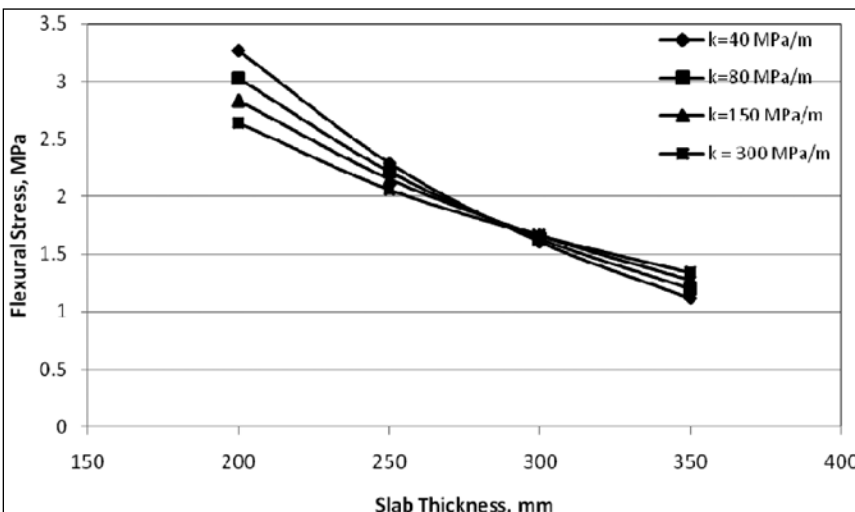


Fig. IV.66 Stress due to Tandem Axle Load of 240 kN, $\Delta T = 13^\circ\text{C}$, Without Concrete Shoulder

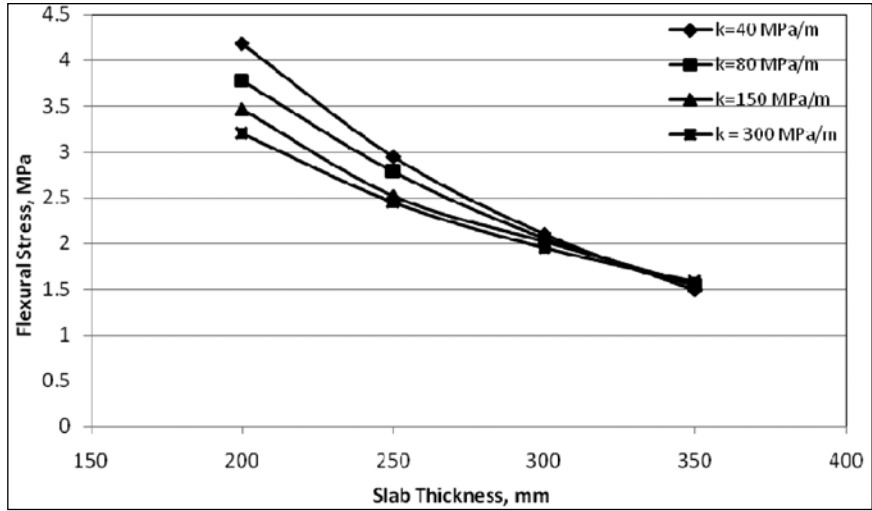


Fig. IV.67 Stress due to Tandem Axle Load of 320 kN, $\Delta T = 13^\circ\text{C}$, Without Concrete Shoulder

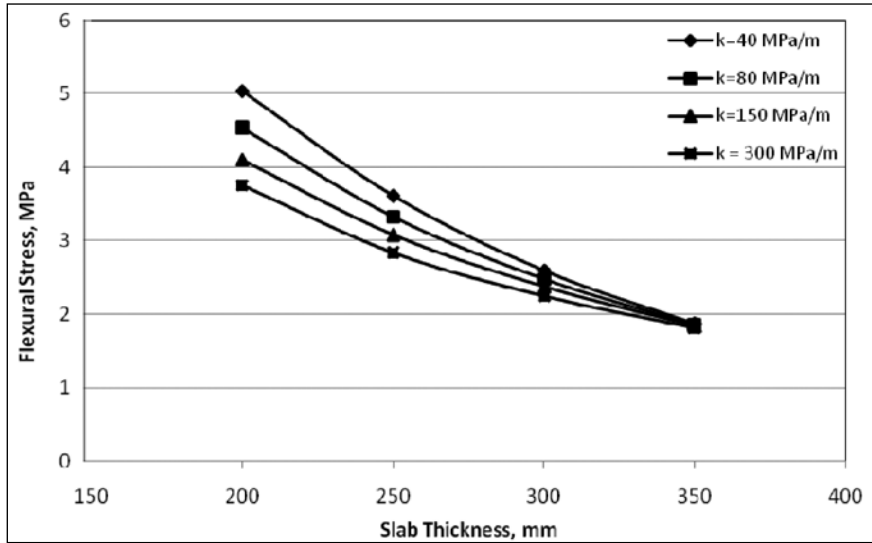


Fig. IV.68 Stress due to Tandem Axle Load of 400 kN, $\Delta T = 13^\circ\text{C}$, Without Concrete Shoulder

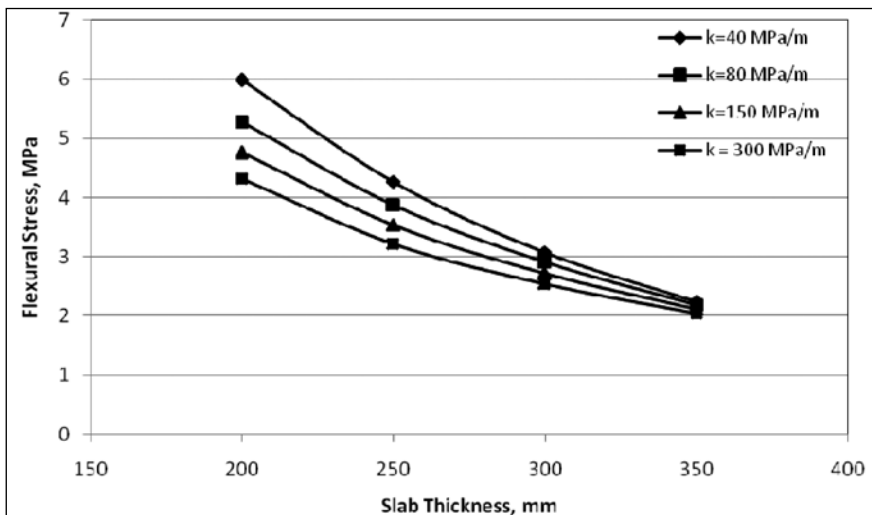


Fig. IV.69 Stress due to Tandem Axle Load of 480 kN, $\Delta T = 13^\circ\text{C}$, Without Concrete Shoulder

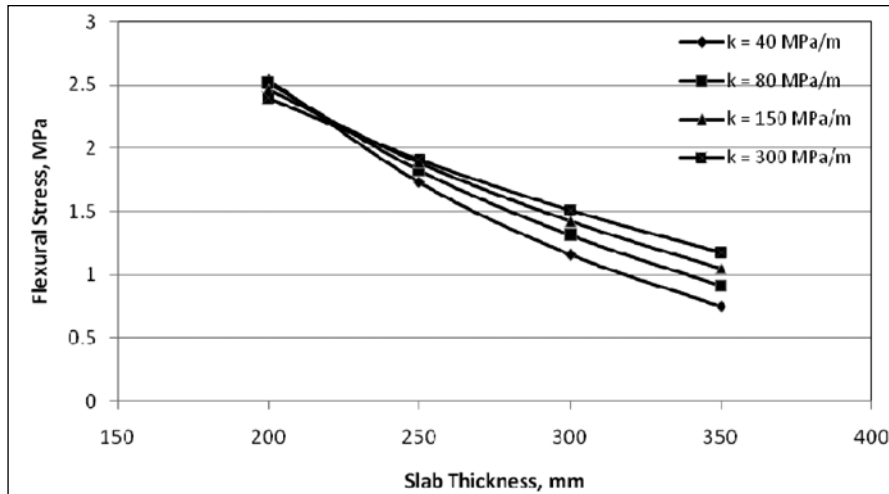


Fig. IV.70 Stress due to Tandem Axle Load of 160 kN, $\Delta T = 17^\circ\text{C}$, Without Concrete Shoulder

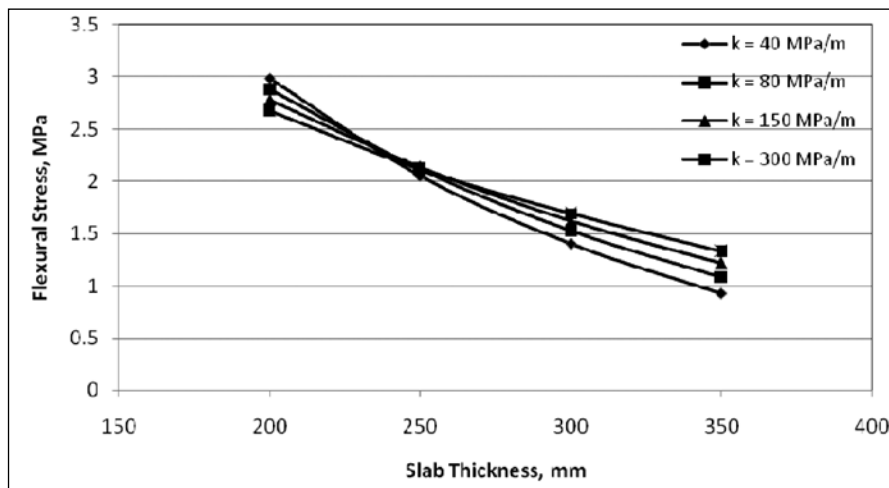


Fig. IV.71 Stress due to Tandem Axle Load of 200 kN, $\Delta T = 17^\circ\text{C}$, Without Concrete Shoulder

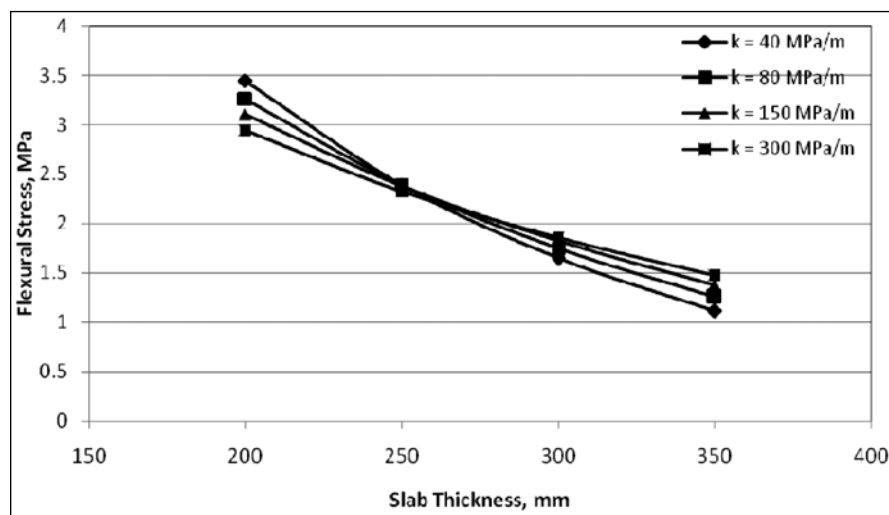


Fig. IV.72 Stress due to Tandem Axle Load of 240 kN, $\Delta T = 17^\circ\text{C}$, Without Concrete Shoulder

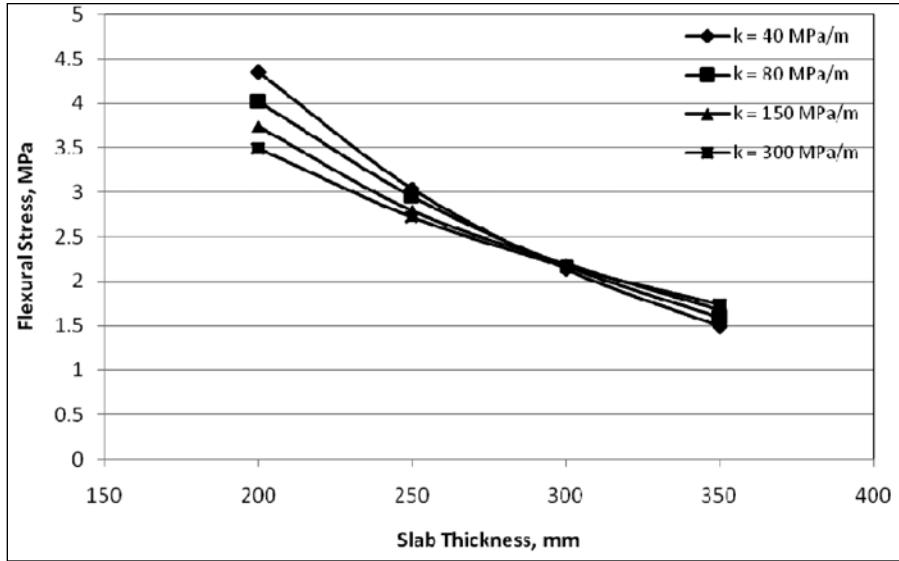


Fig. IV.73 Stress due to Tandem Axle Load of 320 kN, $\Delta T = 17^\circ\text{C}$, Without Concrete Shoulder

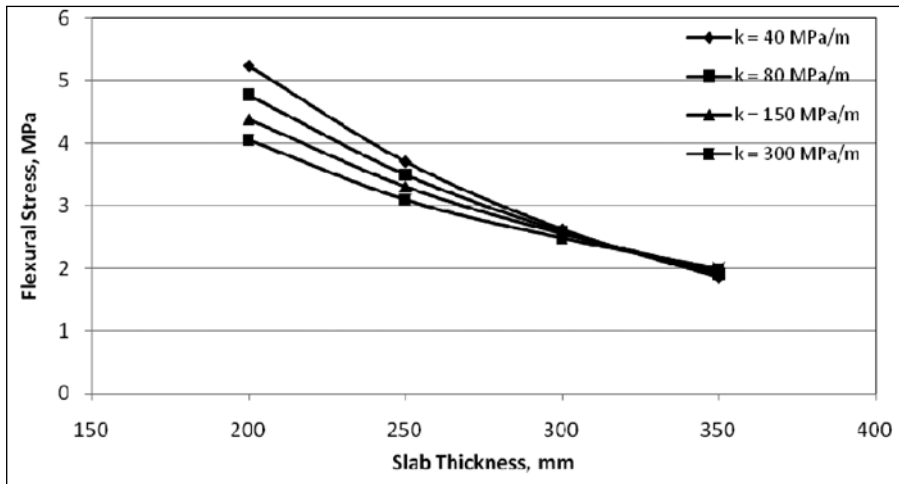


Fig. IV.74 Stress due to Tandem Axle Load of 400 kN, $\Delta T = 17^\circ\text{C}$, Without Concrete Shoulder

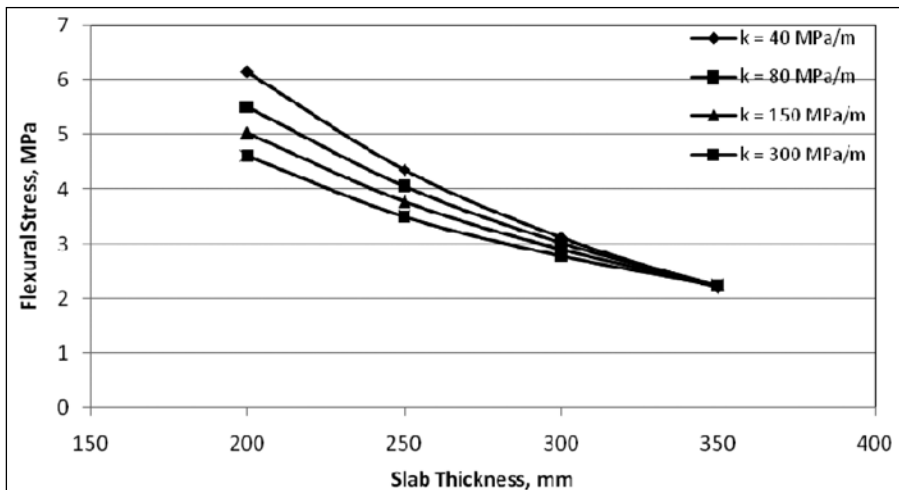


Fig. IV.75 Stress due to Tandem Axle Load of 480 kN, $\Delta T = 17^\circ\text{C}$, Without Concrete Shoulder

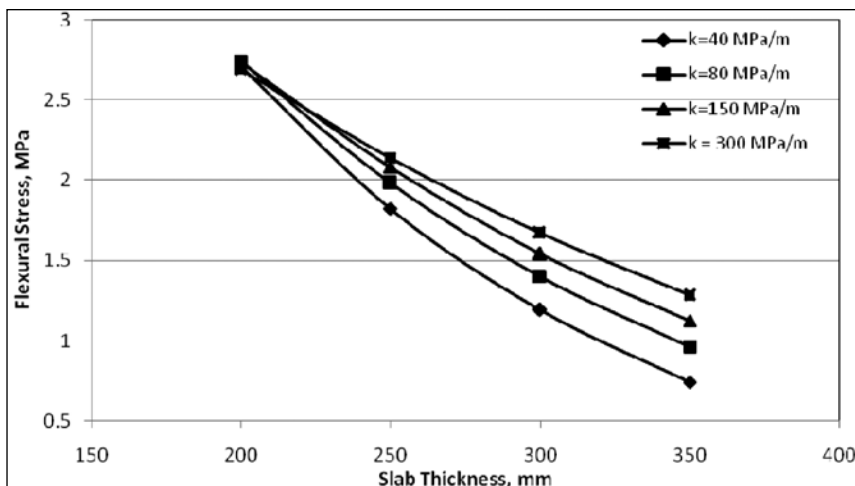


Fig. IV.76 Stress due to Tandem Axle Load of 160 kN, $\Delta T = 21^\circ\text{C}$, Without Concrete Shoulder

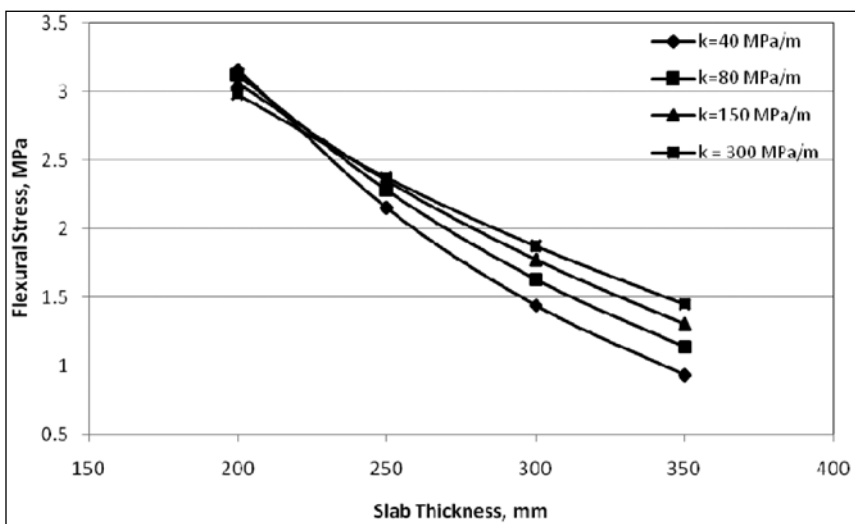


Fig. IV.77 Stress due to Tandem Axle Load of 200 kN, $\Delta T = 21^\circ\text{C}$, Without Concrete Shoulder

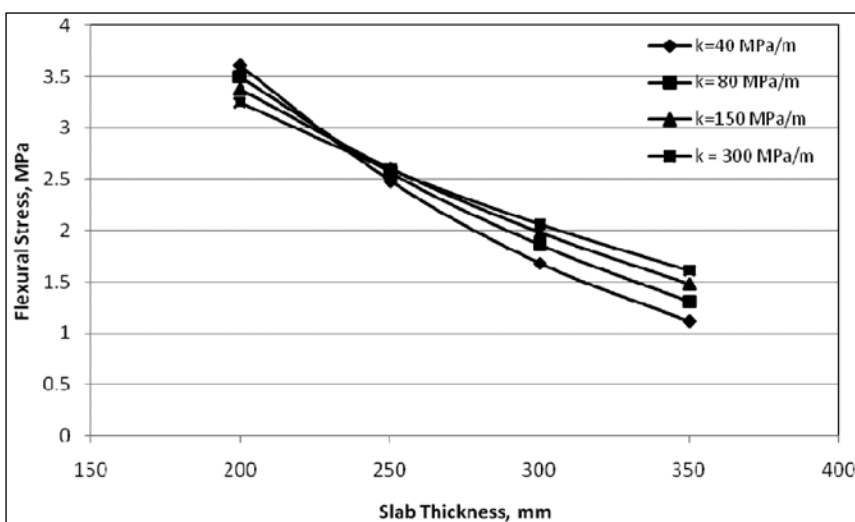


Fig. IV.78 Stress due to Tandem Axle Load of 240 kN, $\Delta T = 21^\circ\text{C}$, Without Concrete Shoulder

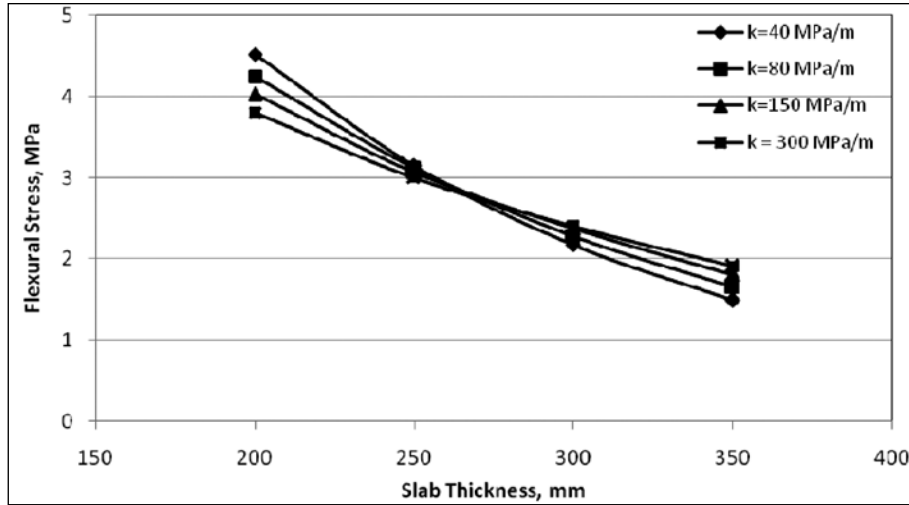


Fig. IV.79 Stress due to Tandem Axle Load of 320 kN, $\Delta T = 21^\circ\text{C}$, Without Concrete Shoulder

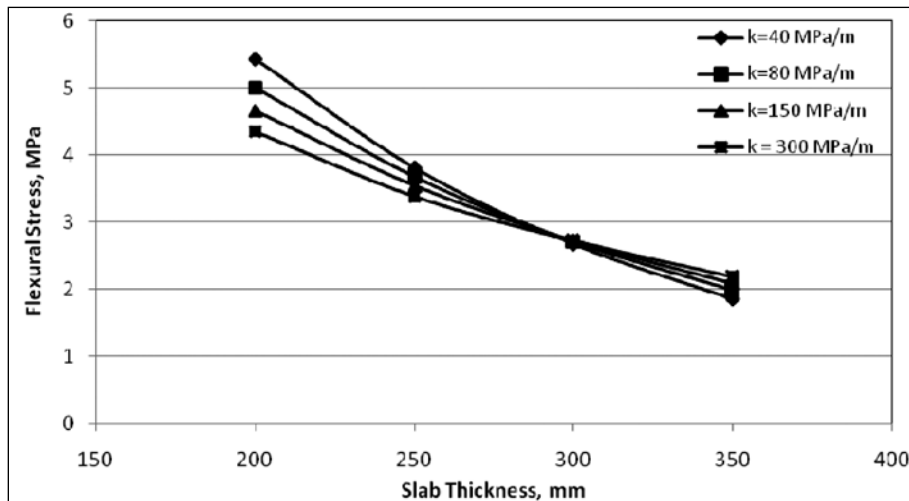


Fig. IV.80 Stress due to Tandem Axle Load of 400 kN, $\Delta T = 21^\circ\text{C}$, Without Concrete Shoulder

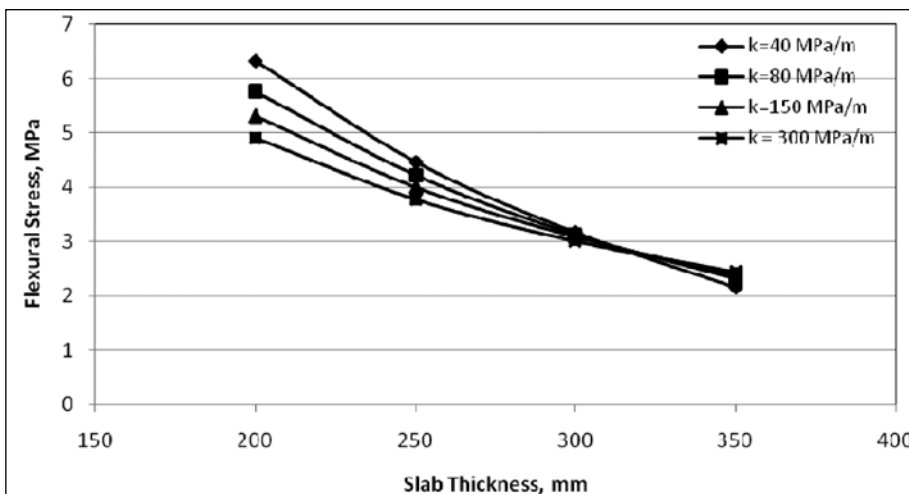


Fig. IV.81 Stress due to Tandem Axle Load of 480 kN, $\Delta T = 21^\circ\text{C}$, Without Concrete Shoulder

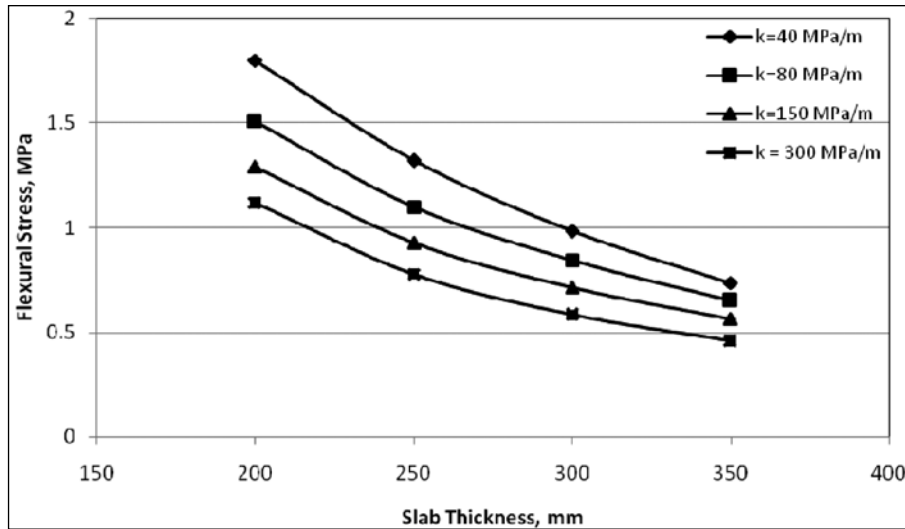


Fig. IV.82 Stress due to Tandem Axle Load of 160 kN, $\Delta T = 0^\circ\text{C}$, With Tied Concrete Shoulders

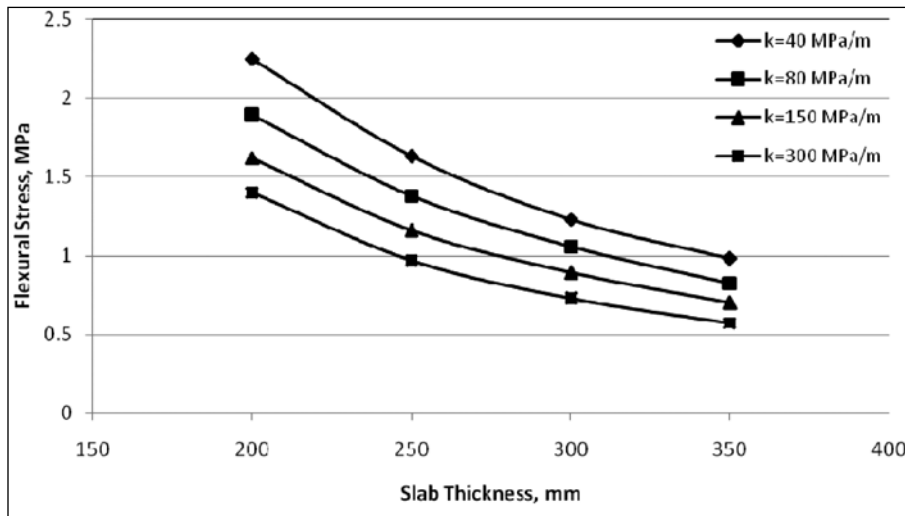


Fig. IV.83 Stress due to Tandem Axle Load of 200 kN, $\Delta T = 0^\circ\text{C}$, With Tied Concrete Shoulders

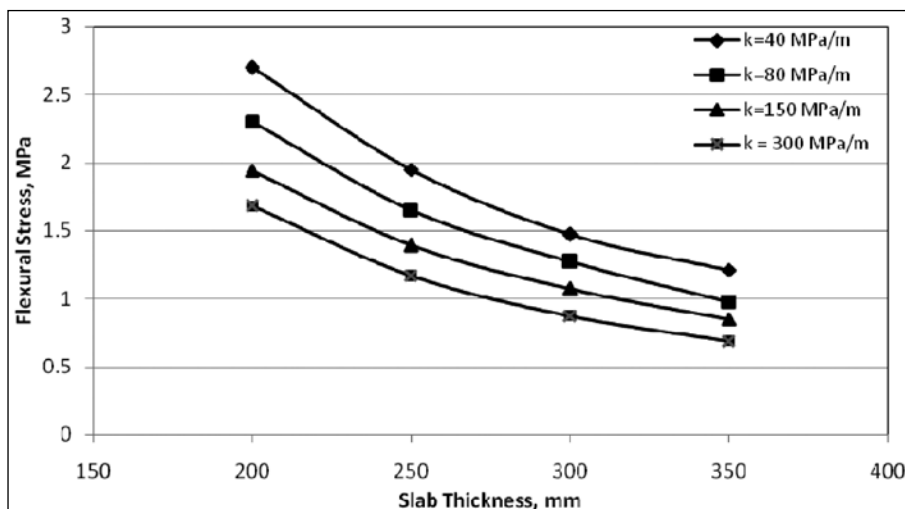


Fig. IV.84 Stress due to Tandem Axle Load of 240 kN, $\Delta T = 0^\circ\text{C}$, With Tied Concrete Shoulders

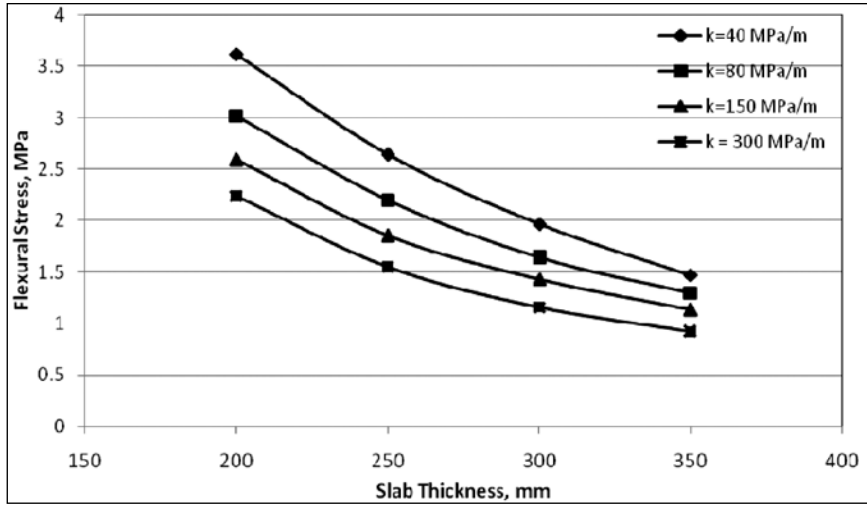


Fig. IV.85 Stress due to Tandem Axle Load of 320 kN, $\Delta T = 0^\circ\text{C}$, With Tied Concrete Shoulders

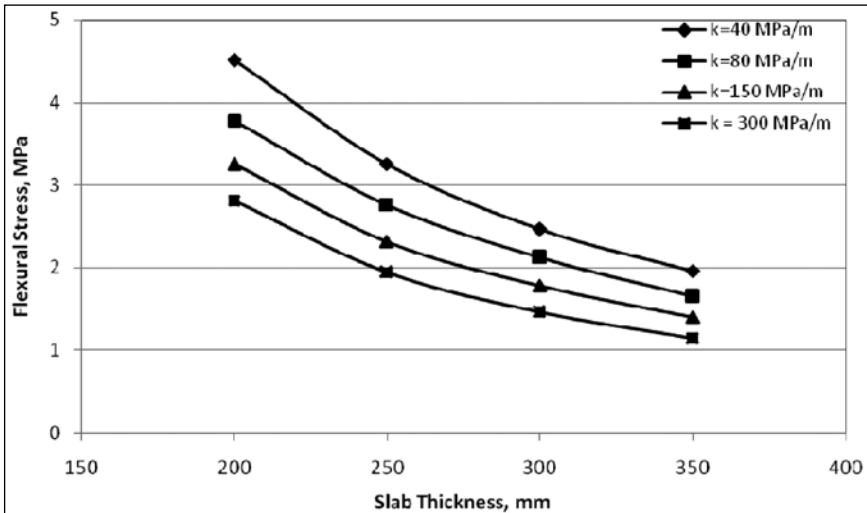


Fig. IV.86 Stress due to Tandem Axle Load of 400 kN, $\Delta T = 0^\circ\text{C}$, With Tied Concrete Shoulders

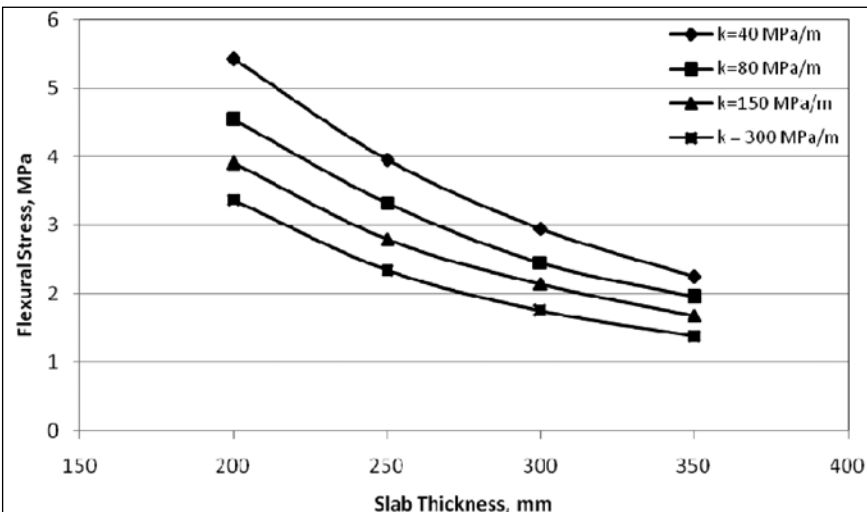


Fig. IV.87 Stress due to Tandem Axle Load of 480 kN, $\Delta T = 0^\circ\text{C}$, With Tied Concrete Shoulders

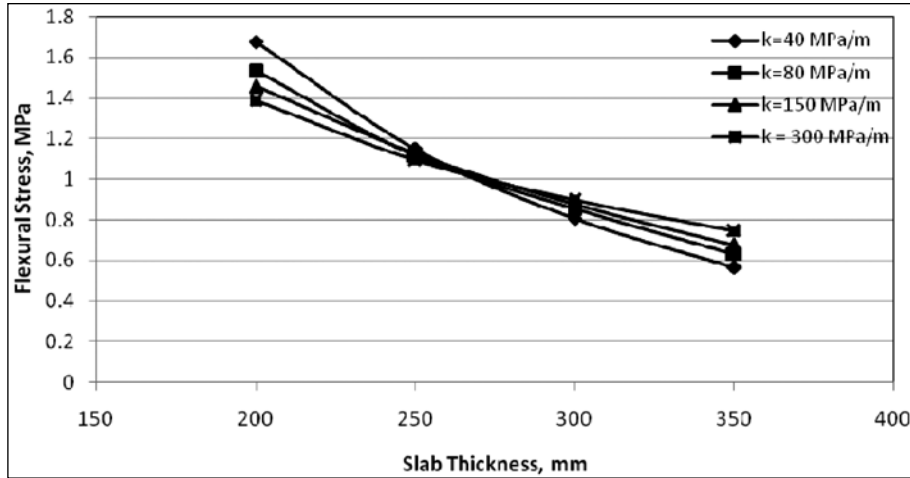


Fig. IV.88 Stress due to Tandem Axle Load of 160 kN, $\Delta T = 8^{\circ}\text{C}$, With Tied Concrete Shoulders

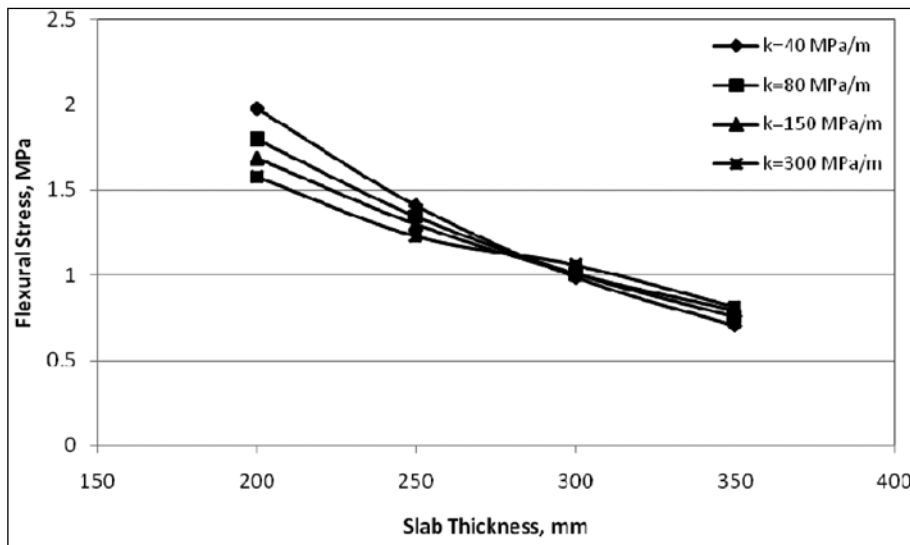


Fig. IV.89 Stress due to Tandem Axle Load of 200 kN, $\Delta T = 8^{\circ}\text{C}$, With Tied Concrete Shoulders

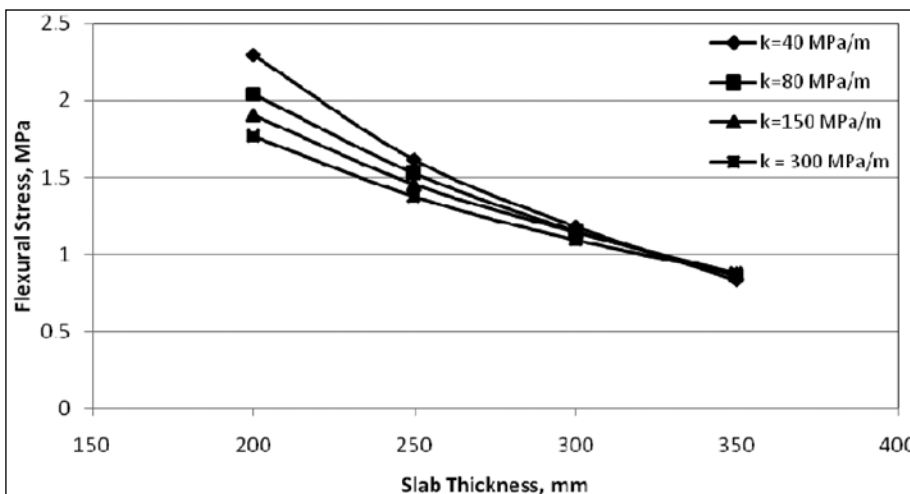


Fig. IV.90 Stress due to Tandem Axle Load of 240 kN, $\Delta T = 8^{\circ}\text{C}$, With Tied Concrete Shoulders

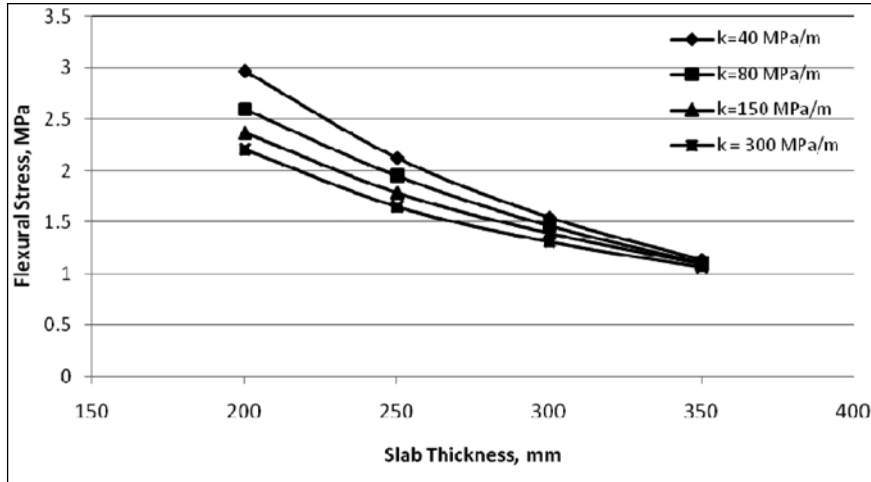


Fig. IV.91 Stress due to Tandem Axle Load of 320 kN, $\Delta T = 8^\circ\text{C}$, With Tied Concrete Shoulders

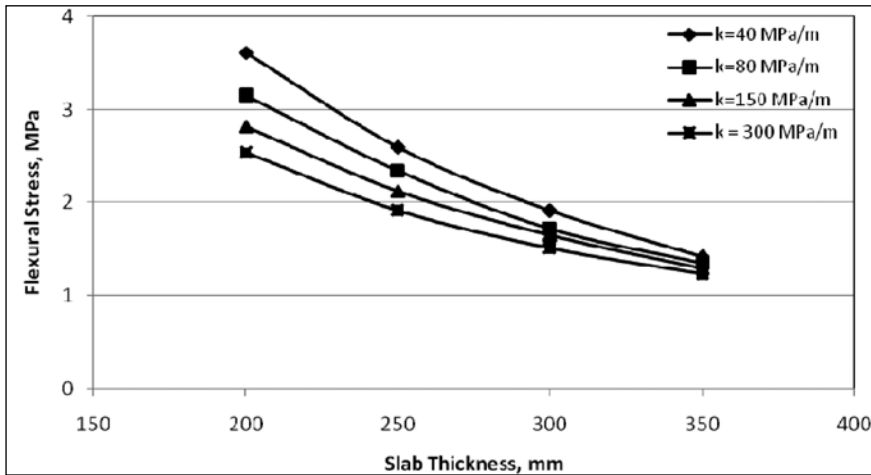


Fig. IV.92 Stress due to Tandem Axle Load of 400 kN, $\Delta T = 8^\circ\text{C}$, With Tied Concrete Shoulders

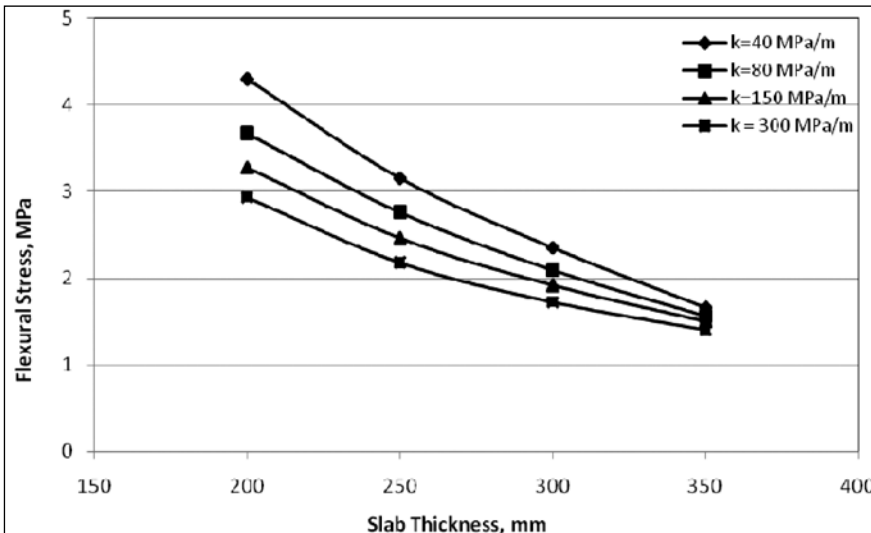


Fig. IV.93 Stress due to Tandem Axle Load of 480 kN, $\Delta T = 8^\circ\text{C}$, With Tied Concrete Shoulders

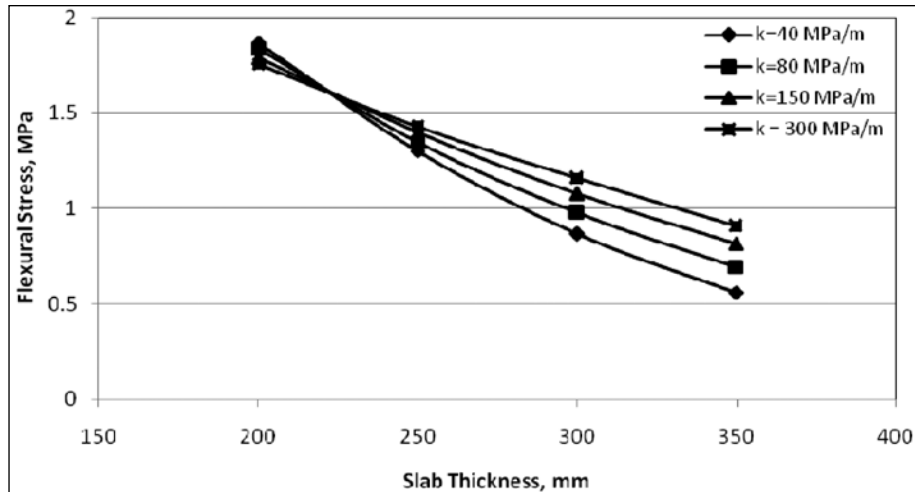


Fig. IV.94 Stress due to Tandem Axle Load of 160 kN, $\Delta T = 13^\circ C$, With Tied Concrete Shoulders

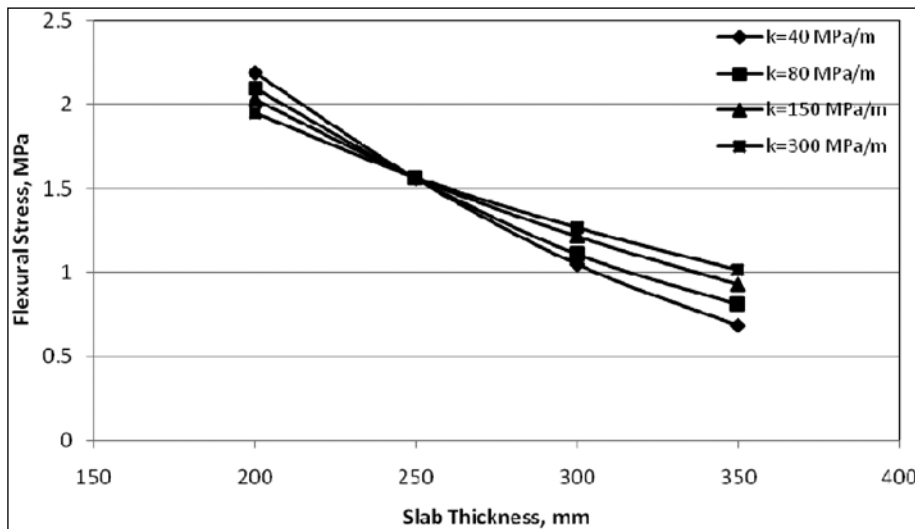


Fig. IV.95 Stress due to Tandem Axle Load of 200 kN, $\Delta T = 13^\circ C$, With Tied Concrete Shoulders

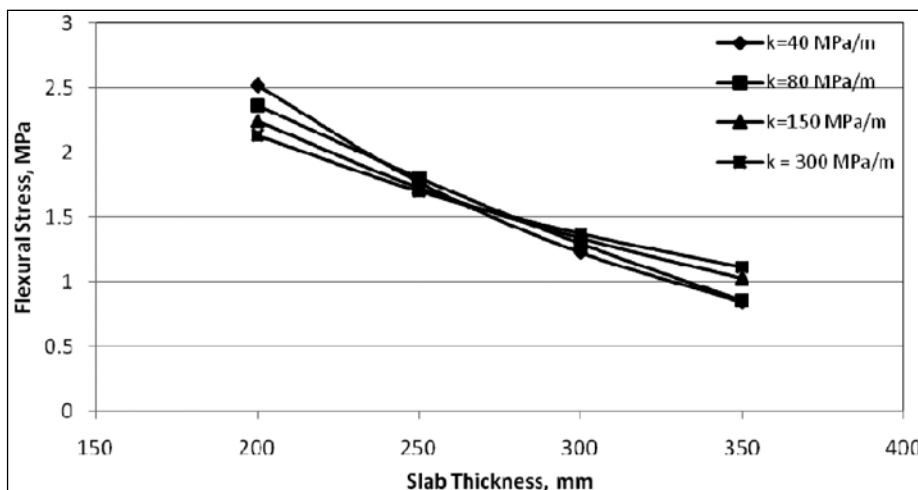


Fig. IV.96 Stress due to Tandem Axle Load of 240 kN, $\Delta T = 13^\circ C$, With Tied Concrete Shoulders

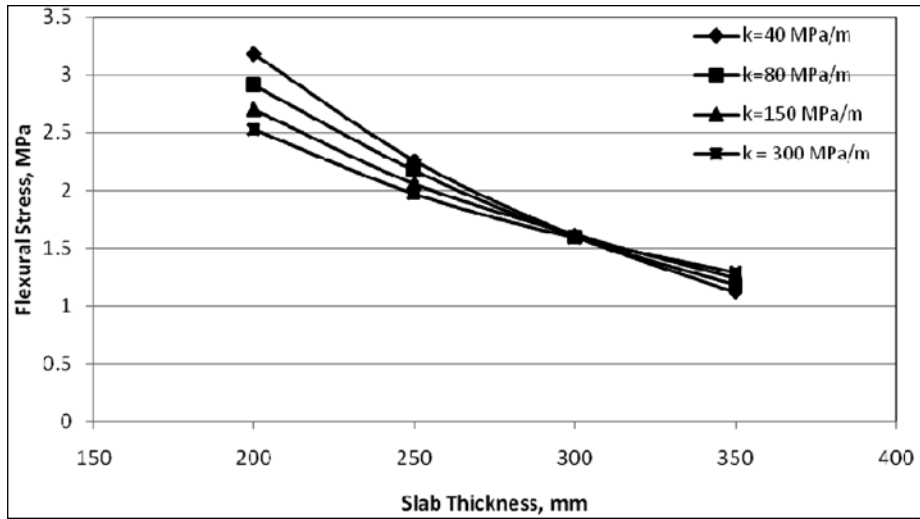


Fig. IV.97 Stress due to Tandem Axle Load of 320 kN, $\Delta T = 13^\circ\text{C}$, With Tied Concrete Shoulders

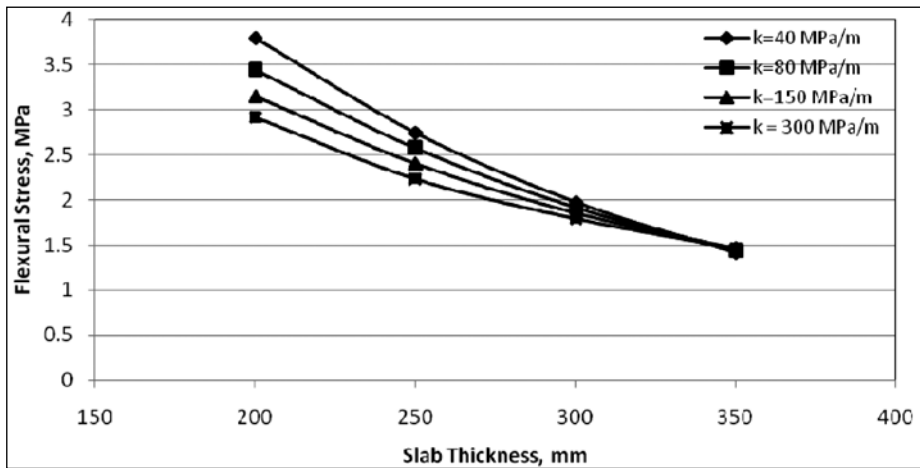


Fig. IV.98 Stress due to Tandem Axle Load of 400 kN, $\Delta T = 13^\circ\text{C}$, With Tied Concrete Shoulders

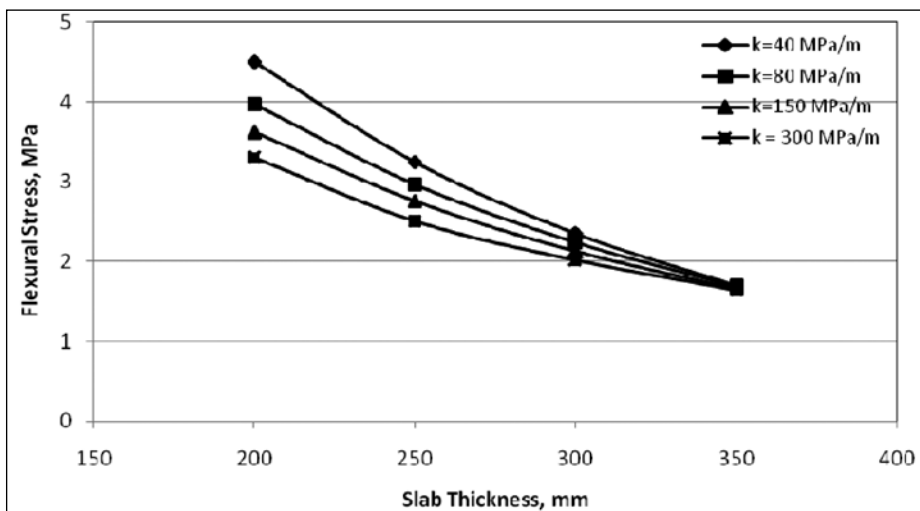


Fig. IV.99 Stress due to Tandem Axle Load of 480 kN, $\Delta T = 13^\circ\text{C}$, With Tied Concrete Shoulders

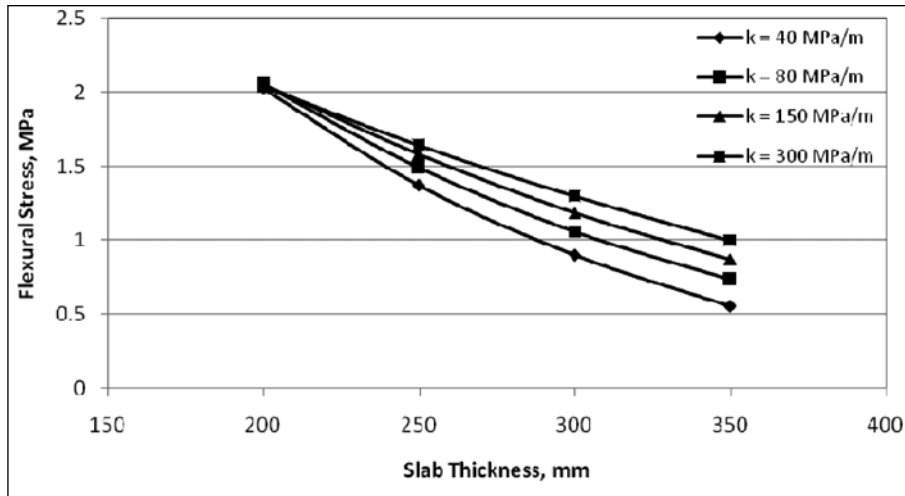


Fig. IV.100 Stress due to Tandem Axle Load of 160 kN, $\Delta T = 17^\circ\text{C}$, With Tied Concrete Shoulders

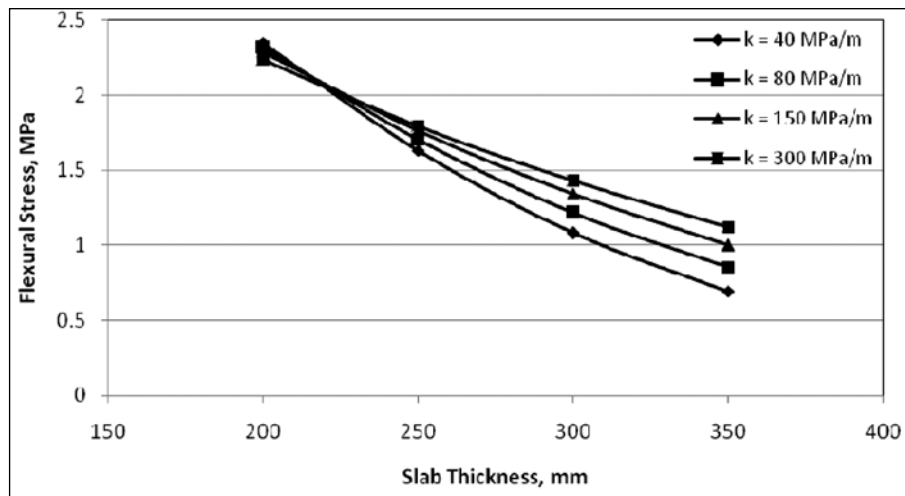


Fig. IV.101 Stress due to Tandem Axle Load of 200 kN, $\Delta T = 17^\circ\text{C}$, With Tied Concrete Shoulders

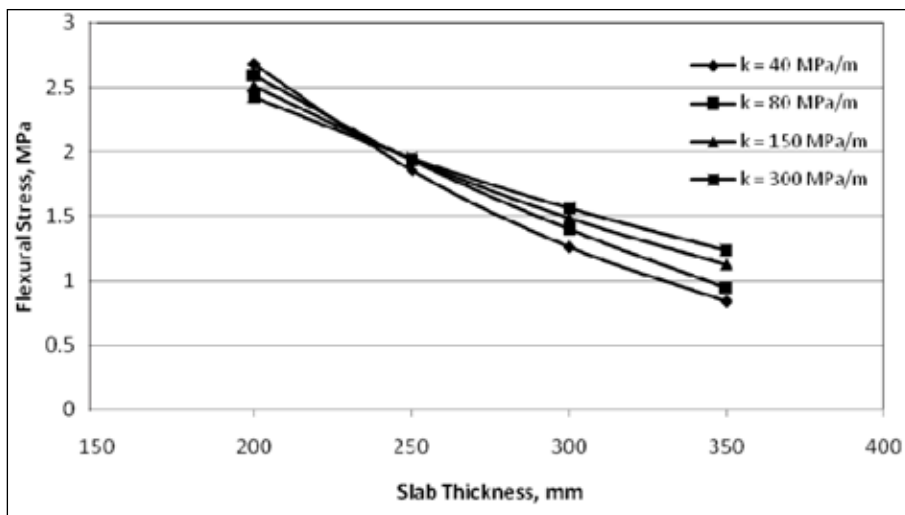


Fig. IV.102 Stress due to Tandem Axle Load of 240 kN, $\Delta T = 17^\circ\text{C}$, With Tied Concrete Shoulders

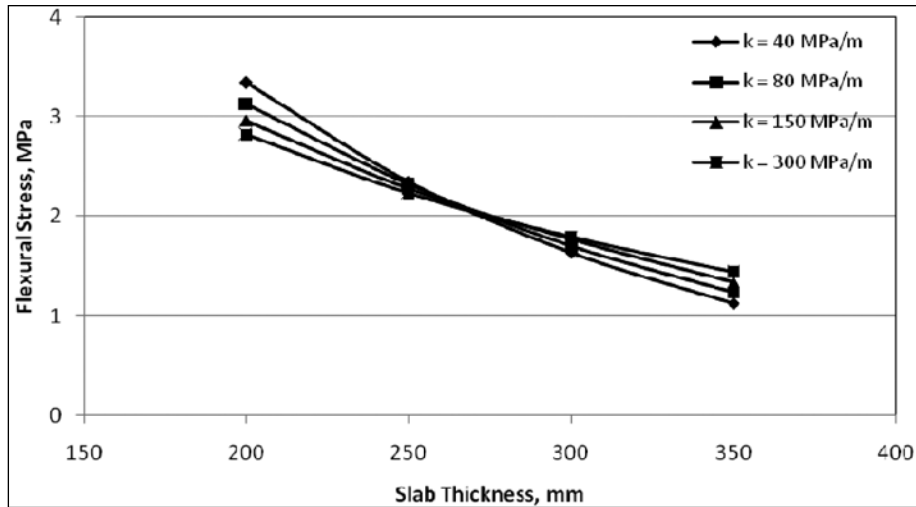


Fig. IV.103 Stress due to Tandem Axle Load of 320 kN, $\Delta T = 17^\circ\text{C}$, With Tied Concrete Shoulders

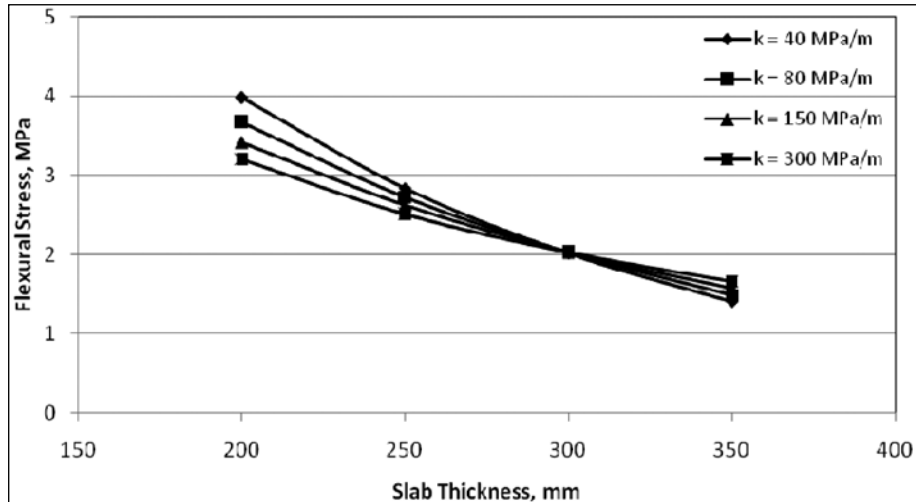


Fig. IV.104 Stress due to Tandem Axle Load of 400 kN, $\Delta T = 17^\circ\text{C}$, With Tied Concrete Shoulders

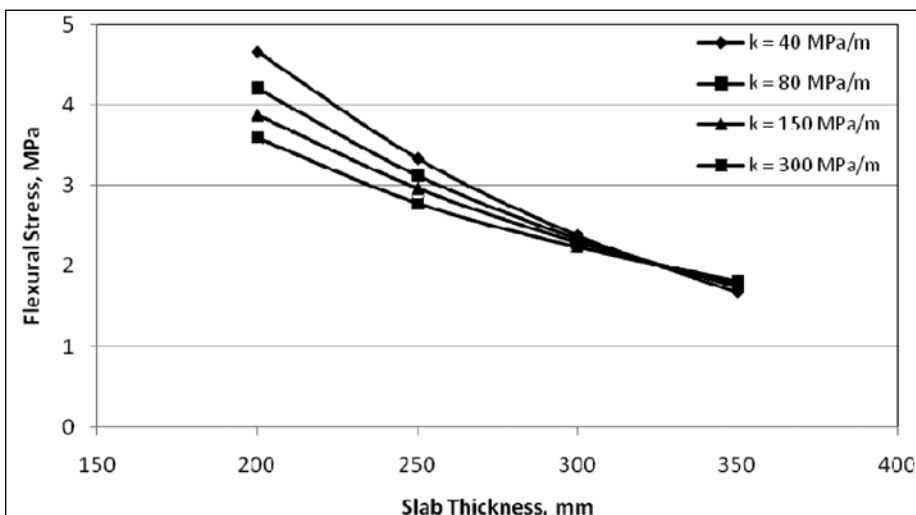


Fig. IV.105 Stress due to Tandem Axle Load of 480 kN, $\Delta T = 17^\circ\text{C}$, With Tied Concrete Shoulders

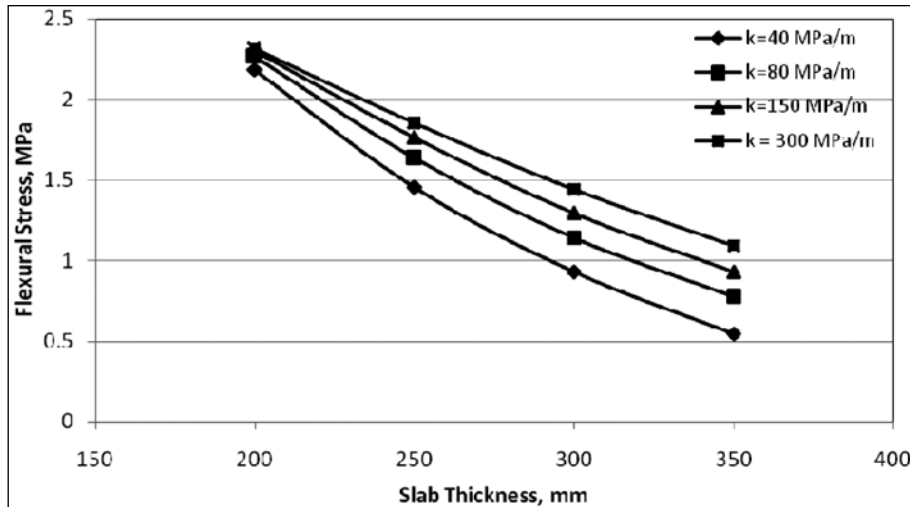


Fig. IV.106 Stress due to Tandem Axle Load of 160 kN, $\Delta T = 21^\circ\text{C}$, With Tied Concrete Shoulders

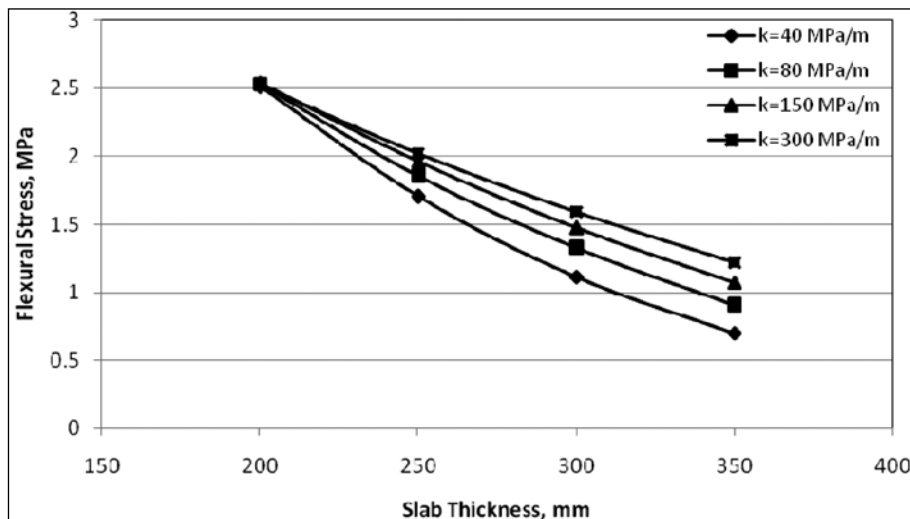


Fig. IV.107 Stress due to Tandem Axle Load of 200 kN, $\Delta T = 21^\circ\text{C}$, With Tied Concrete Shoulders

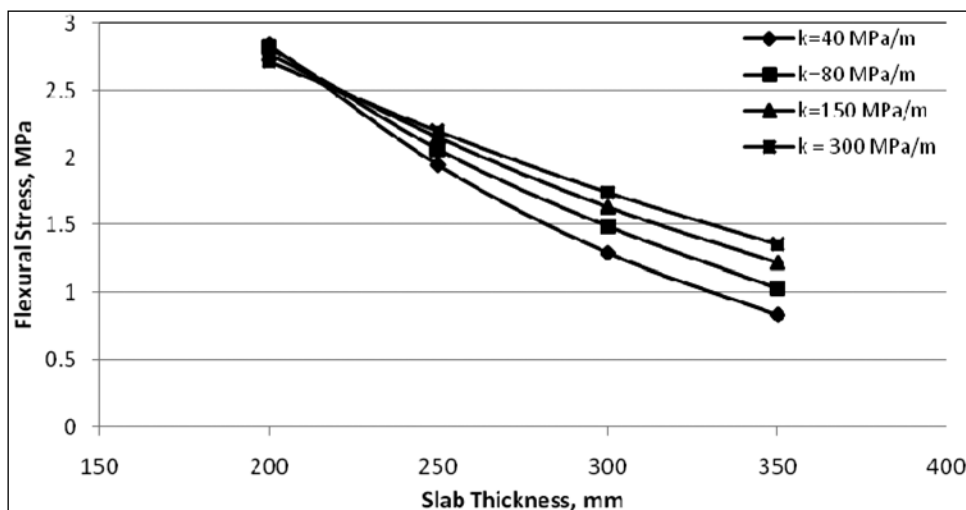


Fig. IV.108 Stress due to Tandem Axle Load of 240 kN, $\Delta T = 21^\circ\text{C}$, With Tied Concrete Shoulders

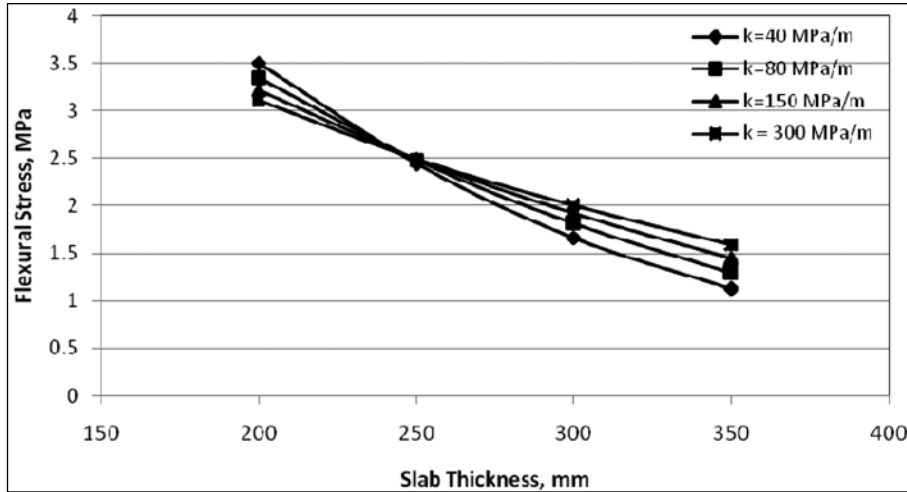


Fig. IV.109 Stress due to Tandem Axle Load of 320 kN, $\Delta T = 21^\circ\text{C}$, With Tied Concrete Shoulders

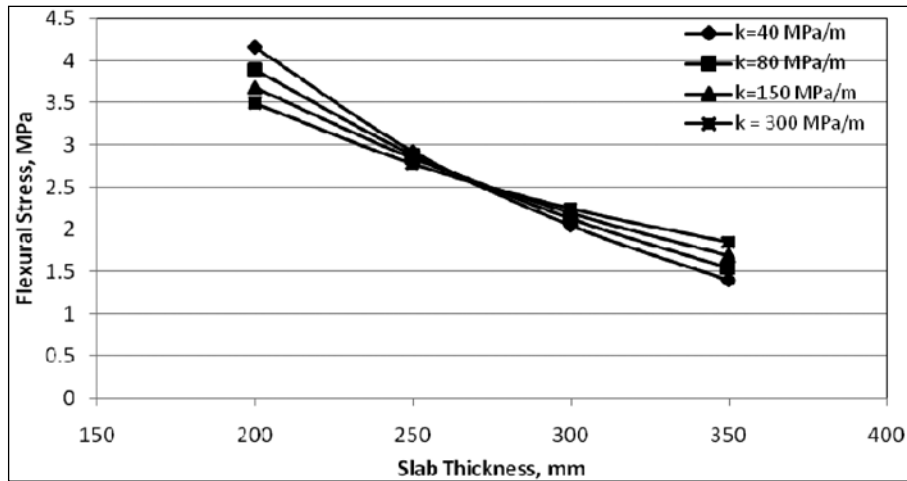


Fig. IV.110 Stress due to Tandem Axle Load of 400 kN, $\Delta T = 21^\circ\text{C}$, With Tied Concrete Shoulders

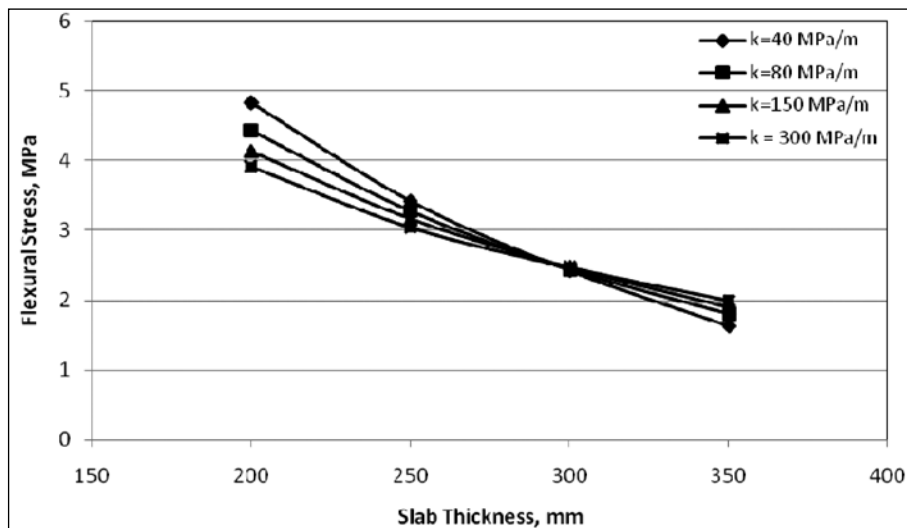


Fig. IV.111 Stress due to Tandem Axle Load of 480 kN, $\Delta T = 21^\circ\text{C}$, With Tied Concrete Shoulders

Appendix - V

Regression Equations for Flexural Stress in Concrete Slab

Regression equations are given in this Appendix for the estimation of the maximum tensile stress in the slab in the edge region due to the combined effect of axle loads and temperature differentials. The equations are included for bottom-up cracking case illustrated in **Figs. 3 and 4** and for top-down case depicted in **Figs. 5 and 6**. Flexural stress for bottom-up cracking has been computed for non-linear positive temperature differential occurring in the slab during day time. The stress for top-down cracking also is due to simultaneous application of axle loads and linear negative temperature differential in the slab in night time.

For the computation of stress for bottom-up cracking analysis, only the rear axles (single as well as tandem) with two wheels (dual wheel sets) on either side of each axle have been considered as the front axles do not contribute to any significant fatigue damage. For top-down cracking, rear axle is considered at one end of the pavement slab and the front axle at the other end. As shown in **Fig. 6**, only one axle of the tandem and tridem axles is assumed to be placed on the slab under consideration. Thus, for a tandem axle, 50% of the tandem axle weight is considered for analysis. For a tridem axle, 33% of the tridem axle weight may be taken for analysis. The corresponding front axle (see **Figs. 5 and 6**) is taken as 50% of the rear axle, (25% of rear tandem axle or one sixth of rear tridem axle loads).

V.1 Expressions for Maximum Tensile Stress at the Bottom of the Slab (for Bottom-up Cracking Case)

Single axle – Pavement with tied concrete shoulders

(a) $k \leq 80$ MPa/m

$$S = 0.008 - 6.12 (\gamma h^2/k^2) + 2.36 Ph/(k^4) + 0.0266 \Delta T \quad \dots (V.1)$$

(b) $k > 80$ MPa/m, $k \leq 150$ MPa/m

$$S = 0.08 - 9.69 (\gamma h^2/k^2) + 2.09 Ph/(k^4) + 0.0409 \Delta T \quad \dots (V.2)$$

(c) $k > 150$ MPa/m

$$S = 0.042 + 3.26 (\gamma h^2/k^2) + 1.62 Ph/(k^4) + 0.0522 \Delta T \quad \dots (V.3)$$

Single axle – Pavement without concrete shoulders

(a) $k \leq 80$ MPa/m

$$S = -0.149 - 2.60 (\gamma h^2/k^2) + 3.13 Ph/(k^4) + 0.0297 \Delta T \quad \dots (V.4)$$

(b) $k > 80$ MPa/m, $k \leq 150$ MPa/m

$$S = -0.119 - 2.99 (\gamma h^2/k^2) + 2.78 Ph/(k^4) + 0.0456 \Delta T \quad \dots (V.5)$$

(c) $k > 150$ MPa/m

$$S = -0.238 + 7.02 (\gamma h^2/k^2) + 2.41 Ph/(k^4) + 0.0585 \Delta T \quad \dots (V.6)$$

Tandem axle – Pavement with tied concrete shoulders

(a) $k \leq 80$ MPa/m

$$S = - 0.188 + 0.93 (\gamma h^2/k^2) + 1.025 Ph/(k^4) + 0.0207 \Delta T \quad \dots (V.7)$$

(b) $k > 80$ MPa/m, $k \leq 150$ MPa/m

$$S = - 0.174 + 1.21 (\gamma h^2/k^2) + 0.87 Ph/(k^4) + 0.0364 \Delta T \quad \dots (V.8)$$

(c) $k > 150$ MPa/m

$$S = - 0.210 + 3.88 (\gamma h^2/k^2) + 0.73 Ph/(k^4) + 0.0506 \Delta T \quad \dots (V.9)$$

Tandem axle – Pavement without concrete shoulders

(a) $k \leq 80$ MPa/m

$$S = - 0.223 + 2.73 (\gamma h^2/k^2) + 1.335 Ph/(k^4) + 0.0229 \Delta T \quad \dots (V.10)$$

(b) $k > 80$ MPa/m, $k \leq 150$ MPa/m

$$S = - 0.276 + 5.78 (\gamma h^2/k^2) + 1.14 Ph/(k^4) + 0.0404 \Delta T \quad \dots (V.11)$$

(c) $k > 150$ MPa/m

$$S = - 0.3 + 9.88 (\gamma h^2/k^2) + 0.965 Ph/(k^4) + 0.0543 \Delta T \quad \dots (V.12)$$

V.2 Expression for Maximum Tensile Stress at the Top of the Slab (for Top-down Cracking Case)

For the analysis of top-down cracking, only rear axle load is the input. Front axle load is assumed to be 50% of the rear axle load (tandem/tridem).

$$S = - 0.219 + 1.686BPh/k^4 + 168.48h^2/k^2 + 0.1089 \Delta T \quad \dots (V.13)$$

The symbols in the equations have the following meaning:

S	=	flexural stress in slab, MPa
ΔT	=	maximum temperature differential in °C during day time for bottom-up cracking
	=	sum of the maximum night time negative temperature differential and built-in negative temperature differential in °C for top-down cracking
h	=	thickness of slab, m
k	=	effective modulus of subgrade reaction of foundation, MPa/m
l	=	radius of relative stiffness = $\{Eh^3/(12k(1-\mu^2))\}^{0.25}$
E	=	elastic modulus of concrete, MPa
μ	=	Poisson's ratio of concrete
γ	=	unit weight of concrete (24 kN/m ³ , density = 2400 kg/m ²)
P	=	For Bottom-up cracking analysis :- single/tandem rear axle load (kN). No fatigue damage is computed for front (steering) axles for bottom-up cracking case.

- = For Top-down cracking analysis :- 100% of rear single axle, 50% of rear tandem axle, 33% of rear tridem axle. Front axle weight is not required to be given as input for top-down cracking case in equation V.13. 50% of rear single axle, 25% of rear tandem axle, 16.5% of rear tridem axle, have been considered in the finite element analysis as the front axle weights for single, tandem and tridem rear axles respectively.
- B
 - = 0.66 for transverse joint with dowel bars (load transfer efficiency was taken as 50%)
 - = 0.90 for transverse joint without dowel bars (load transfer efficiency was taken as 10%)

Appendix - VI

Permeability of Drainable Subbase and Design of Drainage Layer

VI-I International Practice for Drainage Layers

A good subsurface drainage is a standard practice in all major highways in developed countries. A drainage layer must have enough permeability to drain away the water in accordance with the design criteria and must have enough stability during the construction Phase. Thus, the drainage layer must meet the necessary requirements for both permeability and stability. These requirements are at opposite ends of a materials spectrum. The more permeable a materials; the more unstable it will be and vice versa. Hence proper balance pf permeability and stability is desirable. Various gradations of aggregates for the drainage layer are in use due to a large variation in climate in different regions depending upon the local experience but most of them have high permeability. Federal Highway Administration of USA recommends a minimum permeability of 300 metre per day (1000 feet/day) for drainage layer for high volume roads with a rider that the regional experience shall govern the choice of the drainage materials. American Concrete Pavement Association (APCA) recommends a permeability of about 107 m/day for the unstabilised aggregate drainage layer below concrete pavements. A number of gradations for permeable drainage layers commonly used by different Departments of Transport in USA including those from AASHTO 93 pavement design guide are shown **Table VI-I**. Highly permeable AASHTO 57 grading of the Table is also used by many state highway agencies in USA. Engineers have a wide range of choice and any of the gradations that are available can be selected. Stabilisation is necessary for the stability of open graded aggregates. Conservative design for drainage layer is necessary to guard against pavement failure observed in India within five years of the construction due to deformation in GSB and the subgrade layers due to heavy loads and moisture.

Table VI-I Gradations and Permeability of Granular Subbase for Drainage as per US Practice

Sieve Size, mm	AASHTO57 Cement/ Bitumen Treated	California Bitumen Treated	Wisconsin Cement Treated	New Jersey Bitumen Treated	Viginia Cement Treated	AASHTO 93, Page I-19 Grading 4,5 and 6 (Unstabilised)		
	1	2	3	4	5	6	7	8
53								
37.5	100							
25.4	95-100	100	100	100	100			
19.5		96-100	90-100	95-100		100	100	100
12.5	25-60	35-65		85-100	25-60	81.5	79.5	75
9.5		20-45	20-55	60-90		72.5	69.5	63
4.75	0-10	0-10	0-10	15-25	0-10	49	43.5	32
2.36	0-5	0-5	0-5	2-10	0-5	29.5	22	5.8
1.18						16	5	0
0.30						0	0	0

Sieve Size, mm	AASHTO57 Cement/ Bitumen Treated	California Bitumen Treated	Wisconsin Cement Treated	New Jersey Bitumen Treated	Viginia Cement Treated	AASHTO 93, Page I-19 Grading 4,5 and 6 (Unstabilised)		
	1	2	3	4	5	6	7	8
0.075	0-2	0-2	0-5	2-5		0	0	0
Permeability Approximately (Averagem per day)	6600 m/day	5000 m/ day	3000 m/ day	300 m/day	3000 m/day)	350 m/ day	850 m/day	950 m/day

As per the US practice, the concrete pavement slab is laid directly over the cement treated drainage layer known as permeable base and hence the stability of the drainage layer is vital for good performance of concrete pavement. The open graded cement treated permeable base is also required to stand the construction traffic. In India, a much stronger DLC layer bears all the construction traffic and it also provides a strong support to the pavement slab. Hence, any of the grading 4, 6 and 7 of **Table VI-I** containing relatively higher fines contents than the others can be used without stabilization to form to provide a proper balance between permeability and stability. For gradations 1, 2, 3, 5 and 8, stabilization may be necessary to impart stability. The aggregates for the highly permeable drainage layers are predominantly coarser than 4.75 mm. The filter/separation layer placed above the subgrade must prevent intermixing of the subgrade soil and the drainage layer by preventing entry of the subgrade soil into the drainage layer and should satisfy the criteria laid down in IRC:37, IRC:SP:42 and IRC:SP:50.

VI-II Permeability of Single Size Aggregates

Effect of bitumen treatment on permeability of aggregates is shown in **Table VI-II**

Table VI-II Effect of Bitumen Treatment on Permeability (Cedergren)

S. No.	Aggregate size, mm	Permeability m/day	
		Untreated	Treated with 2% Bitumen
1	38-25.4 mm	46000	40000
2	20-9.5 mm	33000	31600
3	4.75-2.36 mm	2600	2000

It can be seen that the effect of bitumen treatment is only marginal if open graded aggregates are treated with bitumen. Cement treatment also will have similar effect. The open graded aggregates with maximum sizes of 20 mm and 4.75 mm shown in S.N. 2 and 3 of **Table VI-II** can also have a high permeability and a thickness of 75 mm also may be sufficient to drain away the water. The minimum recommended thickness for the drainage layer is 100mm for which the maximum aggregate size should be about 40 mm.

VI-III Relation Between Effective Aggregate Size, Uniformity Coefficient and Coefficient of Permeability

It may not always be possible to determine the permeability of the drainage layer. Some simple well established guidelines can be used to adopt the right type of drainage layer which will have reasonably good permeability. The permeability of a drainage layer depends to a great extent upon the effective aggregate size (D_{10}) and Uniformity coefficient (C_u).

where,

D_{10} = effective aggregate size mm, (corresponding to 10% finer than D_{10})

D_{60} = particle size, mm (corresponding to 60% finer than D_{60}),

$$C_u = D_{60}/D_{10}$$

Greater the value of D_{10} , greater is the permeability. The value of D_{10} greater than 2 mm is adopted for highly permeable aggregates. $C_u = 1$ for single size aggregates. Lower the value of C_u , greater is the permeability and but lower is the stability. $C_u = 40$ for dense graded aggregates. The Uniformity Coefficient, C_u , is an indicator of the spread of the particle sizes between the 10 and 60 percent particle sizes. This, in turn, is an indicator of the gradation's permeability and stability:

For a good drainage layer, C_u should be between 2 and 8. If C_u is less than 4, the drainage layer has a high permeability but the layer is unstable and it must be stabilised with cement or bitumen for heavy traffic pavements.

VI-IV Permeability of Granular Subbase as per the MORTH

The granular subbase having as per Section 401.2.2 of MORTH have permeability values less than 12 m/day as per the laboratory tests and they are not suitable for drainage layers. Only lower gradation limits of Grades III and VI have the C_u values close to 5 and will have the required permeability. The gradations for good drainage layers are shown in **Tables VI-I**. Thickness of highly permeable layer can be much less if permeability is high as shown in the example given in the section later.

While a new concrete pavement is practically impermeable, longitudinal and transverse joints open up due to oxidation of the sealing material, expansion and contraction of the slabs. Cracks in the pavement slabs may also form due to deformation of the foundation caused by heavy commercial vehicles aggravated in the presence of moisture or by settlement. Water may thus enter into the pavements through the joints and cracks.

VI-V Quantum of Water Entering into Pavements

There two methods of estimation of the amount water that enters into a pavement.

- I) Infiltration ratio method (Cedergrain)
- II) Crack infiltration method (Ridgeway)

Certain percentage(50 to 67%)of hourly rainfall of one year frequency is assumed to enter into a rigid pavement in the infiltration ratio method. In the crack infiltration method, water

enters through joints and cracks in the pavement. Any method can be used but widely used crack infiltration method of Ridgeway is adopted in the guidelines.

VI-VI Estimation of Permeability Requirement

The required permeability of the drainage layer can be estimated by two methods as discussed below.

- I) In the first method, the permeability of the drainage layer is selected depending upon the quality of drainage selected as defined in AASHTO 93 Pavement Design Guide. The quality of drainage is determined by the time required for the pavement to drain from a saturated condition. The time is less than two hours for an excellent drainage for a high volume pavement and less than one day for a good drainage (AASHTO 93). The time-to-drain approach is based on water entering the pavement until the permeable base is saturated. Excess run off will not enter the pavement section after it is saturated because the water will simply run off on the pavement surface. After the stoppage of rain, the base will drain to embankment slope or into the edge-drain system if provided. Engineers may select a permeability of the drainage layer to drain relatively quickly to prevent the pavement from being damaged. The quantum of water entering into the pavement can be estimated by infiltration ratio method or by crack infiltration method.
- II) In the second method, the permeability is so selected that total outflow capacity of the drainage layer is be greater than the inflow of rainwater into the pavement. This approach has been adopted in the example given below. The time to drain approach also can be adopted as per the AASHTO 93 guidelines.

VI-VII Water from Median

Water entering into the pavements from earthen medians may be very damaging if care is not taken to prevent entry of water along with fines into the drainage layer. Choking of drainage layer with soils entering into the drainage layer in the median side should be avoided by using a filter layer or nonwoven geotextile. Cares should be taken to ensure that the exposed drainage layer along the embankment slope is not covered with earth while rectifying the erosion of the side slope after the rain. Blockage of a drainage layer may cause a much serious problem than with no drainage layer. Several cases of drainage problems are described in IRC:37, IRC:42 and IRC:50.

VI-VIII Example of Design of a Drainage Layer

A four-lane divided cement concrete pavement will be constructed for a high traffic volume road in an area having an annual rainfall of 1500 mm/year. The width of each carriageway will be 7.0 m. 2.5 m wide shoulders (1.5 m concrete, 1.0 m unpaved) will be provided. Transverse joint spacing will be 4.5 m. The highway has a longitudinal gradient of 3 percent and a camber of 2.5 percent. Side slopes of embankment are 2:1 (horizontal to vertical). The pavement has

a 300 mm thick concrete slab placed over 150 mm thick DLC layer. Estimate the requirement of permeability of the drainage layer material to be used if the layer thickness is 150 mm.

Solution:

- Combined thickness of the slab and DLC layer = 300 + 150 = 450 mm.
- The drainage layer will be provided below the DLC layer at a depth of 450 mm from pavement surface. The drainage layer will be extended to the full width of embankment.
- Width of drainage layer = 7 m (pavement) + 2.5 m (shoulder) + 2 x 0.45 m = 10.4 m
- **Fig. VI.1** indicates the direction of flow of water along AD (diagonal)
- In **Fig. VI.1**, AB = 10.4 m; AC = 10.4 x (0.03/0.025) = 12.48 m; AD = $(10.4^2 + 12.48^2)^{0.50} = 16.24$ m
- Drop of elevation along AC = 12.48 x 0.03 = 0.374 m; Elevation drop along CD = 10.4 x 0.025 = 0.26 m; Elevation drop along AD = 0.374 + 0.260 = 0.634 m
- Gradient along AD = I = drop along AD/ length of AD = 0.634/16.24 = 0.039

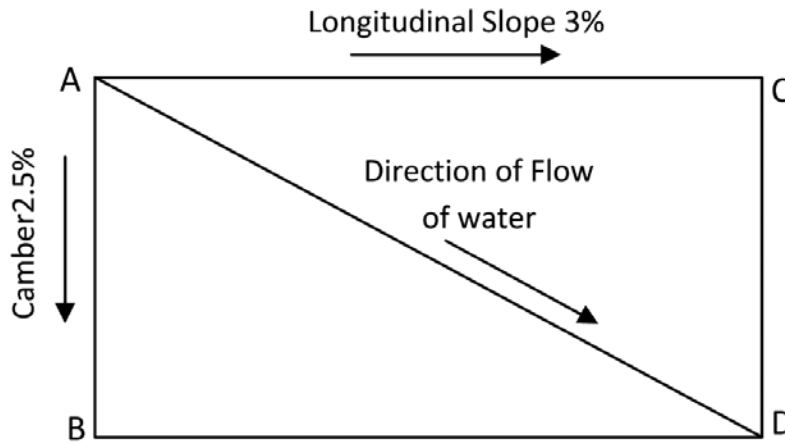


Fig. VI.1 Direction of Water Flow

- The infiltration rate per unit area q_i can be estimated using equation 9 of the guidelines. The equation is reproduced here for convenience.

- $q_i = I_c \left(\frac{N_c}{W_p} + \frac{W_c}{C_s W_p} \right) + K_p$

where,

- I_c = crack infiltration rate = 0.223 m³/day/m
- N_c = number of longitudinal joints/cracks = 3 (joint between lanes, between lane and shoulder and paved shoulder edge)
- W_p = width of pavement subjected to infiltration = 7.0 + 2.5 = 9.5 m

- W_c = length of the transverse cracks or joints = $7.0 + 1.5 = 8.5$ m
- C_s = spacing of transverse joints = 4.5 m
- D_p = rate of infiltration through un-cracked pavement surface = nil(0 m³/day/m²)
- Thus, the rate of infiltration of water into pavement, $q_i = 0.115$ m³/day/m²
 - Amount of infiltrated water per meter length flowing along the path AD of the drainage layer, $Q = 16.24$ (length of AD)* 0.115 = 1.868 m³/day per meter width of drainage layer along AD. Let K = coefficient of permeability (m/day), A = area of the drainage layer along AD per metre width
 - Rate of flow through drainage layer, $Q = KIA$. Since $I = 0.039$, $KA = 1.868/0.039 = 47.89$.
 - $A = 1 \times 0.15 = 0.15$ m² assuming depth of the drainage layer as 150 mm.
 - Hence, the required coefficient of permeability, $K = 47.89/0.15 = 319$ m/day.
 - If thickness of the drainage layer is 300 mm, the required $K = 160$ m/day.

Appendix - VII

Illustrative Examples of Thickness Design

Example

A cement concrete pavement is to be designed for a four-lane divided National Highway with two lanes in each direction in the state of Bihar. Design the pavement for a period of 30 years. Lane width = 3.5 m; transverse joint spacing = 4.5 m.

It is expected that the road will carry, in the year of completion of construction, about 3000 commercial vehicles per day in each direction. Axle load survey of commercial vehicles indicated that the percentages of front single (steering) axle, rear single axle, rear tandem axle and rear tridem axle are 45%, 15%, 25% and 15% respectively. The percentage of commercial vehicles with spacing between the front axle and the first rear axle less than 4.5 m is 55%. Traffic count indicates that 60% of the commercial vehicles travel during night hours (6 PM to 6 AM).

Details of axle load spectrum of rear single, tandem and tridem axles are given in **Table VII.1**. Front (steering) axles are not included. The average number of axles per commercial vehicle is 2.35 (due to the presence of multi-axle vehicles).

Table VII.1 Axle Load Spectrum for Example

Single Axle		Tandem Axle		Tridem Axle	
Axle Load Class kN	Frequency (% of Single Axles)	Axle Load Class kN	Frequency (% of Tandem Axles)	Axle Load Class kN	Frequency (% of Tridem Axles)
185-195	18.15	380-400	14.5	530-560	5.23
175-185	17.43	360-380	10.5	500-530	4.85
165-175	18.27	340-360	3.63	470-500	3.44
155-165	12.98	320-340	2.5	440-470	7.12
145-155	2.98	300-320	2.69	410-440	10.11
135-145	1.62	280-300	1.26	380-410	12.01
125-135	2.62	260-280	3.9	350-380	15.57
115-125	2.65	240-260	5.19	320-350	13.28
105-115	2.65	220-240	6.3	290-320	4.55
95-105	3.25	200-220	6.4	260-290	3.16
85-95	3.25	180-200	8.9	230-260	3.1
< 85	14.15	< 180	34.23	< 230	17.58
	100		100		100

Effective CBR of compacted subgrade = 8 %.

Design a concrete pavement for the following options (i) concrete pavement with tied concrete shoulder with doweled transverse joints (ii) concrete pavement without tied concrete shoulder

and without doweled transverse joints (Only for illustration since dowel bar is necessary for heavy traffic for eliminating faulting) (iii) concrete pavement with widened outer lane and (iv) concrete pavement bonded to dry lean concrete layer

Solution for Example

Typical cross-section of a concrete pavement is shown in **Fig. VII.1**.

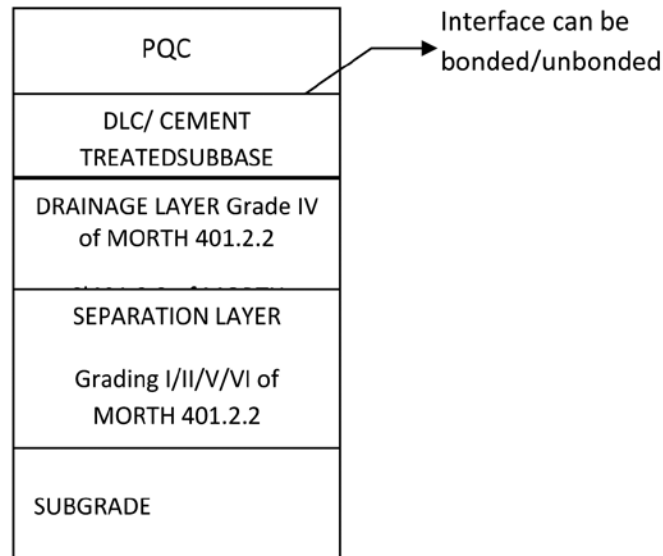


Fig. VII.1 Typical Cross-Section of Concrete Pavement

- a) Selection of modulus of subgrade reaction :-
 - Effective CBR of compacted subgrade = 8%. Modulus of subgrade reaction = 50.3 MPa/m (from **Table 2**)
 - Provide 150 mm thick granular subbase
 - Provide a DLC subbase of thickness 150 mm with a minimum 7 day compressive strength of 7 MPa
 - Effective modulus of subgrade reaction of combined foundation of subgrade + granular subbase and DLC subbase (from **Table 4** by interpolation) = 285 MPa/m
 - Provide a debonding layer of polythene sheet of 125 micron thickness between DLC and concrete slab.
- b) Selection of Flexural Strength of Concrete :-
 - 28-day compressive strength of cement concrete ≥ 40 MPa minimum
 - 90-day compressive strength of cement concrete ≥ 48 MPa
 - 28-day Flexural strength of cement concrete = 4.5 MPa (minimum)
 - 90-day Flexural strength of cement concrete = $4.5 \times 1.1 = 4.95$ MPa
- (c) Selection of Design Traffic for Fatigue Analysis :-
 - Design period = 30 years

- Annual rate of growth of commercial traffic (expressed in decimal) = 0.075 (assumed)
- Two-way commercial traffic volume per day = 6000 commercial vehicles/day
- % of traffic in predominant direction = 50% (3000 CVs in each direction)
- Total two-way commercial vehicles during design period,

$$C = \frac{365 \times 6000 \{ (1 + 0.075)^{30} \}}{0.075}$$

- = 226,444,692 CVs
- Average number of axles (steering/single/tandem/tridem) per commercial vehicle = 2.35
- Total two-way axle load repetitions during the design period = 226,444,692 X 2.35 = 532,145,025 axles
- Number of axles in predominant direction = 532,145,025 X 0.5 = 266,072,513
- Design traffic after adjusting for lateral placement of axles (25% of predominant direction traffic for multi-lane highways) = 266,072,513 X 0.25 = 66,518,128
- Night time (12-hour) design axle repetitions = 66,518,128 * 0.6 (60% traffic during night time) = 39,910,877
- Day time (12-hour) design axle repetitions = 66,518,128 * (1-0.6) = 26,607,251
- Day-time Six-Hour axle load repetitions = 26,607,251 / 2 = 13,303,626
- Hence, design number of axle load repetitions for **bottom-up cracking analysis = 13,303,626**
- Night-time Six-Hour axle load repetitions = 39,910,877/2 = 19,955,439
- % of commercial vehicles having the spacing between the front (steering) axle and the first axle of the rear axle unit less than 4.50 m = 55%
- Hence, the Six-hour night-time design axle load repetitions for Top-down cracking analysis (wheel base < 4.5 m) = 19,955,439 X 0.55 = 10,975,491
- The axle load category-wise design axle load repetitions for bottom-up and top-down fatigue cracking analysis are given in the following table:

Axle Category	Proportion of the Axle-Category	Category-Wise Axle Repetitions for Bottom-up Cracking Analysis	Category-Wise Axle Repetitions for Top-Down Cracking Analysis
Front (steering) single	0.45	5986632	4938971
Rear single	0.15	1995544	1646324
Tandem	0.25	3325906	2743873
Tridem	0.15	1995544	1646324

- c) Cumulative Fatigue Damage (CFD) analysis for Bottom-Up Cracking (BUC) and Top-Down Cracking (TDC) and Selection of Slab Thickness :-
- Effective modulus of subgrade reaction of foundation, $k = 285 \text{ MPa/m}$
 - Elastic Modulus of concrete, $E = 30,000 \text{ MPa}$
 - Poisson's ratio of concrete, $\mu = 0.15$
 - Unit weight of concrete, $\gamma = 24 \text{ kN/m}^3$
 - Design flexural strength of concrete = 4.95 MPa
 - Max. day-time Temperature Differential in slab (for bottom-up cracking) = 16.8°C (for Bihar)
 - Night-time Temperature Differential in slab (for top-down cracking) = $\text{day-time diff}/2 + 5 = 13.4^\circ\text{C}$

Pavement Option I - Concrete pavement with tied concrete shoulder with dowel bars across transverse joints

- Trial thickness of slab, $h = 0.28 \text{ m}$
- Radius of relative stiffness, $l = (Eh^3/(12k(1-\mu^2)))^{0.25} = 0.78758 \text{ m}$
- 'Beta' factor in the stress equations will be 0.66 for doweled transverse joints for carrying out TDC analysis

Computation of bottom-up and top-down cumulative fatigue damage is illustrated in **Tables VII.2 and VII.3**. It can be seen from the calculations given in the tables that for the slab thickness of 0.28 m, the total fatigue damage for bottom-up and top down cracking is $0.976 + 0.274 + 0.445 + 0.036 = 1.731$ which is greater than 1.0. Hence, the trial thickness of 0.28 m is not adequate. Increase thickness to 290 mm, Total CFD = 0.527, Hence 290 mm is acceptable. If two retexturing is considered in 30 years, a thickness of 300 mm will be appropriate.

Table VII.2 Cumulative Fatigue Damage Analysis for Bottom-up Cracking (Mid Point of the Axle Load Class from Table VII-1 is Adopted for Stress Computation)

Bottom-up Cracking Fatigue Analysis for Day-time (6 hour) traffic and Positive Temperature Differential									
Rear Single Axles(as per Table VII-1, 1st col)					Rear Tandem Axles(as per Table VII-1, 3rd col)				
Expected Rep (ni)	Flex Stress MPa	Stress Ratio (SR)	Allowable Rep. (Ni)	Fatigue Damage (ni/Ni)	Expected Rep. (ni)	Flex Stress MPa	Stress Ratio (SR)	Allowable Rep. (Ni)	Fatigue Damage (ni/Ni)
362191	2.503	0.506	588331	0.616	482256	2.118	0.428	infinite	0.000
347823	2.422	0.489	1344185	0.259	349220	2.045	0.413	infinite	0.000
364586	2.341	0.473	4072762	0.090	120730	1.972	0.398	infinite	0.000
259022	2.260	0.457	22079767	0.012	83148	1.899	0.384	infinite	0.000
59467	2.179	0.440	infinite	0.000	89467	1.826	0.369	infinite	0.000
32328	2.099	0.424	infinite	0.000	41906	1.754	0.354	infinite	0.000
52283	2.018	0.408	infinite	0.000	129710	1.681	0.340	infinite	0.000
52882	1.937	0.391	infinite	0.000	172615	1.608	0.325	infinite	0.000
52882	1.856	0.375	infinite	0.000	209532	1.535	0.310	infinite	0.000
64855	1.775	0.359	infinite	0.000	212858	1.462	0.295	infinite	0.000
64855	1.695	0.342	infinite	0.000	296006	1.39	0.281	infinite	0.000
282369	1.614	0.326	infinite	0.000	1138458	1.317	0.266	infinite	0.000
1995544	Fat Dam from Single Axles =			0.976	3325906	Fat Dam from Tandem Axles =			0.000

**Table VII.3 Cumulative Fatigue Damage Analysis for Top-Down Cracking
(Mid Point of the Axle Load Class from Table VII-1 is Adopted for Stress Computation)**

Top-Down Cracking Fatigue Analysis for Night-time (6 hour) traffic and Negative Temperature Differential														
Rear Single Axles(as per Table VII-1 1st col)				Rear Tandem Axles (as per Table VII-1 3rd col) (Stress computed for 50% of axle load)				Rear Tridem Axles (as per Table VII-1 5th col) (Stress computed for 33% of axle load)						
Expected Rep. (ni)	Flex Stress MPa	Stress Ratio (SR)	Allowable Rep. (Ni)	Fat. Dam. (ni/Ni)	Expected Rep. (ni)	Flex Stress MPa	Stress Ratio (SR)	Allowable Rep. (Ni)	Fat. Dam. (ni/Ni)	Expected Rep. (ni)	Flex Stress MPa	Stress Ratio (SR)	Allowable Rep. (Ni)	Fat. Dam. (ni/Ni)
298808	2.399	0.485	1768731	0.169	397862	2.427	0.490	1267085	0.314	86103	2.353	0.475	3370878	0.026
286954	2.344	0.473	3899961	0.074	288107	2.371	0.479	2564487	0.112	79847	2.297	0.464	9089367	0.009
300783	2.288	0.462	11091781	0.027	99603	2.316	0.468	6308978	0.016	56634	2.242	0.453	38025932	0.001
213693	2.233	0.451	52048021	0.004	68597	2.26	0.457	21946523	0.003	117218	2.186	0.442	Infinite	0.000
49060	2.177	0.440	infinite	0.000	73810	2.205	0.445	infinite	0.000	166443	2.131	0.430	Infinite	0.000
26670	2.122	0.429	infinite	0.000	34573	2.149	0.434	infinite	0.000	197723	2.075	0.419	Infinite	0.000
43134	2.066	0.417	infinite	0.000	107011	2.094	0.423	infinite	0.000	256333	2.02	0.408	Infinite	0.000
43628	2.011	0.406	infinite	0.000	142407	2.038	0.412	infinite	0.000	218632	1.964	0.397	Infinite	0.000
43628	1.955	0.395	infinite	0.000	172864	1.983	0.401	infinite	0.000	74908	1.909	0.386	Infinite	0.000
53506	1.900	0.384	infinite	0.000	175608	1.927	0.389	infinite	0.000	52024	1.853	0.374	Infinite	0.000
53506	1.844	0.373	infinite	0.000	244205	1.872	0.378	infinite	0.000	51036	1.798	0.363	Infinite	0.000
232955	1.789	0.361	infinite	0.000	939228	1.816	0.367	infinite	0.000	289424	1.742	0.352	Infinite	0.000
1646324	Fat Dam from Sing. Axles =			0.274	2743873	Fat Dam from Tand Axles =			0.445	1646324	Fat Dam from Tridem Axles =			0.036

Table VII.4 Gives the Cumulative fatigue damage values for five trial thicknesses.

**Table VII.4 Cumulative Fatigue Damage Values for Different Trial Thicknesses
(for the Data Considered in the Example)**

Slab Thickness, m	CFD for BUC Case			CFD for TDC Case				Sum of BUC and TDC CFD	Remarks
	Due to Rear Single Axles	Due to Tandem Axles	Total CFD	Due to Rear Single Axles	Due to Tandem Axles	Due to Rear Tridem Axles	Total CFD		
0.24	36.27	2.992	39.262	7.064	8.69	1.489	17.243	56.505	Unsafe
0.25	14.924	0.812	15.737	3.537	4.475	0.674	8.686	24.423	Unsafe
0.26	6.488	0.136	6.624	1.671	2.245	0.285	4.201	10.825	Unsafe
0.28	0.976	0.00	0.976	0.274	0.445	0.036	0.755	1.731	Unsafe
0.29	0.282	0.00	0.282	0.078	0.157	0.009	0.245	0.527	Safe

Pavement Option II - Concrete pavement with no concrete shoulder and without dowel bars across transverse joints. This is for illustration since dowel bar is essential for heavy traffic to prevent faulting, erosion and pumping at transverse joints.

- Trial thickness of slab, $h = 0.33$ m
- Radius of relative stiffness, $l = (Eh^3/(12k(1-\mu^2)))^{0.25} = 0.75358$ m
- ‘Beta’ factor in the stress equations will be 0.90 for transverse joints without dowel bars for carrying out TDC analysis

The cumulative fatigue damage values obtained for bottom-up and top-down cracking analyses are given below.

Bottom-up cracking :-
 (a) CFD due to rear single axles = 0.935
 (b) CFD due to tandem axles = 0.000
 (c) Total CFD = 0.935

Top-down cracking :
 (a) CFD due to rear single axles = 0.233
 (b) CFD due to tandem axles = 0.390
 (c) CFD due to tridem axles = 0.030
 (d) Total CFD = 0.654

Total CFD for BUC and TDC=1.589 >1,0

Hence, the trial thickness of 330 mm is not adequate. A thickness of 340 mm is needed. This clearly shows that for heavy traffic, dowel bar is necessary to lower CFD for TDC. This also illustrates that CFD for BUC is large for pavement without concrete shoulder.

Pavement Option III - Concrete pavement with widened outer lanes

The reduction of flexural stress due to widening of the outer lane by 0.5 m to 0.6 m is of the same order as that of providing tied concrete shoulder. Hence, the thickness of the pavement will be the same as that obtained for Option I (with tied concrete shoulders). Hence, design

thickness of concrete pavement slab = 290 mm. The thickness may be increased by 10 mm for two retexturing during the pavement's life time.

Pavement Option IV- Concrete pavement bonded to dry lean concrete layer.

A 7 day strength of 10 MPa or higher for the DLC is necessary for a bonded pavement. There is no upper strength limit for DLC for bonded cases.

- Provide a granular subbase of 250 mm thickness above the subgrade
- Effective modulus of subgrade reaction of foundation consisting of subgrade (8% CBR) and granular subbase (from **Tables 2 and 3**) = 72 MPa/m
- Assuming that doweled transverse joints and tied concrete shoulders will be provided, the thickness of slab required for the given traffic and other design data = 0.30 m.
- Referring to **Fig. 6**, $E_1 = 30000$ MPa, $E_2 = 13600$ MPa, $\mu_1 = 0.15$, $\mu_2 = 0.20$
- Provide a DLC thickness of 0.15 m. For bonded condition, DLC of 10 MPa strength at 7 days is considered. Higher strength DLC will give lower thickness of PQC slab
- Depth of neutral axis (computed using equation 11) = 0.16 m
- Assume a trial slab thickness (to be bonded to 0.15 m thick DLC layer) = 0.235 m
- Stiffness of the slab to be placed over DLC layer (Equation 12) = 46.65 MN.m
- Stiffness of the DLC layer (Equation 13) = 23.28 MN.m
- Combined stiffness of slab and DLC = 46.65 + 23.28 = 69.93 MN.m
- Stiffness of the design slab of 0.3 m thickness (Equation 10) = 69.05 MN.m
- Combined stiffness is more than the design stiffness requirement. Hence OK.

Appendix - VIII

Design of Dowel Bars

Example

Input data considered for dowel bar design

- Slab thickness, h = 330 mm
- Joint width, z = 20 mm (expansion joint), 5mm (for contraction joint)
- Modulus of subgrade reaction, k = 80 MPa/m
- Radius of relative stiffness, l = 1035.3 mm
- E for dowel bar = 2×10^5 MPa
- Modulus of dowel support, k_{mds} = 415000 MPa/m
- Maximum single axle load = 190 kN
- Maximum single wheel load = $190/2 = 95$ kN (considering dual wheel as single wheel for a safe design)
- Assume a load transfer of 30% at terminal stage to the tied concrete shoulder. If no concrete shoulders are provided, no load transfer to shoulder may be assumed
- Wheel load for dowel bar design = $95 \times 0.7 = 66.5$ kN
- Safety of the dowel bar is examined for a wheel load of 66.5 kN
- Assume the percentage of load transfer through dowel bar as 50% for 100% joint efficiency. The load to be transferred = 33.25 kN
- Permissible bearing stress in concrete is calculated (using equation 15) as:-

$$F_b = (101.6 - b_d) f_{ck} / 95.25$$

Where,

f_{ck} = characteristics compressive = 40 MPa for M40 grade

b_d = diameter of the dowel bar = 38 mm (assumed)

F_b = $(101.6 - 38) * 40 / 95.25$ = 26.7 MPa

- Spacing between the dowel bars (assumed) = 300 mm
- First dowel bar is placed at a distance of 150 mm from the pavement edge
- Assumed length of the dowel bar = 500 mm
- Dowel bars up to a distance of $1.0 \times$ radius of relative stiffness (l), from the point of load application are effective in load transfer

- Number of dowel bars participating in load transfer when the wheel load is just over the dowel bar close to the edge of the slab = $1 + l/\text{spacing} = 1 + 1035.3/300 = 4$ dowels
- Assuming that the load transferred by the first dowel is P_t and that the load on dowel bar at a distance of l from the first dowel is zero, the total load transferred by dowel bar system = $(1 + (1035.3 - 300)/1035.3 + (1035.3 - 600)/1035.3 + (1035.3 - 900)/1035.3) P_t = 2.26 P_t$
- Load carried by the outer dowel bar, $P_t = (33.25)/2.26 = 14.71$ kN
- Check for Bearing Stress
- Moment of Inertia of Dowel = $\pi(b_d)^4/64 = \pi \times (38)^4/64 = 102302.0$ mm⁴
- Relative stiffness of dowel bar embedded in concrete, $\beta = \sqrt[4]{\frac{k_{m\text{ds}} b_d}{4EI}}$
 $= [415000 \times 38 / (1000 \times 4 \times 2.0 \times 10^5 \times 102302)]^{1/4} = 0.021$ mm⁻¹
 A factor of 1000 is introduced to match the units
 Bearing stress in dowel bar $F_{b\text{max}} = (P_t \times k_{m\text{ds}}) \times (2 + \beta_z) / (4 \beta^3 EI)$

$$= \frac{14.71 \times 415000 \{2 + (0.021 \times 20)\}}{4 \times 0.021^3 \times 2.0 \times 10^5 \times 102302}$$

 $= 20.19$ MPa which is less than 26.7 MPa

Hence, the dowel bar spacing and diameter assumed are safe.

Even if load transfer to the tied concrete shoulder is not considered and the dual wheels with a wheel spacing of 310 mm each carrying a load of 45 kN is considered separately, the dowel bar designed as per above is safe.

There is practically little Joint opening at transverse contraction joint. 20 mm joint width is assumed for the expansion joint near a structure. Therefore, the dowel bar specifications recommended in **Table 6** will always be safe for contraction joints.

Appendix - IX

Design of Tie Bars

Input Data

- Slab Thickness = 0.33 m
- Lane width, b = 3.5 m
- Coefficient of friction, f = 1.5
- Density of concrete, kN/m^3 = 24
- Allowable tensile stress in plain bars, MPa
(As per IRC:15-2011) = 125.0
- Allowable tensile stress in deformed bars, MPa
(As per IRC:15-2011) = 200.0
- Allowable bond stress for plain tie bars, MPa = 1.75
- Allowable bond stress for deformed tie bars, MPa = 2.46

Design for Plain bars

- Select diameter of tie bar, d_t = 12 mm
- Area of plain steel bar required per metre width of joint to resist the frictional force at slab bottom, A_s = bfW / S_{st}
= $3.5 \times 1.5 \times 0.33 \times 24000 / 125$
= $332.6 \text{ mm}^2/\text{m}$
- Cross sectional area of tie bar, $A = d_t^2 \times \pi/4$ = 113.0 mm^2
- Perimeter of tie bar, $P_{ptb} = \pi d_t$ = 37.7 mm
- Spacing of tie bars, $= A/A_s$ = $100 \times (113/332.6)$
= 339.7 mm
- Provide a spacing of 340 mm c/c
Length of tie bar, $L = 2 \times S_{st} \times A / B^* \times P_{ptb}$ = $2 \times 125 \times 113 / (1.75 \times 7)$
= 428.2 mm
- Increase length by 100 mm for loss of bond due to painting and another 50 mm for tolerance in placement.
- Therefore, the required length of tie bar = $428.2 + 100 + 50 = 578.2 \text{ mm}$
(say 580 mm)

Design for Deformed bars

- Select diameter of tie bar, d_t = 12 mm
- Area of plain steel bar required per metre width of joint to resist the frictional force at slab bottom, A_s = bfW / S_{st}
 = $3.5 \times 1.5 \times 0.33 \times 24000 / 200$
 = 207.9 mm²/m
- Spacing of tie bars, = A / A_s = $100 \times (113 / 207.9)$
 = 543.5 mm
- Provide a spacing of 540 mm c/c
- Length of tie bar, $L = 2 \times S_{st} \times A / B^* \times P_{ptb}$ = $2 \times 200 \times 113 / (2.46 \times 37.7)$
 = 487.4 mm
- Increase length by 100 mm for loss of bond due to painting and another 50 mm for tolerance in placement.
- Therefore, the required length of tie bar = $487.4 + 100 + 50 =$
 637.4 mm
 (say 640 mm)
